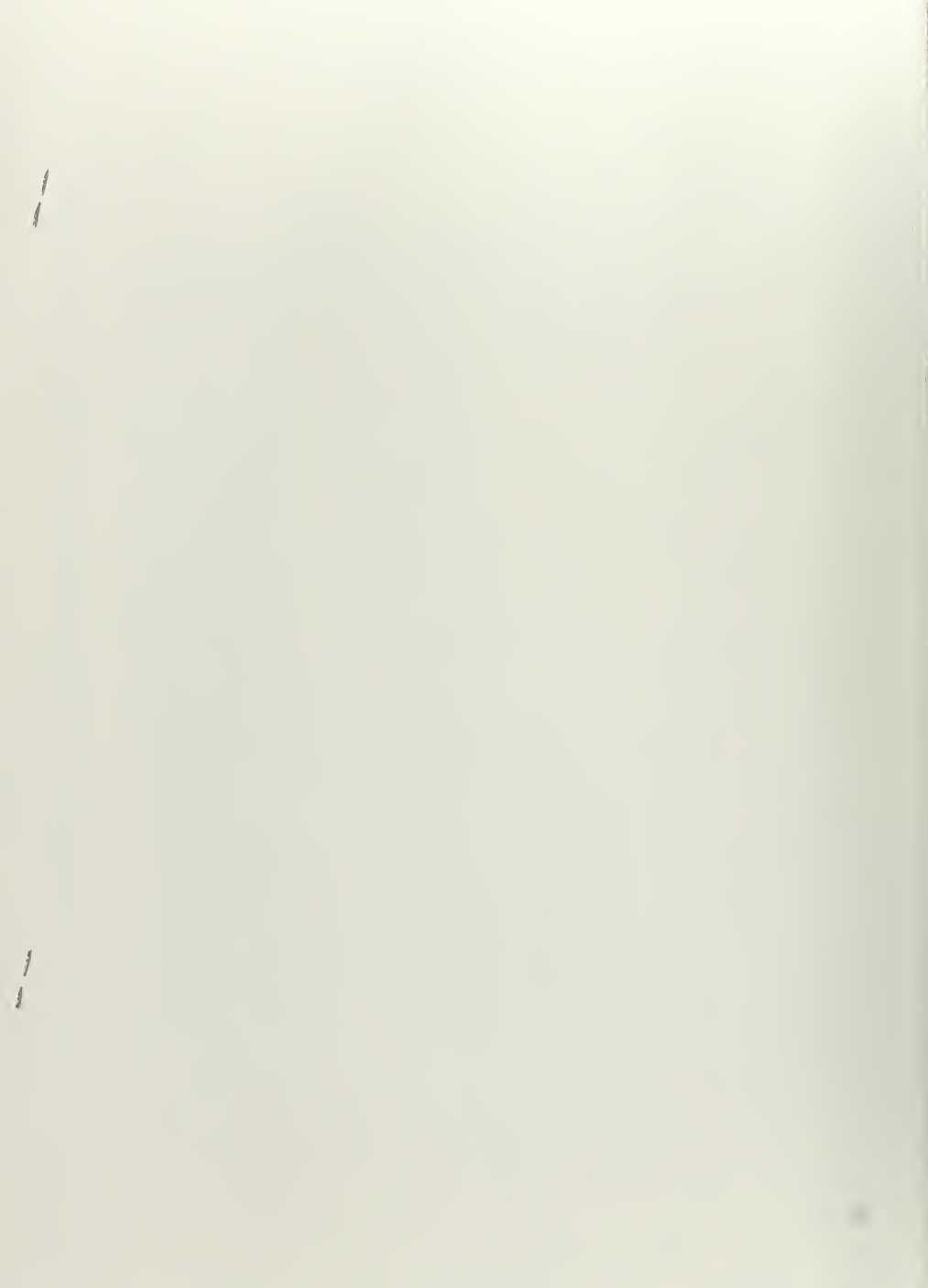


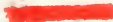
NPS ARCHIVE
1967
HARRISON, R.

AN ANALYSIS OF SINGLE STAGE AXIAL-FLOW
TURBINE PERFORMANCE USING THREE-DIMENSIONAL

CALCULATING METHODS

ROBERT GLEN HARRISON




AN ANALYSIS OF SINGLE STAGE
AXIAL-FLOW TURBINE PERFORMANCE USING
THREE-DIMENSIONAL CALCULATING METHODS

by

Robert Glen Harrison
Lieutenant, United States Navy
B.M.E., University of Louisville, 1959

Submitted in partial fulfillment of the
requirements for the degree of

AERONAUTICAL ENGINEER

from the

NAVAL POSTGRADUATE SCHOOL
September 1967

167
ARRISON, P.

ABSTRACT

The method of turbine performance prediction developed by Vavra and Eckert has been refined in this analysis to realize more of the potential of the three-dimensional calculating methods. Mach number and rotor tip clearance effects on blade outlet angles and loss coefficients have been localized rather than averaged over the blade height. An approximation for streamline curvature has been used.

Performance curves were determined for two single stage axial-flow turbines located at the Propulsion Laboratory of the Naval Postgraduate School. Test results were available for one of the turbines. Agreement between predicted and experimental performance values was generally within 3 per cent.

ERRATA SHEET

<u>Page</u>	<u>Line</u>	<u>Change</u>	<u>To</u>
3	10	Developement	Development
13	21	()	(γ/δ)
13	22	518.4	$T_{to}/518.4$
18	13	development	development
21	Eq.13	reads: $\xi = 1 - \sum \frac{\delta^*}{a} = \frac{H^{***} - 1}{H^{***} - \zeta/2}$	
21	Eq.14	reads: $dA = \xi Z \frac{a}{a_m} dX a_m r_m$	
24	13	representing	representing
26	7/8	calculat-ing	calcula-ting
27	2		insert " α_1 " after "the" at end of line.
27	27/28	proce-dur	proce-dure
36	10	() _w	(η) _w
39	16		insert " ζ_R " after "of" at end of line.
44	13/14	opera-ting	operat-ing
45	23	b unt	blunt
49	8/9	coeffici-ents	coeffi-cients
107	7	glade	blade
147	Item 10	Item 10. should read:	"This document is subject to special export controls and each transmittal to foreign nationals may be made only with prior approval of the Naval Postgraduate School"

TABLE OF CONTENTS

Section	Page
1. Introduction	17
2. Basis for the Analysis	18
3. Technique for Obtaining a Solution	23
4. MOD I and MOD II Turbines	37
5. Conclusions and Recommendations	48
6. Bibliography	88
Appendix	
A. Development of Equations	89
B. Computations of Outlet Angles and Loss Coefficients	101
C. Computer Program	112

LIST OF TABLES

Table	Page
I. Sample Calculations for Stator Outlet Angles	104
II. Sample Calculations for Rotor Outlet Angles	105
III. Sample Calculations for Stator Loss Coefficient	109
IV. Sample Calculations for Stalling Incidence and Rotor Loss Coefficients	110
V. Sample Computer Output for Stator Solution	144
VI. Sample Computer Output for Rotor Solution	145

LIST OF ILLUSTRATIONS

Figure	Page
1. Turbine Thermodynamic Process	50
2. Coordinates and Streamlines	51
3. Velocity Diagrams	52
4. Stator and Rotor Blade Profiles (MOD I)	53
5. Stator and Rotor Blade Profiles (MOD II)	54
6. Stator and Rotor Throat Openings versus Radial Position (MOD I & MOD II)	55
7. Variation of Stator Outlet Angle with Radius (MOD I)	56
8. Variation of Stator Outlet Angle with Mach Number (MOD I)	56
9. Variation of Stator Outlet Angle with Radius (MOD II)	57
10. Variation of Stator Outlet Angle with Mach Number (MOD II)	57
11. Variation of Rotor Outlet Angle with Radius (MOD I)	58
12. Variation of Rotor Outlet Angle with Mach Number (MOD I)	58
13. Variation of Rotor Outlet Angle with Radius (MOD II)	59
14. Variation of Rotor Outlet Angle with Mach Number (MOD II)	59
15. Stator Loss Coefficients as Function of Radius (MOD I & MOD II)	60
16. Variation of Blade Inlet and Stall Incidence Angles with Radius (MOD I & MOD II)	61
17. Rotor Loss Coefficients as Function of Incidence Ratio (MOD I)	62
18. Rotor Loss Coefficients as Function of Incidence Ratio (MOD II)	63

Figure	Page
19. Variation of Referred Flowrate with Referred RPM (MOD I)	64
20. Referred Moment versus Referred RPM (MOD I)	65
21. Total-Static Efficiency versus Referred RPM (MOD I, $k=0.020$ in.)	66
22. Total-Static Efficiency versus Referred RPM (MOD I, $k=0.033$ in.)	67
23. Total-Static Efficiency versus Isentropic Head Coefficient (MOD I)	68
24. Referred Power versus Referred RPM (MOD I)	69
25. Theoretical Degree of Reaction versus Isentropic Head Coefficient (MOD I)	70
26. Theoretical Degree of Reaction versus Referred RPM (MOD I, $P_{t_0}/P_2=1.40$)	71
27. Variation of Referred Flowrate with Referred RPM (MOD II, $k=0.015$ in.)	72
28. Variation of Referred Flowrate with Referred RPM (MOD II, $k=0.033$ in.)	73
29. Referred Moment versus Referred RPM (MOD II, $k=0.015$ in.)	74
30. Referred Moment versus Referred RPM (MOD II, $k=0.033$ in.)	75
31. Total-Static Efficiency versus Referred RPM (MOD II, $P_{t_0}/P_2=1.30, 1.31$)	76
32. Total-Static Efficiency versus Referred RPM (MOD II, $P_{t_0}/P_2=1.40$)	77
33. Total-Static Efficiency versus Referred RPM (MOD II, $P_{t_0}/P_2=1.50, 1.51$)	78
34. Total-Static Efficiency versus Referred RPM (MOD II, $P_{t_0}/P_2=1.60$)	79
35. Total-Static Efficiency versus Isentropic Head Coefficient (MOD II)	80

Figure	Page
36. Referred Power versus Referred RPM (MOD II, $k=0.015$ in.)	81
37. Referred Power versus Referred RPM (MOD II, $k=0.033$ in.)	82
38. Theoretical Degree of Reaction versus Isentropic Head Coefficient (MOD II)	83
39. Theoretical Degree of Reaction versus Referred RPM (MOD II, $P_{t_0}/P_2=1.40$)	84
40. Absolute Flow Outlet Angles as Function of Radius (MOD II, $k=0.015$ in., $P_{t_0}/P_2=1.40$, $RPM/\sqrt{\Theta} = 13,934$)	85
41. Referred Velocities as Function of Radius (MOD II, $k=0.015$ in., $P_{t_0}/P_2=1.40$, $RPM/\sqrt{\Theta} = 13,934$)	86
42. Relative Rotor Flow Outlet Angle as Function of Radius (MOD II, $k=0.015$ in., $P_{t_0}/P_2=1.40$, $RPM/\sqrt{\Theta} = 13,934$)	86
43. Plots of Axial Velocity Ratios versus Radius Ratios at Peak Efficiency (MOD I & MOD II, $P_{t_0}/P_2=1.40$)	87
44. Expansion from Plenum	94
45. Conditions at Exit of Blade Row	96
46. Blade Geometry	102
47. Tip Clearance Factor X as Function of Radius	103

TABLE OF SYMBOLS

Symbols

A	Area (in. ²)
a	Throat opening of blade channel (in.)
B	Shroud factor used in rotor loss coefficient calculations (dimensionless)
b	Blade's departure from being straight-backed (in.)
C ₁	Conversion factor, $2gJ(\text{ft}^2\text{-lb}_m/\text{sec}^2\text{-BTU})$
c	Blade Chord (in.)
c _p	Specific heat, constant pressure (BTU/lb _m -°R)
Ė	Kinetic energy rate (ft-lb/sec)
e	Mean radius of curvature of back of blade (in.)
g	Universal gravitational constant (32.174 lb _m -ft/lb-sec ²)
H	Total enthalpy (BTU/lb _m)
H***	Boundary layer energy parameter ($\frac{\delta^{***}}{\delta^*}$)
h	Static enthalpy (BTU/lb _m)
h	Blade height (in.)
HP	Horsepower
I	Integrand
i	Incidence angle (deg. or radians)
\vec{i}	Unit vector
i _s	Stalling incidence angle (deg. or radians)
J	Conversion factor (778.16 ft-lb/BTU)
j	Distance from throat to trailing edge of blade (in.)
k	Tip clearance (in.)
k _{is}	Isentropic head coefficient (dimensionless)

Symbols

L	Distance between stations 0 and 1 and between stations 1 and 2 (in.)
M	Mach number
M	Moment (ft-lb)
\dot{m}	Mass flowrate (slugs/sec)
m	Exponent used in boundary layer calculations, see Eq. 146 (dimensionless)
P	Pressure (psia)
R	Gas constant for air (53.345 ft-lb/lb _m -°R)
r	Radius (in.)
r*	Theoretical degree of reaction (dimensionless)
s	Blade spacing (in.)
s	Entropy (BTU/lb _m -°R)
s*	Non-dimensional entropy ($\frac{s}{c_p}$)
T	Temperature (°R)
t	Blade thickness (in.)
t	Blade trailing edge thickness (in.)
t*	Projection of blade trailing edge thickness on the exit plane of the blade row (in.)
U	Peripheral velocity (ft/sec)
u	Velocity within a boundary layer (ft/sec)
V	Absolute velocity (ft/sec)
W	Relative velocity (ft/sec)
\dot{w}	Weight flowrate (lb _m /sec)
W_f	Fraction of the total flowrate which passes between the hub and any other streamline (dimensionless)
W_{ref}	Reference flowrate (in. ²)

Symbols

X	Non-dimensional radius $\frac{r}{r_m}$ where r_m is the mean streamline radius
X	Shroud factor for calculation of rotor outlet angles (dimensionless)
X _e	See Eq. 145
Y	Non-dimensional axial velocity $\frac{V_A}{V_{A_m}}$ where V_{A_m} is the mean streamline axial velocity
Y	Pressure loss parameter, see Eq. 167
y	Distance from wall of a point in a boundary layer (in.)
Z	Number of blades

Greek Letters

α	Absolute gas flow angles (deg. or radians)
β	Gas flow angles relative to rotor (deg. or radians)
β_0	Blade inlet angle (deg. or radians)
γ	Specific heat ratio (dimensionless)
ΔR	Streamline displacement, see Fig. 2 (in.)
δ	Boundary layer thickness (in.)
δ	Referred pressure $\frac{P_t}{14.7}$ (dimensionless)
δr	Streamline displacement, see Fig. 2 (in.)
δ^*	Boundary layer displacement thickness (in.)
δ^{***}	Boundary layer energy thickness (in.)
ξ	Loss coefficient (dimensionless)
η	Efficiency (dimensionless)
η	Non-dimensional distance from the wall in a boundary layer ()
θ	Referred temperature 518.4 (dimensionless)
K	Streamline curvature factor (dimensionless)

Greek Letters

λ	Angle between flow and axis of turbine in a meridional plane (deg. or radians)
λ	Factor used in predicting secondary loss coefficients, see Eq. 171 (dimensionless)
ξ	Area restriction factor (dimensionless)
ρ	Density (lb_m/ft^3)
Φ	Non-dimensional flow function
ω	Angular velocity (radians/sec)

Subscripts

A	Axial
d	Discharge
E	Equivalent
H	Hub
is	Isentropic expansion from total inlet conditions
m	Mean streamline
o	Station ahead of stator
P	Profile
R	Relative
r	Radial
ref	Referred
req.	Required
S	Stator
S	Shroud
s	Isentropic expansion from equivalent total conditions
T	Tip
t	Total

Subscripts

th	Theoretical
u	Tangential
z	Axial direction, cylindrical coordinates
θ	Peripheral direction, cylindrical coordinates
1	Station between stator and rotor
2	Station after rotor

Superscript

**	Refers to predicted values for the mean streamline
----	--

1. Introduction

Turbines form an important part of propulsion systems. To optimize a design it is necessary to know the performance at off-design conditions as well as the performance at the design point. Since the testing of a prototype is very costly and time consuming, it is of great advantage to be able to predict the performance characteristics by means of theoretical methods. The more advanced a system is the more important it becomes to improve the accuracy of these methods. Hence it is necessary to base these methods on the fundamental laws of fluid dynamics rather than on rule-of-thumb approximations. The latter basis is possible only when data on previous designs are available. For new and advanced configurations, it will be necessary to apply refined methods which enable the designer and systems engineer to predict the effect of proposed design changes.

The principal equations that describe the flow properties in turbomachines are well known. These same equations are used as a basis for all proper "three-dimensional" calculating methods that have been cited in the technical literature. The methods differ however in the manner in which these equations are manipulated and applied.

This thesis is concerned with the refinement of the three-dimensional method of analysis developed by Vavra and Eckert. Based on the physical dimensions of particular test turbines that are available at the Turbo-Propulsion Laboratory of the Naval Postgraduate School, performance curves were determined for these machines. Concurrently with the performance analysis, experimental tests were conducted on one of these turbines so that actual experimental results could be used to judge the accuracy of the proposed theoretical performance evaluation.

In addition to his publications and classroom lectures which constituted the foundation for this analysis, Professor Vavra was very generous in providing guidance and counsel during the period of this work. For this I am greatly appreciative. I would also like to thank Lieutenants P. M. Commons and J. A. Messegee for making their experimental results available.

2. Basis for the Analysis

The two conservation equations that must be satisfied to obtain a solution for the flow in a turbine are the equations of motion and continuity. These equations are satisfied at stations between blade rows. The method used is that given by Vavra.¹ Vavra developed the equations of motion and continuity for absolute flows. The equations in this form are readily useable for the position after the stator. Eckert later developed these equations for relative flows to be used for rotor calculations.² Eckert's conversion allows relative flow quantities to be handled directly without conversion to an absolute system. Eckert's approach also avoids iteration procedures to determine the total enthalpy after the rotor.

The assumptions made for the development of the equations used in the performance analysis are:

1. An infinite number of blades in each row so that downstream effects are not felt upstream.

2. Axisymmetric flow at the stations where the equations of motion are solved.

3. Adiabatic and steady flow so that the total enthalpy along any given streamline is constant through the stator and the relative total enthalpy is constant through the rotor.

4. All entropy changes are assumed to occur in the blade channels that are located ahead of the stations where the equations of motion are satisfied. Hence at the calculating stations the flow is assumed to be isentropic along particular streamlines.

With the above assumptions, the equations of motion for absolute and relative flows, respectively, are

$$\nabla H = \bar{V} \times (\nabla \times \bar{V}) + T \nabla s \quad (1)$$

$$\nabla H_R = \bar{W} \times (\nabla \times \bar{W} + 2\bar{\omega}) + T \nabla s \quad (2)$$

¹Vavra, M. H., Aero-Thermodynamics and Flow in Turbomachines. New York, London: John Wiley and Sons, Inc.; 1960, Chapter 16.

²Eckert, R. H., Performance Analysis and Initial Tests of a Transonic Turbine Test Rig (USNPGS Thesis, May 1966), pp. 149-155.

Relative total enthalpy can be written as

$$H_R = h_1 + \frac{W_1^2}{2} - \frac{U_1^2}{2} = h_2 + \frac{W_E^2}{2} - \frac{U_2^2}{2} = h_{2s} + \frac{W_{2th}^2}{2} - \frac{U_2^2}{2} \quad (3)$$

Equivalent enthalpy is defined as

$$H_E = h_{2s} + \frac{W_{2th}^2}{2} = H_R + \frac{U_2^2}{2} \quad (4)$$

Similar to H_R , the equivalent enthalpy H_E is constant along a streamline for the adopted assumptions. Equivalent enthalpy can also be written as

$$H_E = h_2 + \frac{W_E^2}{2} = h_1 + \frac{W_1^2}{2} + \frac{U_2^2 - U_1^2}{2} \quad (5)$$

The introduction of the equivalent enthalpy allows this quantity to be used for the rotor in a manner analogous to the way total enthalpy is used for the stator.

For equations used in this analysis, the subscripts refer to:

0 - station ahead of stator

1 - station ahead of rotor

2 - station after rotor

is - isentropic expansion from P_{t0}

s - isentropic expansion from P_{tE}^0

th - the theoretical value

Figure 1 is a temperature-entropy diagram showing the thermodynamic process along a particular streamline for a single stage turbine. In general, the fluid properties will vary from streamline to streamline. The method in which the loss coefficients are applied is also indicated in Fig. 1. The loss coefficients are defined as

$$y_s = \frac{V_{1th}^2 - V_1^2}{V_{1th}^2} \quad \text{For the Stator} \quad (6)$$

$$y_R = \frac{W_{2th}^2 - W_2^2}{W_{2th}^2} \quad \text{For the Rotor} \quad (7)$$

The coordinate system that will be used in the analysis is indicated in Fig. 2. This figure also shows the general layout of the type turbine to which the prediction performance analysis is applied.

Sign convention for the various angles that are needed in the analysis is indicated in Fig. 3.

The modification of Eq. 2 into a form that can be used for the analysis is given in Appendix A, Section 1. The appropriate form of Eq. 1 can be obtained from the modification of Eq. 2 if the angular velocity ω is set equal to zero. Other differences of the final equations derived from Eqs. 1 and 2 are listed in Appendix A,

Section 1. Equation 1 can then be written

$$\begin{aligned} \frac{d(\ln Y_1^2)}{dX_1} = & -\cos^2 \alpha_1 \left[-K_2 r_m \frac{\delta r}{L^2} - \left(\frac{L^2 + (\Delta R)^2}{L^2} \right) \frac{ds_1^*}{dX_1} \right] - 2 \tan \alpha_1 \frac{d\alpha_1}{dX_1} \\ & - \frac{2}{X_1} \sin^2 \alpha_1 + \frac{C_1 \cos^2 \alpha_1}{Y_1^2 V_{A1m}^2} \frac{dH}{dX_1} - \left[\frac{C_1 H \cos^2 \alpha_1}{Y_1^2 V_{A1m}^2} - \sin^2 \alpha_1 \right] \frac{ds_1^*}{dX_1} \end{aligned} \quad (8)$$

Equation 2 becomes

$$\begin{aligned} \frac{d(\ln Y_2^2)}{dX_2} = & -\cos^2 \beta_2 \left[K_2 r_m \frac{\delta r}{L^2} - \left(\frac{L^2 + (\Delta R)^2}{L^2} \right) \frac{ds_2^*}{dX_2} \right] - 2 \tan \beta_2 \frac{d\beta_2}{dX_2} - \frac{2}{X_2} \sin^2 \beta_2 \\ & - \frac{4U_m \cos \beta_2 \sin \beta_2}{W_{A_m} Y_2} - \frac{2U_m U_2 \cos^2 \beta_2}{W_{A_m} Y_2^2} + \frac{C_1 \cos^2 \beta_2}{W_{A_m} Y_2^2} \frac{dH_E}{dX_2} - \left[\frac{C_1 H_E \cos^2 \beta_2}{W_{A_m} Y_2^2} - \sin^2 \beta_2 \right] \frac{ds_2^*}{dX_2} \end{aligned} \quad (9)$$

where:

$Y = \frac{V_A}{V_{A_m}}$ or $\frac{W_A}{W_{A_m}}$	for Eqs. 8 and 9 respectively (subscript m refers to mean streamline)
$X = \frac{r}{r_m}$	
$K = 5.0$	streamline curvature factor
δr	streamline displacements shown in Fig. 2
ΔR	
$L = \frac{L_1 + L_2}{2}$	(see Fig. 2)
$s^* = \frac{s}{c_p}$	
$C_1 = 2gJ$	

The equation of continuity is used in its non-dimensional form by introducing a flow function Φ . Development of Φ is given in Appendix A, Section 2. In differential form the equations for absolute and relative flows can then be expressed by

$$\frac{d\dot{W} \sqrt{T_{T_0}}}{P_{T_0}} \sqrt{\frac{R}{g}} = dA \Phi = dA \sqrt{\frac{2\gamma}{\gamma-1} \left[\left(\frac{P}{P_{T_0}} \right)^{\frac{2}{\gamma}} - \left(\frac{P}{P_{T_0}} \right)^{\frac{\gamma+1}{\gamma}} \right]} \quad (10)$$

and

$$\frac{d\dot{W} \sqrt{T_{T_E}}}{P_{T_E}} \sqrt{\frac{R}{g}} = dA \bar{\Phi} = dA \sqrt{\frac{2\gamma}{\gamma-1} \left[\left(\frac{P}{P_{T_E}} \right)^{\frac{2}{\gamma}} - \left(\frac{P}{P_{T_E}} \right)^{\frac{\gamma+1}{\gamma}} \right]} \quad (11)$$

The differential element of area dA is

$$dA = \int_{\theta}^{\theta} \bar{z} \, d\theta \quad (12)$$

where:

Z = number of blades

a = blade exit opening (see Fig. 46)

ϵ_{res} = arc restriction coefficient

Since Φ is valid for isentropic flow only, the restriction factor ϵ_{res} must be introduced to correct the actual flow area to an effective area which accounts for the restrictions due to the boundary layers on both sides of the flow channel.

The factor ϵ_{res} can be expressed by³

$$\epsilon_{\text{res}} = 1 - \sum \frac{\xi^*}{a} = \frac{H^{***} - 1}{H^{***} - 1 + \frac{\zeta}{2}} \quad (13)$$

In Eq. 13, ξ^* is the boundary layer displacement thickness and H^{***} is the so-called energy parameter defined as the energy thickness divided by the displacement thickness. The term $\frac{\zeta}{2}$ represents the loss that is assumed to occur from the inlet to the throat of the blade channel, where ζ is the loss coefficient representing all the losses across the row of blades. The profile loss coefficient was used by Eckert⁴ to represent the loss prior to the blade throat. Percentage of the total loss due to profile losses will vary considerably depending on blade geometry, radial position, and the incidence of the flow on the leading edge of the blade. Since secondary flow and tip clearance effects result in losses in the blade channel, half the total loss coefficient provides a better average representation of the losses in the blade channel prior to the throat. The basis for the development of ϵ_{res} and H^{***} as used is given in Appendix A, Sections 3 and 4.

By multiplying and dividing by $\alpha_m \sin$ Eq. 12 is

$$1/\rho = \frac{1}{\rho} - \dots \quad (14)$$

³Yavira, M. H., Problems of Fluid Mechanics in Radial Turbomachines (Rhode-Saint-Genese, Belgium: Von Kármán Institute for Fluid Dynamics, 1965) VKI Course Note 55b, pp. G46-50.

⁴Eckert, *op. cit.*, p. 44.

After integration Eqs. 10 and 11 become, respectively,

$$\frac{\dot{W}\sqrt{T_{T0}}}{P_{T0}}\sqrt{\frac{R}{g}} = a_m Z r_m \int_{x_H}^{x_T} \frac{a}{a_m} \sum \Phi dX \quad (15)$$

and

$$\frac{\dot{W}\sqrt{T_{TE}}}{P_{TE}}\sqrt{\frac{R}{g}} = a_m Z r_m \int_{x_H}^{x_T} \frac{a}{a_m} \sum \Phi dX \quad (16)$$

The flowrate \dot{W} can be computed from the conditions ahead of the stator. Then a reference flowrate is defined by

$$W_{ref} \equiv \left[\frac{\dot{W}\sqrt{T_{T0}}}{P_{T0}}\sqrt{\frac{R}{g}} \right] \quad (17)$$

where W_{ref} is in square inches. Continuity will be satisfied for the stator by

$$\left[a_m Z r_m \int_{x_H}^{x_T} \frac{a}{a_m} \sum \Phi dX \right]_{STATOR} = W_{ref} \quad (18)$$

Similarly for the rotor

$$\left[a_m Z r_m \int_{x_H}^{x_T} \frac{P_{TE}}{P_{T0}} \sqrt{\frac{T_{T0}}{T_{TE}}} \frac{a}{a_m} \sum \Phi dX \right]_{ROTOR} = W_{ref} \quad (19)$$

The influence of the leakage flow through the radial tip clearance has not been accounted for in Eq. 19.

The element of area between the blade tips and the shroud is

$$dA = 2\pi r dr \quad (20)$$

The flow through the tip clearance area is

$$\left[\frac{\dot{W}\sqrt{T_{TE}}}{P_{TE}}\sqrt{\frac{R}{g}} \right]_{TIP\ CLEARANCE} = 2\pi a_m Z r_m^2 \int_{x_T}^{x_S} \frac{X}{Z a_m} \sum \Phi dX \quad (21)$$

Since the tip clearance is relatively small, the values of Φ , \sum , P_{TE} , T_{TE} , and X_2 for the tip will be used in Eq. 21.

With these assumptions Eq. 19 can be expressed by

$$\left[\int_{x_H}^{x_T} \frac{P_{TE}}{P_{T0}} \sqrt{\frac{T_{T0}}{T_{TE}}} \frac{a}{a_m} \sum \Phi dX + 2\pi r_m \int_{x_T}^{x_S} \left(\frac{P_{TE}}{P_{T0}} \sqrt{\frac{T_{T0}}{T_{TE}}} \sum \Phi X \right)_{TIP} \frac{dX}{Z a_m} \right]_{ROTOR} = \frac{W_{ref}}{[a_m Z r_m]_{ROTOR}} \quad (22)$$

The assumptions used to arrive at Eq. 22 are obviously incorrect in two respects. First, the flow represented by Φ_T is not

perpendicular to the tip clearance area. Second, the effective area represented by ξ_T is larger than that which probably occurs because of the relatively large boundary layers that exist on the shroud and blade tips. The exact behavior of the flow in the small region between the shroud and the blade tips is impossible to predict without further tests. However, it is felt that the flowrate through this space as represented in Eq. 22 is too large for the reasons just mentioned. Therefore a more accurate approximation of this flowrate will be obtained if the last term on the left side of Eq. 22 is divided by 2, yielding

$$\left[\int_{X_H}^{X_T} \frac{P_T}{P_0} \sqrt{\frac{T_0}{T_E}} \frac{a}{a_m} \xi_T dX + \pi r_m \left(\frac{P_T}{P_0} \sqrt{\frac{T_0}{T_E}} \xi_T \Phi \right)_{TIP} \frac{dX}{Z a_m} \right]_{ROTOR} = \frac{W_{ref}}{[a_m Z r_m]_{ROTOR}} \quad (23)$$

The tip clearance flow included in Eq. 23 can be obtained by integration,

$$\begin{aligned} \pi r_m \int_{X_T}^{X_S} \left(\frac{P_T}{P_0} \sqrt{\frac{T_0}{T_E}} \xi_T \Phi \right)_{TIP} \frac{dX}{Z a_m} &= \frac{\pi r_m}{Z a_m} \left(\frac{P_T}{P_0} \sqrt{\frac{T_0}{T_E}} \xi_T \Phi \right)_{TIP} [X_S - X_T] \\ &= \frac{\pi r_m}{Z a_m} \left(\frac{P_T}{P_0} \sqrt{\frac{T_0}{T_E}} \xi_T \Phi \right)_{TIP} \frac{k}{r_m} = \frac{\pi k r_T}{a_m Z r_m} \left(\frac{P_T}{P_0} \sqrt{\frac{T_0}{T_E}} \xi_T \Phi \right)_{TIP} \end{aligned} \quad (24)$$

Introducing this expression into Eq. 23 gives

$$\left[\int_{X_H}^{X_T} \frac{P_T}{P_0} \sqrt{\frac{T_0}{T_E}} \frac{a}{a_m} \xi_T \Phi dX + \frac{\pi k r_T}{a_m Z r_m} \left(\frac{P_T}{P_0} \sqrt{\frac{T_0}{T_E}} \xi_T \Phi \right)_{TIP} \right]_{ROTOR} = \frac{W_{ref}}{[a_m Z r_m]_{ROTOR}} \quad (25)$$

3. Technique for Obtaining Solution

With the equations of motion and continuity in the forms given by Eqs. 8, 9, 18 and 25, a method has been developed to analyze single stage axial turbines, in particular, those available for test in the Turbine Test Rig of the Turbo-Propulsion Laboratory of the Naval Postgraduate School. The method of analysis predicts turbine performance for specified values of inlet total pressure, inlet total temperature, rotor speed and the ratio of total inlet to static discharge pressure P_t/P_2 . This method is similar to that described by Eckert.⁵ However, Eckert's analysis neglected some effects which

⁵Ibid, Section 3.

have been accounted for in this development. Some significant changes made in this method are listed below:

1. Stator and rotor outlet angles for a particular radial location are computed using a calculated Mach number for that location rather than an assumed Mach number or the Mach number of the mean streamline.
2. Variation of loss coefficients due to changes in blade geometry in the radial direction is accounted for.
3. The influence of rotor tip clearance on the rotor outlet angles and loss coefficients is concentrated near the tip of the blade rather than averaging these effects over the full blade height.
4. Fourth order polynomials are used to better approximate the curves representing blade characteristics as a function of radius and the curves of rotor loss coefficients as a function of incidence.
5. Streamline curvature effects have been accounted for in the solution of the equations of motion.

In addition to the assumptions that were mentioned in Section 2 for the development of the particular form of the equation of motion, the conditions ahead of the stator are assumed to be uniform; that is, the total temperature, velocity, and entropy are assumed constant and the flow axial in direction. It is realized that completely uniform conditions are difficult to obtain, but any other assumption would be extremely difficult to develop mathematically.

Direct solution of the equations of motion is not possible since they are nonlinear in the dependent variable Y . Likewise, no direct method is possible to satisfy continuity. Solutions of these equations must therefore be gained by making initial assumptions for the values of the axial velocities which must be improved by successive iterations until the equations are satisfied. To account for streamline curvature and slope, a complete solution of the flow through the stator and rotor must first be made by neglecting the effects of curvature in order to determine streamline locations. Then the iteration to account for these effects may progress. These requirements make the use of a high-speed computer a necessity.

This analysis has been programmed for the IBM 360 computer using FORTRAN IV. The program is described in Appendix C. The following paragraphs set forth the procedural steps of the program. The equations are listed in general form without referring to specific streamline locations. In the interest of clarity, however, some relationships will be written in forms similar to those used in the program. For example, $P_1(z)/P_{t0} = [T_{1is}(z)/T_{t0}]^{\frac{\gamma}{\gamma-1}}$ will represent the isentropic relationship for the number 2 streamline.

Five streamlines are utilized for the analysis with the number 1 streamline located at the hub and the number 5 streamline located at the tip as shown in Fig. 2. The number 3 streamline will be used as the mean streamline, and the radius of this streamline will be referred to as the mean radius. The radial locations of the streamlines ahead of the stator will be such that the mass flowrate between adjacent streamlines is 25 per cent of the total flowrate. Positions for the streamlines after the stator and after the rotor are initially assumed. The locations of streamlines 2, 3, and 4 then vary during the solution as necessary so that the percentage of the total flowrate between adjacent streamlines does not change. This continuity requirement will be called streamline continuity.

Besides the radii, sufficient input information must be used to effectively reflect the physical characteristics of the stator and rotor blading. Some of the physical properties are introduced directly; such as, the number of stator blades, the number of rotor blades, and the rotor tip clearance. The other quantities used which reflect blade characteristics are throat opening dimensions for the blade channels, discharge angles, rotor blade inlet angles, loss coefficients, and stalling incidences for the rotor.

Throat opening dimension "a" is a function of radius. The best method for introducing this characteristic into the analysis is to enter the measured values of "a" together with the corresponding radii. Then, utilizing the method of least squares, a fourth order polynomial curve is fitted through these points. From the resulting polynomial, the value of "a" for any radius required by streamline continuity can be determined.

Discharge angles are predicted by using a combination of the methods of Vavra and Ainley.⁶ Outlet angles are first calculated using the formula which Vavra established from the experimental data of Beer.⁷ These angles are then corrected for tip clearance, blade curvature, and Mach number effects with the methods given by Ainley. Stator and rotor discharge angles are predicted at three radii; namely, the hub, mean radius, and tip. The method used for calculating these angles is explained in Appendix B, Section 1.

Values of stator gas outlet angles α_1 for the mean streamline are determined for Mach numbers M_1 of 0.5, 0.7, 0.75, 0.8, and 1.0. These values are represented by two parabolic curves of the form

$$\alpha_1 = a + b M_1 + c M_1^2 \quad (26)$$

The first curve is used for Mach numbers M_1 from 0.5 to 0.75 and the second established interim values of α_1 for M_1 between 0.75 and 1.0. From these curves the flow angle α_1 for the mean streamline can be found for any Mach number M .

The flow angle α_1 is also a function of radius r_1 . Therefore the changes of α_1 for the hub and tip with reference to the mean radius, called $\Delta\alpha_H$ and $\Delta\alpha_T$ respectively, must be used. The flow angle α_1 can then be determined for any r_1 by assuming a linear variation of α_1 between the hub and the mean radius and between the mean and the tip. With this assumption and using the Mach number M_1 in Eq. 26 corresponding to the number 2 streamline, the flow angle α_1 for this streamline would be

$$\alpha_1(r) = \alpha_1^{**} + \frac{r_1(r) - r_1^{**}}{r_1(l) - r_1^{**}} \Delta\alpha_H \quad (27)$$

⁶Ainley, D. G. and Mathieson, G. C. R., A Method of Performance Estimation for Axial-Flow Turbines. Aeronautical Research Council, R & M No. 2974, 1957. pp. 3-4.

⁷Beer, R., Aerodynamic Design and Estimated Performance of a Two-Stage Curtis Turbine for the Liquid Oxygen Turbopump of the M-1 Engine. NASA CR 54764 (AGC 8800-12), Nov. 19, 1965. p. 29.

The superscript ** is used with r_1 and α_1 in Eq. 27 to indicate the radius initially assumed for the mean streamline and the computed for that radius. Equation 27 can then be used throughout the analysis even though the radial location of the mean streamline may change due to streamline continuity requirements. A similar approach is used to establish the flow angle β_2 at the rotor discharge.

The rotor blade inlet angles β_0 are measured from the manufacturing drawings of the blade profiles. Using the values of β_0 for the hub, mean, and tip streamlines, a parabolic curve is determined which gives β_0 as a function of X_1 .

Loss coefficients and stalling incidences are predicted by using the methods of Ainley.⁸ For the present method, the stalling incidence i_s is defined as that at which the loss coefficient is twice the value of the minimum loss coefficient. Following Ainley's methods, loss coefficients are computed as a function of the ratio of flow incidence to stalling incidence $\frac{i}{i_s}$. Loss coefficients are also a function of blade geometry or radius. Since the stator has zero incidence, its loss coefficient is a function of the radius only.

Stator and rotor loss coefficients and rotor stalling incidences are calculated for the hub, mean, and tip radial locations. Rotor loss coefficients ζ are determined for values of $\frac{i}{i_s}$ ranging from -2.0 to 1.6. Curves of ζ_R vs. $\frac{i}{i_s}$ are drawn for each of the three radial locations, and values of ζ_R , along with the corresponding quantities $\frac{i}{i_s}$, are used to determine fourth order polynomials which approximate these curves. A similar procedure is followed to obtain a fourth order polynomial representing stalling incidence i_s as a function of radius r_1 . Sample calculations for the prediction of stator and rotor loss coefficients and stalling incidences are contained in Appendix B, Section 2.

⁸ Ainley, op. cit., pp. 4-5.

Variation of loss coefficients with radial location is accounted for by assuming a linear variation of these quantities between the hub and the mean radius and between the mean and the tip. To demonstrate the procedure followed in computing rotor loss coefficients, the following example is given. For a particular incidence, the first step in the determination of ψ_R for the number 2 streamline would be to calculate i_s by using the radius r_1 of that streamline and the polynomial of the form $i_s = i_s(r_1)$. Loss coefficients for the hub and mean radius would then be computed using the resulting $\frac{i}{s}$ in the polynomials, for these radii, of the form $\psi_R = \psi_R(\frac{i}{s})$. With the assumed linear variation $\psi_R(z)$ would be

$$\psi_R(z) = \psi_R(1) + \left[\frac{r_1(z) - r_1(1)}{r_1^{**} - r_1(1)} \right] \left[\psi_R^{**} - \psi_R(1) \right] \quad (28)$$

The reason for using the superscript ** on the mean streamline values is the same as previously mentioned in connection with Eq. 27.

For the first approximation, the Mach number M_0 ahead of the stator is assumed, and the static properties and flowrate at station 0 are found by

$$T_0 = \frac{T_{T_0}}{1 + \frac{\gamma-1}{2} M_0^2} \quad (29)$$

$$V_0 = \sqrt{\gamma g R T_0} M_0 \quad (30)$$

$$P_0 = \frac{P_{T_0}}{\left(1 + \frac{\gamma-1}{2} M_0^2\right)^{\gamma/(\gamma-1)}} \quad (31)$$

$$\rho_0 = \frac{P_0}{R T_0} \quad (32)$$

$$A_0 = \pi (r_T^2 - r_H^2) \quad (33)$$

$$\dot{W} = \rho_0 A_0 V_0 \quad (34)$$

$$\dot{\Phi} A = \frac{\dot{W}}{P_{T_0}} \sqrt{\frac{R T_{T_0}}{g}} = W r c f \quad (35)$$

The reference flowrate W_{ref} will be used to check continuity at stations 1 and 2.

The next step is to determine axial velocities after the stator that satisfy the equation of motion. Total enthalpy after the stator is constant by assumption, and streamline curvature effects are neglected at this stage of the analysis. With these conditions, Eq. 8 simplifies to

$$\frac{d(\ln Y_1^2)}{dX_1} = 2 \tan \alpha_1 \frac{d\alpha_1}{dX_1} - \frac{2}{X_1} \sin^2 \alpha_1 + \left(1 - \frac{C_1 H \cos^2 \alpha_1}{Y_1^2 V_{A1m}^2} \right) \frac{ds_1^*}{dX_1} = I \quad (36)$$

This equation can be integrated to give

$$\ln Y_1^2 = \int_{X_0}^X I dX + \ln C^2 \quad (37)$$

where X_0 is arbitrary and $\ln C^2$ is the constant of integration. Using the boundary condition $Y = 1.0$ at $X = 1.0$, $\ln C^2$ can be found by

$$0 = \int_{X_0}^1 I dX + \ln C^2 \quad \text{or} \quad \ln C^2 = - \int_{X_0}^1 I dX$$

then

$$\ln Y_1^2 = \int_{X_0}^X I dX - \int_{X_0}^1 I dX = \int_1^X I dX \quad (38)$$

Equation 38 must be expressed in a form that can be utilized in the computer. Expansion by infinite series yields

$$Y = e^{\frac{1}{2} \int_1^X I dX} = 1 + n + \frac{n^2}{2} + \frac{n^3}{6} + \frac{n^4}{24} + \frac{n^5}{120} + \dots; \quad n = \frac{1}{2} \int_1^X I dX \quad (39)$$

The quantities contained in I , Eq. 36, must be evaluated before proceeding with the solution. For the first approximation, assumptions are made for the values of Y_1 , M_1 , and V_A . The flow angles α_1 are then calculated by using Eqs. 26 and ^m27. After the value of α_1 has been determined for each streamline, $\frac{d\alpha_1}{dX_1}$ is computed. This derivative and all others needed in the analysis are found by finite difference methods.

Enthalpy is computed by

$$H = c_p T_e \quad (40)$$

and the entropy term is found by the method of Vavra.⁹

⁹Vavra, M. H., Aero-Thermodynamics and Flow in Turbomachines. New York, London: John Wiley and Sons, Inc., 1960. pp. 445-447.

$$S^* = \ln \left[\frac{1 - \frac{Y_1^2 V_{A1m}^2}{C_1 H \cos^2 \alpha_1}}{1 - \frac{Y_1^2 V_{A1m}^2}{C_1 H \cos^2 \alpha_1 (1 - y_s)}} \right] \quad (41)$$

The stator loss coefficients y_s are determined by equations similar to Eq. 28.

Each time a solution to Eq. 36 is found, the new values of Y_1 are then used for the next iteration. After five iterations, α_1 and $\frac{d\alpha_1}{dX_1}$ are recalculated using the new stator exit Mach numbers. The Mach number for each streamline is found by

$$V_{A1} = Y_1 V_{A1m} \quad (42)$$

$$V_1 = \frac{V_{A1}}{\cos \alpha_1} \quad (42a)$$

$$T_1 = T_{t0} - \frac{V_1^2}{2gJc_p} \quad (43)$$

$$M_1 = \frac{V_1}{\sqrt{\gamma g R T_1}} \quad (44)$$

With the new values for α_1 and $\frac{d\alpha_1}{dX_1}$, five more iterations are made to determine the corrected values of Y_1 .

The quantities represented by Eqs. 42-44 are recomputed after satisfying the equation of motion and additional quantities determined by

$$V_{U1} = V_{A1} \tan \alpha_1 \quad (45)$$

$$T_{1is} = T_{t0} - \frac{T_{t0} - T_1}{1 - y_s} \quad (46)$$

$$P_1 = P_{t0} \left(\frac{T_{1is}}{T_{t0}} \right)^{\gamma/\gamma-1} \quad (47)$$

The flowrate through the stator is computed next and compared with that required to satisfy continuity. Reference flowrate between the hub and each streamline is found from

$$SUM = a_m Z r_m \int_{x_H}^x \frac{a}{a_m} \oint \Phi dX = a_m Z r_m \int_{x_H}^x WI dX \quad (48)$$

where

$$\Phi = \left\{ \frac{2\gamma}{\gamma-1} \left[\left(\frac{P}{P_{t0}} \right)^{2/\gamma} - \left(\frac{P}{P_{t0}} \right)^{\delta+1/\gamma} \right] \right\}^{\frac{1}{2}} \quad (49)$$

The "a" and "a_m" in Eq. 48 are found from the polynomial which represents throat opening as a function of radius.

Before Eq. 48 is solved, the pressure ratio is compared with the critical pressure ratio. If the critical pressure ratio has been exceeded, the flow is choked at that radial location and the critical pressure ratio is used in calculating $\frac{\dot{m}}{W_f}$ and $\frac{dX}{dW_f}$.

The fraction of the total flowrate passing between the hub and each streamline is computed by

$$W_f = \frac{\int_{x_h}^x WI \, dx}{\int_{x_h}^x WI \, dx} \quad (50)$$

Total flowrate, as found by the denominator of Eq. 50 multiplied by $a_m \bar{z} r_m$, is then compared with the reference flowrate. Overall continuity is satisfied if the difference is less than 0.0002.

If required and computed flowrates are not within this tolerance, the axial velocity for the mean streamline is adjusted by

$$V_{m \text{ (NEW)}} = V_{m \text{ (OLD)}} + \frac{\dot{W}_{req} - \dot{W}_{computed}}{0.00065} \quad (51)$$

\dot{W}_{req} is the required reference flowrate divided by $a_m \bar{z} r_m$, and $\dot{W}_{computed}$ is the denominator of Eq. 50.

Solutions to the equation of motion and continuity are successively found until overall continuity is satisfied.

The fractions of the total flowrate determined for each streamline by Eq. 50 are then compared with the corresponding flowrate fractions ahead of the stator. Streamline continuity is satisfied if agreement is within 0.002 for each streamline. If streamline continuity has not been satisfied, the streamlines in error are adjusted by

$$X_{NEW} = X_{OLD} + \left[\frac{\dot{W}_{f \text{ req}} - \dot{W}_{f \text{ computed}}}{\dot{W}_f} \right] \frac{dX}{dW_f} \quad (52)$$

Equation 52 applies only to streamlines 2, 3, and 4 since $W_f = 0$ at the hub and $W_f = 1.0$ at the tip.

If streamline positions have been adjusted, new streamline radii are found by

$$r_{NEW} = X_{NEW} r_{m_OLD} \quad (53)$$

and new values of X for each streamline are obtained by

$$X = \frac{r_{NEW}}{r_{m_NEW}} \quad (54)$$

With the new streamline radii the equation of motion and overall continuity must be satisfied again.

The following values are determined after streamline continuity is satisfied:

$$U_1 = \frac{\pi R F M_1}{(30)(12)} r_1 \quad (55)$$

$$U_2 = \frac{r_2}{r_1} U_1 \quad (56)$$

$$W_{u1} = V_{u1} - U_1 \quad (57)$$

$$\beta_1 = \text{TAN}^{-1} \left(\frac{W_{u1}}{V_{A1}} \right) \quad (58)$$

$$W_1 = \frac{V_{A1}}{\cos \beta_1} \quad (59)$$

$$T_{tE} = T_1 + \frac{W_1^2}{2gJc_p} + \frac{U_2^2 - U_1^2}{2gJc_p} \quad (60)$$

$$H_E = T_{tE} c_p \quad (61)$$

$$P_{tE} = P_1 \left(\frac{T_{tE}}{T_1} \right)^{\gamma/\gamma-1} \quad (62)$$

Rotor blade inlet angles are determined for each streamline by means of the parabola which establishes β_o as a function of X_1 . Incidence is found by

$$i = \beta_1 - \beta_o \quad (63)$$

Stalling incidences and rotor loss coefficients are then determined using the procedure described in connection with Eq. 28. If the incidence ratio $\frac{i}{i_s}$ is less than -2.0 or greater than 1.6, the value for $\frac{i}{i_s}$ is set equal to -2.0 or 1.6, respectively.

One of the quantities necessary for the equation of motion after the rotor is $\frac{ds_2^*}{dX_2}$. This quantity is separated into two parts,

$$\frac{ds_2^*}{dX_2} = \frac{ds_{10}^*}{dX_2} + \frac{ds_{21}^*}{dX_2} \quad (64)$$

$\frac{ds_{10}^*}{dX_2}$ represents the entropy gradient due to changes of entropy across the stator and referred to station 2. The term $\frac{ds_{21}^*}{dX_2}$ represents the entropy gradient due to the different entropy changes through the rotor. The entropy increase through the rotor is computed by using the corresponding values of the rotor in Eq. 41; for example, H_E would be used instead of H.

Neglecting streamline curvature and slope, Eq. 9 can be re-written

$$\begin{aligned} \frac{d(\beta_2 Y_2^2)}{dX_2} = & -i \tan^2 \beta_2 \frac{d\beta_2}{dX_2} \sin^2 \beta_2 - \frac{4 U_m \cos \beta_2 \sin \beta_2}{Y_2 W_{A2m}} \\ & - \frac{2 U_m U_2 \cos^2 \beta_2}{Y_2^2 W_{A2m}^2} + \frac{C_1 \cos^2 \beta_2}{Y_2^2 W_{A2m}^2} \frac{dH_E}{dX_2} + \left(1 - \frac{C_1 H_E \cos^2 \beta_2}{Y_2^2 W_{A2m}^2}\right) \frac{ds_2^*}{dX_2} \end{aligned} \quad (65)$$

The discharge angle β_2 and its derivative $\frac{d\beta_2}{dX_2}$ are found in the same manner as previously described for the stator discharge angles. The method for solving Eq. 65 is similar to that used for Eq. 36 with the exception that iterations are carried out until corresponding values of Y change by less than 0.005, or until 13 iterations have been completed. The extra iterations are necessary because there may be a slower convergence of the values of Y at station 2. After satisfying the equation of motion, values at station 2 corresponding to those represented by Eqs. 42-47, are computed. It should be noted that where absolute velocity terms are used in Eqs. 42-47, the corresponding equations for the rotor will employ relative velocities. Therefore M_2 is the Mach number of the flow relative to the rotating rotor blade.

Overall continuity is checked at the rotor discharge using the same procedure utilized for the stator; however, the reference flowrate is increased according to Eq. 25 to account for the flowrate between the blade tips and the surrounding shroud.

After overall continuity has been satisfied at station 2, streamline continuity is checked. In addition to the functions performed for the check after the stator, there are certain quantities that must be adjusted for streamline relocation. These are

$$\left(\frac{dH_E}{dX_2}\right)_{NEW} = \left(\frac{dH_E}{dX_2}\right)_{OLD} + \frac{d^2 H_E}{dX_2^2} (X_{NEW} - X_{OLD}) \quad (66)$$

$$H_{L_{NEW}} = H_{L_{OLD}} + \frac{dH_E}{dX_2} (X_{NEW} - X_{OLD}) \quad (67)$$

$$\left(\frac{dS_{10}^*}{dX_2}\right)_{NEW} = \left(\frac{dS_{10}^*}{dX_2}\right)_{OLD} + \frac{d^2 S_{10}^*}{dX_2^2} (X_{NEW} - X_{OLD}) \quad (68)$$

$$U_{2_{NEW}} = (U_{2_{OLD}}) \frac{X_{NEW}}{X_{2,OLD}} \quad (69)$$

A solution exists when the equations of motion, and overall and streamline continuity have been satisfied; however, this solution has neglected streamline curvature and streamline slope. To obtain a solution which accounts for streamline curvature effects, the terms in Eqs. 8 and 9 that contain δr or ΔR must be included when solving the equations of motion.

The streamline displacements δr and ΔR , shown in Fig. 2, are computed for each streamline by

$$\delta r = r_1 - \frac{r_0 + r_2}{2} \quad (70)$$

and

$$\Delta R = r_0 - r_2 \quad (71)$$

Equation 70 is based on the assumption that the radii of any streamline at stations 0 and 2 are not greatly different. Therefore the cosine of the angle between the line connecting these points and the axis of the machine is approximately equal to unity. The length L, also shown in Fig. 2, is taken to be half the distance from 0.1 inch ahead of the stator to 0.1 inch after the rotor.

After a solution is obtained which accounts for streamline curvature effects, the resultant pressure ratio $\frac{P_{t_o}}{P_2}$ is compared with the $\frac{P_{t_o}}{P_2}$ specified initially. Ideally $\frac{P_{t_o}}{P_2}$ for each streamline will be the same. However, computer solutions for this quantity may vary slightly from streamline to streamline. Therefore a mass-flow-weighted value of $\frac{P_{t_o}}{P_2}$, called $\left(\frac{P_{t_o}}{P_2}\right)_w$, is found by

$$\left(\frac{P_{t_o}}{P_2}\right)_w = \sum_{i=1}^4 \left(\frac{P_{t_o}}{P_2}_{(i+1)} + \frac{P_{t_o}}{P_2}_i \right) \left(\frac{W_{f_{(i+1)}} - W_{f_i}}{2} \right) \quad (72)$$

If the specified $\frac{P_{t_o}}{P_2}$ and $\left(\frac{P_{t_o}}{P_2}\right)_w$ differ by more than 0.0003, the Mach number of the flow ahead of the stator is properly adjusted and another solution is found.

After the iterations for $\frac{P_{t_o}}{P_2}$ have been completed, additional quantities are determined for each streamline, using

$$\Delta H = H_1 - H_2 = (U_1 V_{U1} - U_2 V_{U2}) \frac{1}{gJ} \quad (73)$$

$$T_{t_2} = T_{t_o} - \frac{\Delta H}{C_p} \quad (74)$$

$$T_{2_{iS}} = T_{t_o} \left(\frac{P_2}{P_{t_o}} \right)^{\frac{\gamma-1}{\gamma}} \quad (75)$$

Overall efficiency is then computed by

$$\eta = \frac{\Delta H}{\Delta h_{iS}} = \frac{T_{t_o} - T_{t_2}}{T_{t_o} - T_{2_{iS}}} \quad (76)$$

The ideal change in enthalpy Δh_{iS} is the isentropic enthalpy drop from the total inlet pressure P_{t_o} to the static discharge pressure P_2 . Equation 76 is used to compute the efficiency of a

single stage turbine because the kinetic energy leaving the rotor cannot be utilized. The efficiency defined by Eq. 76 will be referred to as total-static efficiency.

Theoretical degree of reaction r^* and head coefficient k_{is} are given by

$$r^* = \frac{T_{1s} - T_{2s}}{T_{t0} - T_{2s}} \quad (77)$$

and

$$k_{is} = \frac{\Delta h_{is}}{U_1^2/2gJ} = \frac{2C_p(T_{t0} - T_{2s})gJ}{U_1^2} \quad (78)$$

For turbine performance curves it is desirable to obtain the mass-flow-weighted values of efficiency $(\eta)_{\dot{w}}$, head coefficient $(k_{is})_{\dot{w}}$, theoretical degree of reaction $(r^*)_{\dot{w}}$, horsepower $(HP)_{\dot{w}}$, and moment $(M_R)_{\dot{w}}$. The last two quantities are found from

$$(HP)_{\dot{w}} = \frac{(\Delta H)_{\dot{w}} J \dot{w}}{550} \quad (79)$$

and

$$(M_R)_{\dot{w}} = \frac{(HP)_{\dot{w}} (550)}{\omega} \quad (80)$$

The mass-flow-weighted ΔH , called $(\Delta H)_{\dot{w}}$, as well as $(\eta)_{\dot{w}}$, $(k_{is})_{\dot{w}}$, and $(r^*)_{\dot{w}}$ are computed using equations similar to Eq. 72.

Referred values are obtained, following NASA practice.

For $\gamma = 1.4$:

$$HP_{ref} = \frac{(HP)_{\dot{w}}}{\sqrt{\theta} \delta} \quad (81)$$

$$M_{Rref} = \frac{(M_R)_{\dot{w}}}{\delta} \quad (82)$$

$$RPM_{ref} = \frac{RPM}{\sqrt{\theta}} \quad (83)$$

$$\dot{W}_{ref} = \frac{\dot{w} \sqrt{\theta}}{\delta} \quad (84)$$

$$V_{ref} = \frac{V}{\sqrt{\theta}} \quad (84a)$$

where:

$$\theta = \frac{T_{t0}}{T_{STD.}} = \frac{T_{t0}}{518.4} \quad (85)$$

$$\delta = \frac{P_{t0}}{P_{STD.}} = \frac{P_{t0}}{14.7} \quad (86)$$

4. MOD I and MOD II Turbines

The method of analysis as presented was used to determine performance curves for the so-called MOD I and MOD II turbines. Both turbines are single stage axial-flow machines. Experimental tests were conducted on the MOD II turbine by Commons and Messegee and are described in Refs. 4 and 6. The test results are plotted with appropriate predicted performance curves.

The so-called MOD I turbine was designed for free-vortex flow and has highly twisted blades. Outer diameter of this turbine is 9.898 inches. The hub diameters of the stator inlet and rotor discharge are 6.930 and 5.970 inches, respectively. The stator contains 13 blades and the rotor 22 blades. Blades of the MOD I turbine are generally thin. The stator and rotor profiles used to predict outlet angles and loss coefficients are shown in Fig. 4.

The MOD II turbine is approximately the same size as the MOD I, but its blading is considerably different. The blades of the MOD II turbine are thick with blunt leading edges and constant profiles over the blade height. Outer diameters of the MOD II turbine stator and rotor are 9.701 and 9.836 inches, respectively. The stator has a hub diameter of 6.796 inches, and the hub diameter of the rotor is 6.598 inches. There are 19 stator blades and 18 rotor blades. Stator and rotor blade profiles for the MOD II turbine are shown in Fig. 5.

Throughout the remainder of this thesis the MOD I and MOD II turbines will be referred to simply as MOD I and MOD II.

The minimum throat opening "a" of the blade channels is a very critical dimension. Slight variations of this quantity have a considerable effect on turbine performance. Since this quantity is so sensitive, values of "a" measured from the actual hardware were used for the analysis rather than those obtained from the manufacturing

drawings. Then errors due to manufacturing will not be a factor in comparison of predicted and experimental results. Figure 6 shows the throat openings "a" as a function of radius for the stator and rotor blading of both turbines.

Predicted stator outlet angle α_1 as a function of radius r_1 for the MOD I is plotted in Fig. 7. The assumed linear variation of α_1 between the hub and the mean radius and between the mean and the tip is readily apparent in this figure. Figure 8 shows the predicted variations of α_1 with Mach number M_1 for the MOD I. Figures 9 and 10 are the corresponding plots for the MOD II.

Relative discharge angles β_2 were computed for two radial tip clearances k for each turbine; namely, 0.020 and 0.033 inches for the MOD I, and 0.015 and 0.033 inches for the MOD II. The predicted flow angles β_2 are plotted in the same manner as previously described for the flow angles α_1 . Figures 11 and 12 show β_2 as a function of radius r_2 and as a function of Mach number M_2 , respectively, for the MOD I, where M_2 refers to the Mach number of the flow relative to the rotor. Figures 13 and 14 show the corresponding plots for the MOD II. The predicted effect of radial tip clearance on the discharge angles β_2 can be seen in Figs. 11 - 14.

Stator loss coefficients ζ_s were computed for the radial locations corresponding to the hub, mean radius, and tip. Figure 15 shows ζ_s as a function of radius r_1 for both the MOD I and MOD II. The straight lines in this figure between the values of ζ_s at the hub and mean radius, and between the mean and the tip, reflect the assumed linear variation of ζ_s in these regions.

Variation of rotor blade inlet angle β_c with radius r_1 is plotted for both turbines in Fig. 16. The difference between the untwisted and the free-vortex blades is easily noted in this plot. Also shown in this figure are curves representing the variation of stalling incidence i_s with r_1 . The change of the MOD I rotor blade profiles with radius is reflected by a considerable variation of i_s whereas just the opposite is true for the MOD II.

Curves for the MOD I showing predicted rotor loss coefficients ζ_R as a function of incidence ratio $\frac{i}{t_s}$ for the hub, mean radius, and tip are shown in Fig. 17. Since the loss coefficients between the mean radius and the tip are dependent on tip clearance, there are two curves for the tip. One curve holds for the tip clearance of 0.020 inches; the other is for the larger tip clearance of 0.033 inches. For negative incidence ratios between -0.5 and -2.0 the curves for the tip are estimations. This was necessary because the computations by the method shown in Appendix B, Section 2, gave unrealistically low values of ζ_R as the flow inlet angle β_1 approached -90° . The situation is more easily understood when it is noted that the blade inlet angle is -33.7° and the stalling incidence is 37° at the rotor blade tip. Figure 17 shows that the loss coefficients for the hub ($r_1=3.300$ in.) are relatively large. The loss coefficients at the hub are larger for most incidence ratios than those at the tip for a tip clearance of 0.020 inches. The larger value of at the hub reflects the higher losses that are associated with an impulse type blade. It can be seen in Fig. 4 that the blade shape varies from a reaction type profile at the tip to an impulse type profile at the hub.

Loss coefficients for the MOD II rotor are plotted in Fig. 18 for tip clearances of 0.015 and 0.033 inches. The predicted similarity of the curves for the hub and mean radius is to be expected since the blading differs only in solidity. Although the blade profile is the same at all radii, the losses due to tip clearance result in larger loss coefficients for the tip profile.

For convenience, the blade properties used for calculating the MOD II rotor loss coefficients were those at the hub, mean and tip radii of the rotor discharge. Since the annulus area at the rotor discharge is larger than the annulus area at the stator discharge and since the flow incidence is a significant parameter for the rotor loss coefficients, it would have been more appropriate to use the blade characteristics at the hub, mean, and tip radii of the rotor inlet. However, the error is insignificant because the blade profile does not change along the radius.

It may be noted from Fig. 4 that the minimum radius, for which a blade profile is given, is 3.597 inches whereas the radius at the hub of the MOD I stator exit is 3.300 inches. The outlet angle and loss coefficient for the hub were found by extrapolation, using the values computed for the radii of 4.125 and 3.597 inches and assuming a linear variation of these quantities with radius. The relative outlet angle for the hub of the MOD I rotor was found in a similar manner.

Performance curves for the two turbines were determined for the rotor tip clearances mentioned earlier. The total inlet to static discharge pressure ratios investigated were 1.30, 1.40, 1.50, and 1.60, with the exception that pressure ratios of 1.31 and 1.51 were used for the MOD II with 0.033 inch rotor tip clearance. These pressure ratios agree more closely with those experimentally investigated by Commons and Messegue.

The axial distances L used for the determination of the curvatures depend on the axial clearance between the stator and rotor as well as on the blade geometries. Axial clearances of 0.4 and 1.0 inches were used for the analyses of the MOD I and MOD II, respectively.

Curves representing the performance of the MOD I are plotted in Figs. 19 through 26. Performance values plotted are mass-flow-weighted values unless stated otherwise. Figure 19 shows referred flowrate as a function of referred RPM. The increase in flowrate due to an increase in rotor tip clearance can be seen in this figure. Although the flowrate is greater for the larger tip clearance, the torque developed is greater at the smaller tip clearance. The decrease in torque for the larger tip clearance results from the increased losses and decrease in turning angle of the flow through the rotor near the tip. The predicted effect of tip clearance on torque is shown in Fig. 20 where referred moment is plotted versus referred RPM.

The variation of total-static efficiency with referred RPM for the two tip clearances can be seen in Figs. 21 and 22. The referred RPM at which maximum efficiency occurs increases when the total inlet to static discharge pressure ratio is increased. Blade losses

and the kinetic energy of the flow leaving the rotor affect the total-static efficiency. As pressure ratio is increased the absolute velocity leaving the stator and the relative velocity leaving the rotor increase. Therefore the peripheral speed of the rotor must increase to obtain conditions where the absolute velocity leaving the rotor is in an axial direction and where the relative flow ahead of the rotor has zero incidence. The RPM where the flow has zero incidence on the rotor will not necessarily be that at which the absolute velocity leaving the rotor is axial. At any RPM, flow incidence and absolute discharge angles vary from streamline to streamline, and the above statements refer to mass-flow-weighted values.

It may be noted in Figs. 21 and 22 that the peak total-static efficiency decreases somewhat as the pressure ratio increases. At higher pressure ratios the ratio of kinetic energy leaving the rotor to the work done on the rotor increases. Since the kinetic energy leaving the rotor is lost energy for a single stage turbine, the total-static efficiency declines. The effects of pressure ratio and tip clearance on efficiency can be seen in Fig. 23 where total-static efficiency is plotted as a function of the isentropic head coefficient.

The variation of referred power with referred RPM can be seen in Fig. 24. Peak power does not occur at the same referred RPM at which peak efficiency occurs. The peak referred power occurs at the referred RPM where the product of total-static efficiency and referred flowrate is greatest.

Theoretical degree of reaction is plotted as a function of isentropic head coefficient in Fig. 25. It may be noted that the theoretical degree of reaction increases with increasing pressure ratio and decreases with increasing tip clearance for any given isentropic head coefficient. The predicted effects are considerably different from the results of the radial turbine tests conducted by Riley.¹⁰ Riley found that theoretical degree of reaction was independent of pressure ratio and axial clearance for radial turbines.

¹⁰Riley, M. W., The Effect of Axial Clearance on the Performance of a Dual Discharge Radial Turbine (USNPG Thesis, December 1966), p. 70.

Performance values for each streamline are obtained from the computer solution. However, plots utilizing values for each streamline would be difficult to analyze. The deviation of the hub and tip values from that of the mass-flow-weighted average may be seen in Fig. 26. In this figure, hub, tip, and mass-flow-weighted values of theoretical degree of reaction are plotted as functions of referred RPM for a total inlet to static discharge pressure ratio of 1.40.

Performance curves for the MOD II corresponding to those presented for the MOD I are plotted in Figs. 27 through 39. Additional plots have been used for the MOD II because of the inclusion of experimental results. An axial clearance of 1.0 inches was used for the theoretical prediction. Therefore, only experimental data for that axial clearance are shown.

Comments made concerning the performance curves of the MOD I are applicable to the MOD II performance curves also. Differences in the performance of the two turbines will be discussed later.

Plots of the variation of referred flowrate with referred RPM are shown in Figs. 27 and 28 for two rotor tip clearances. The quantitative values as well as the curve shapes agree well with the experimental data. The maximum difference between predicted and experimental referred flowrates occurs at a pressure ratio of 1.51 for a tip clearance of 0.033 inches. There are two experimental points for this pressure ratio and tip clearance that differ from the predicted curve by about 2 per cent. The predicted and experimental values for all pressure ratios and tip clearances have an average difference of less than 1 per cent.

Figures 29 and 30 show curves of referred moment versus referred RPM. The trends expressed by the predicted curves are in excellent agreement with the experimental data. Although the quantitative agreement between theoretical and experimental values is very good for three of the curves, the experimental torque is generally lower than the predicted torque. The average difference between predicted and experimental values is about 3 per cent.

Figures 31 through 34 show total-static efficiency as a function of referred RPM. The shapes of the predicted curves generally agree well with the experimental results. However, there is an indication that experimental efficiencies decrease more rapidly at high RPM than is predicted by the theoretical curves. In the high RPM region the upper part of the rotor blade has a large negative flow incidence. In the prediction analysis when the incidence ratio i_5 had a value less than -2.0, the value of -2.0 was used for computing loss coefficients. This limitation may be the reason that the predicted efficiencies in the high RPM range do not decrease as rapidly as the test data indicate.

The quantitative agreement between predicted and experimental efficiencies varies considerably between different pressure ratios and tip clearances. There are two data points at a pressure ratio of 1.31 and tip clearance of 0.033 inches where the experimental efficiencies are over five points below the predicted values. At a pressure ratio of 1.50 and a tip clearance of 0.015 inches the average difference between predicted and experimental efficiencies is 1.5 points. Giving equal weight to all experimental values the average difference between experimental and predicted values is 2.6 points.

The calculations gave a decrease in efficiency by about two points as the tip clearance was increased from 0.015 to 0.033 inches. The decrease in experimental efficiencies for the increased tip clearance varied with the different pressure ratios. However, the average decrease in efficiency is close to the predicted decrease.

Total-static efficiency as a function of isentropic head coefficient k_{is} is shown in Fig. 35 for pressure ratios of 1.40 and 1.60. Figure 38 shows degree of reaction r^* versus k_{is} . No experimental data are plotted in these figures because experimental values of mass-flow-weighted r^* and k_{is} were not available.

Plots of referred power as a function of referred RPM are shown in Figs. 36 and 37. The comments made earlier concerning the referred moment plots apply to these curves also, since the turbine power is proportional to the product of torque and RPM.

Hub, tip, and mass-flow-weighted values of theoretical degree of reaction are plotted in Fig. 39 for a pressure ratio of 1.40. The experimental values for the hub and tip are also plotted in this figure. The trend of the experimental data is in close agreement with the predicted trend; however, the quantitative agreement is poor, especially at the hub. The decrease in degree of reaction, as the tip clearance is increased, is considerably greater than predicted. Both predicted and experimental results indicate that an axial flow turbine differs from a radial turbine inasmuch as the theoretical degree of reaction changes if rotor tip clearance is changed.

Figure 40 shows the absolute flow angles α_1 and α_2 as a function of radius for the stator and rotor outlets, respectively, of the MOD II. Experimental data were obtained for the same operating conditions; namely, $P_{t0}/P_2=1.40$, $k=0.015$ inches, $RPM/\sqrt{r} = 13,394$. The experimental and predicted stator outlet angles have an average difference of less than half a degree over the blade height. Predicted and experimental agreement for the absolute flow angles at the rotor outlet is not as close. If the experimental point near the hub is neglected, the average difference between predicted and experimental values of α_2 is about 3.5 degrees. The experimental flow angles α_2 are larger than the predicted angles over most of the blade height, which explains why the predicted torque was generally larger than the measured torque.

Velocity distributions at the stator and rotor exits of the MOD II are shown in Fig. 41 for the operating conditions listed in the preceding paragraph. The experimentally found stator discharge velocities varied only slightly more from hub to tip than predicted. The average difference between predicted and experimental stator exit velocities was about 1 1/2 per cent.

The experimentally determined absolute rotor exit velocities, which are shown in Fig. 41, are considerably larger than the predicted velocities except at the hub and tip. Although experimental points could be taken only at distances greater than 0.16 inches from the inner diameter of the shroud, the trend of the data points indicates that the experimental velocities are less than predicted at the tip.

Near the hub the experimental velocities were less than predicted. The decrease in experimental velocities near the hub and tip is the result of separated flow in these regions. The reader is referred to ref. 6 for additional information concerning the experimental data and for photographs of the rotor showing indications of separation.

Experimental relative rotor discharge angles β_2 were determined for the known rotor speed from the measured values of absolute rotor outlet angles and velocities, which are plotted in Figs. 40 and 41, respectively. The experimental and predicted values of β_1 are shown in Fig. 42. The magnitudes of the experimental values of β_1 near the hub are larger than predicted. Over approximately the outer three fourths of the rotor blade height the magnitudes of the experimental values of β_1 are less than predicted. At a radius of 4.4 inches, for instance, the experimental value of β_1 is about -57 degrees whereas the predicted value is about -67 degrees. The average difference between experimental and predicted values of β_1 is about 6.5 degrees. The lower values of β_1 predicted near the hub, provide some compensation in the overall performance for the high values of β_1 predicted for the outer part of the blade.

The MOD II was not designed to achieve the highest possible efficiency. The objectives of the design were to investigate the effects of blunt untwisted bladings of constant profile. This type of blading has the following advantages:

1. Blade cooling passages are easily accommodated.
2. A wider operating RPM range is possible for a specified turbine efficiency variation.
3. Constant profile blades can be manufactured more economically than twisted blades, especially if exotic high strength materials are needed for elevated temperatures.

The following discussion concerning comparison of the MOD I and MOD II is based entirely on the predicted performance of these turbines using the methods described in this thesis. The reader should be aware that Ainley's methods for predicting loss coefficients were not developed for use with rotor blades having blunt leading edges.

Therefore the accuracy of the rotor loss coefficients predicted for the MOD II is probably not as good as for the MOD I.

Figure 43 shows the predicted axial velocity ratios as a function of radius ratio at the stator exit and at the rotor exit for the MOD I and the MOD II. The curves are for the conditions that occur at the maximum efficiency of each turbine. The axial velocities of the MOD I are nearly constant over the blade height at the stator exit and at the rotor exit. The blading of this turbine was originally designed for free-vortex flow by assuming uniform axial velocity components from hub to tip. From Fig. 43 it can be seen that this condition is only approximately satisfied since loss variations and curvature influences produce slight variations from the assumed distribution. Axial velocities for the MOD II decrease from the hub to the tip at the stator exit, and increase from the hub to the tip at the rotor exit, since the bladings of this turbine have constant profiles. The variation of axial velocities for the MOD II is more pronounced at the rotor exit than at the stator exit. At the rotor exit $\frac{V_{A_2}}{V_{A_1}} \approx \frac{V_{A_2}}{V_{A_1}}$ varies from 0.735 at the hub to 1.195 at the tip.

The maximum predicted total-static efficiency of the MOD I at a tip clearance of 0.033 inches is about 84 per cent. The MOD II has a maximum predicted efficiency at that tip clearance of about 80 per cent. The difference in predicted peak efficiencies is due to different factors. The stator loss coefficients are higher for the MOD I than for the MOD II, whereas the loss coefficients for the MOD II rotor at zero incidence are somewhat larger than those for the MOD I at zero incidence. An accurate comparison of loss coefficients is more involved for the rotor than for the stator. Because of its twisted blades, the MOD I rotor has nearly zero incidence at all points along the blade height in the vicinity of the optimum efficiency. Only at one radius of the MOD II rotor blade, however, is the incidence zero. The incidence angles at larger radii are negative and at smaller radii they are positive. Therefore part of the blade is always operating at a loss coefficient larger than the minimum. Of probably even greater significance

for the efficiency decrease is the kinetic energy of the gas leaving the turbine. Minimum kinetic energy is lost when the flow is axial in direction. The design of the MOD I is such that at all points along the blade height the absolute velocity at the rotor exit is nearly axial in the vicinity of the optimum efficiency. The MOD II has only a small radial portion of the rotor blade where the discharge angle α_2 is zero. At radii greater than the radius where α_2 is zero, the absolute flow discharge angle is positive and at smaller radii it is negative. Therefore the kinetic energy leaving the rotor of the MOD II is greater than that of the MOD I when both turbines are operating at peak efficiency.

A comparison of the total-static efficiency versus isentropic head coefficient curves for the MOD I (Fig. 23) and MOD II (Fig. 35), shows a larger variation of efficiency with head coefficient for the MOD I. For example, at $k=0.033$ inches and $\frac{P_{t0}}{P_2}=1.60$, the MOD I efficiency decreases about 11.5 points as the head coefficient increases from 3 to 7 whereas the MOD II efficiency decreases only about 7 points for the same change in head coefficient. This difference in efficiency variation results from the effects of blade twist mentioned earlier.

To investigate the influence of the streamline curvatures on the predicted performance of the MOD I and MOD II the presented flow equations were solved for an axial length of the bladings L of 9×10^5 inches. Increasing L to this value has the same effect as neglecting streamline curvature effects as can be seen from Eqs. 124 and 125. Differences between performance values neglecting streamline curvature, and those where curvature effects were accounted for, were less than 0.2 per cent for both turbines.

5. Conclusions and Recommendations

Effects of streamline curvature were found to be insignificant for the MOD I and MOD II. The small effect on predicted turbine performance due to streamline curvature indicates that the exact value assumed for the curvature factor K will not greatly affect predicted performance. The results of this analysis also indicate that Vavra's method of approximating streamline curvature is of sufficient accuracy for methods of analysis where the flow equations are satisfied at stations between blade rows.

It is recommended that the MOD I be tested. Results of that investigation would provide additional information concerning the general applicability and accuracy of the method of analysis proposed in this thesis.

Predicted and experimental flowrates for the MOD II were in close agreement. Since the restriction factor ξ is a significant factor in the predicted flowrates, the experimental results verify the validity of the theory used in the development of ξ .

Experimental results for the MOD II showed that the predicted rotor torque and turbine efficiency were generally 2 to 3 per cent too high. The angles and velocities predicted for the flow at the stator outlet were in excellent agreement with the experimental results. Therefore the high values predicted for rotor torque and turbine efficiency must be tied to the rotor solution. The measured values of outlet angles and velocities for the rotor discharge also indicate that the predicted rotor solution is not completely correct.

Exactly what parameters are in error in the predicted rotor solution, and to what extent, cannot be stated without more experimental data. More traverses should be taken at the stator and rotor outlets using recently calibrated probes. With this information, loss coefficients and relative discharge angles for the rotor could be determined on a streamline basis. Based on the experimental results included in this thesis, it is suspected that the magnitudes of the predicted discharge angles β_2 are too large. If the predicted turning angles of the flow through the rotor were less, the predicted torque and efficiency would decrease. Also, the separated flow at the hub and tip at the discharge of the MOD II rotor indicates that predicted loss coefficients should be higher for the streamlines at these locations.

To accurately predict turbine performance at off-design as well as design conditions, a streamline analysis is necessary. The experimental verification obtained for the proposed method indicates that the method possesses much potential and that additional development

is warranted. For future development work on this type of analysis it is recommended that the following changes be considered:

1. Use seven streamlines instead of five.
2. Calculate discharge angles using the methods of this thesis but neglecting blade curvature effects. That would decrease the angles by 2 to 3 degrees and be in closer agreement with experimental results.
3. Introduce a multiplying factor for the rotor loss coefficients which would more accurately account for the separated flow at the hub and tip but would not greatly change the average rotor loss coefficient. For example, rotor loss coefficients would first be calculated using the methods of this thesis, and then the loss coefficients for streamlines 1, 2, 6, and 7 would be multiplied by, say, 1.4 and those for streamlines 3, 4, and 5 would be multiplied by 0.6 or 0.7.
4. Calculate rotor loss coefficients for an range of -3.0 to 2.0 instead of -2.0 to 1.6. The increased range would improve performance prediction for turbines with untwisted rotor blades at off-design conditions.

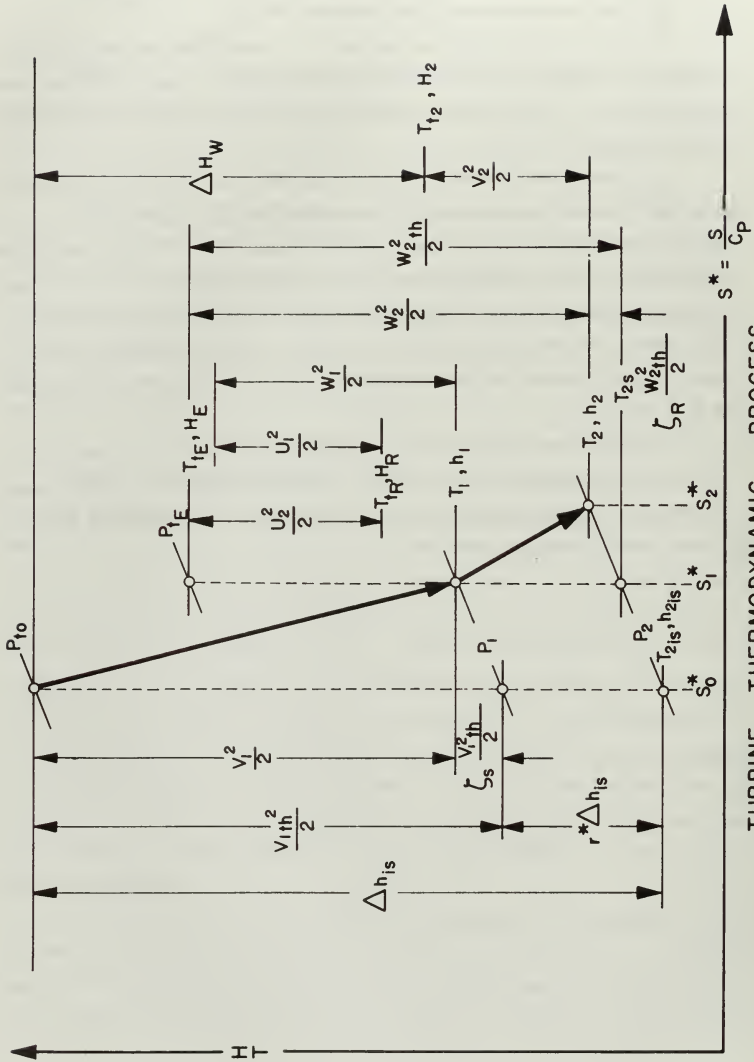
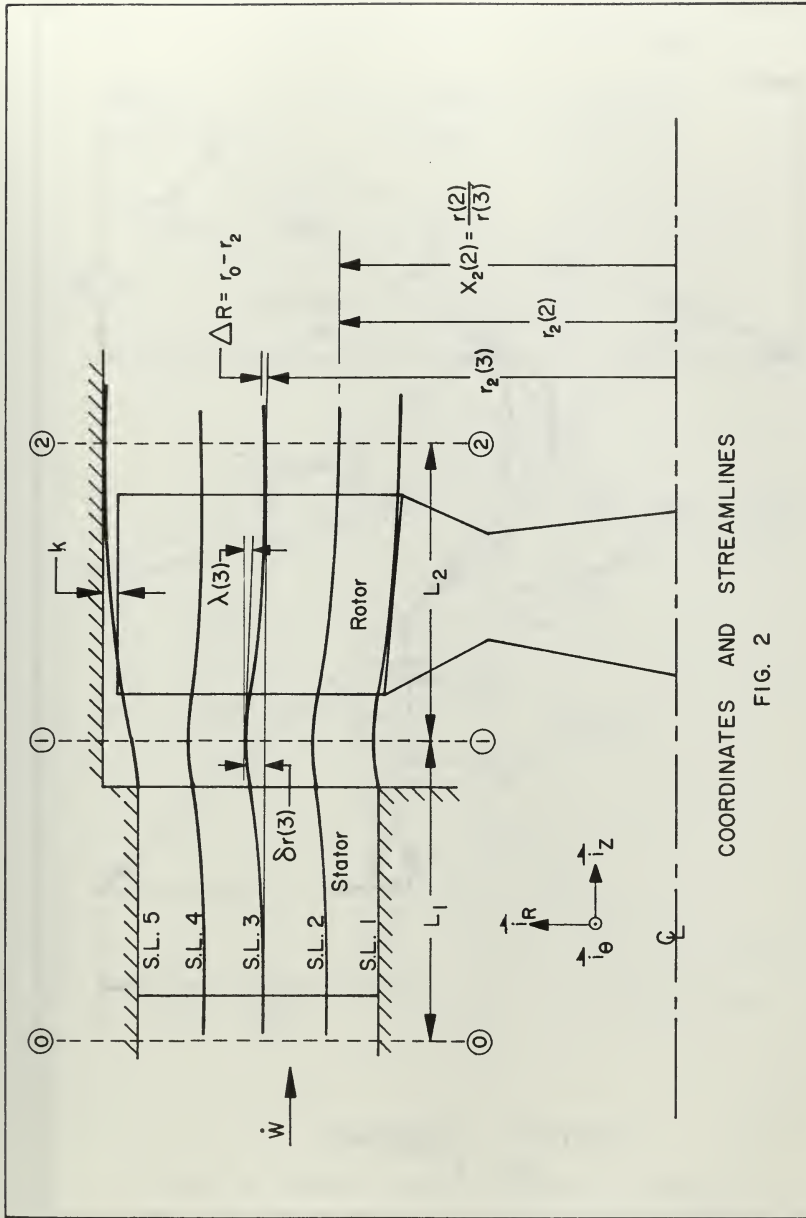
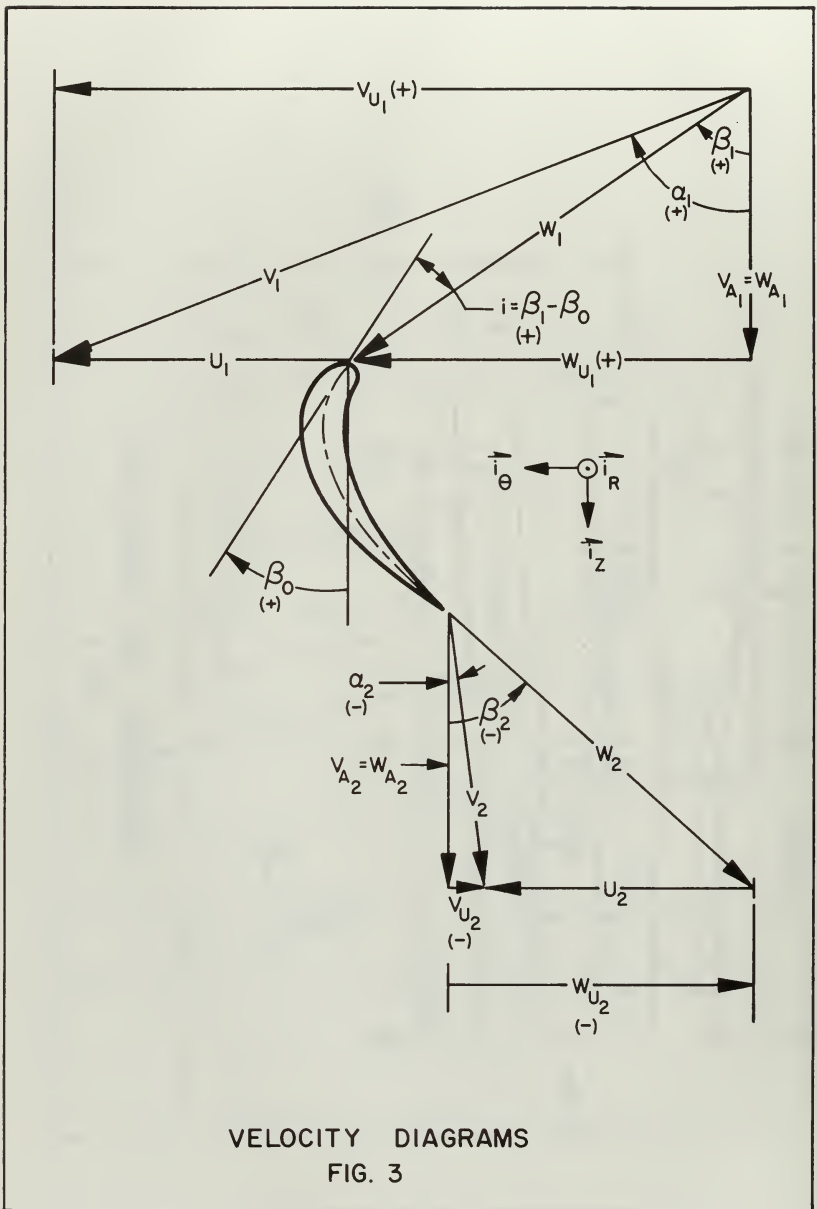


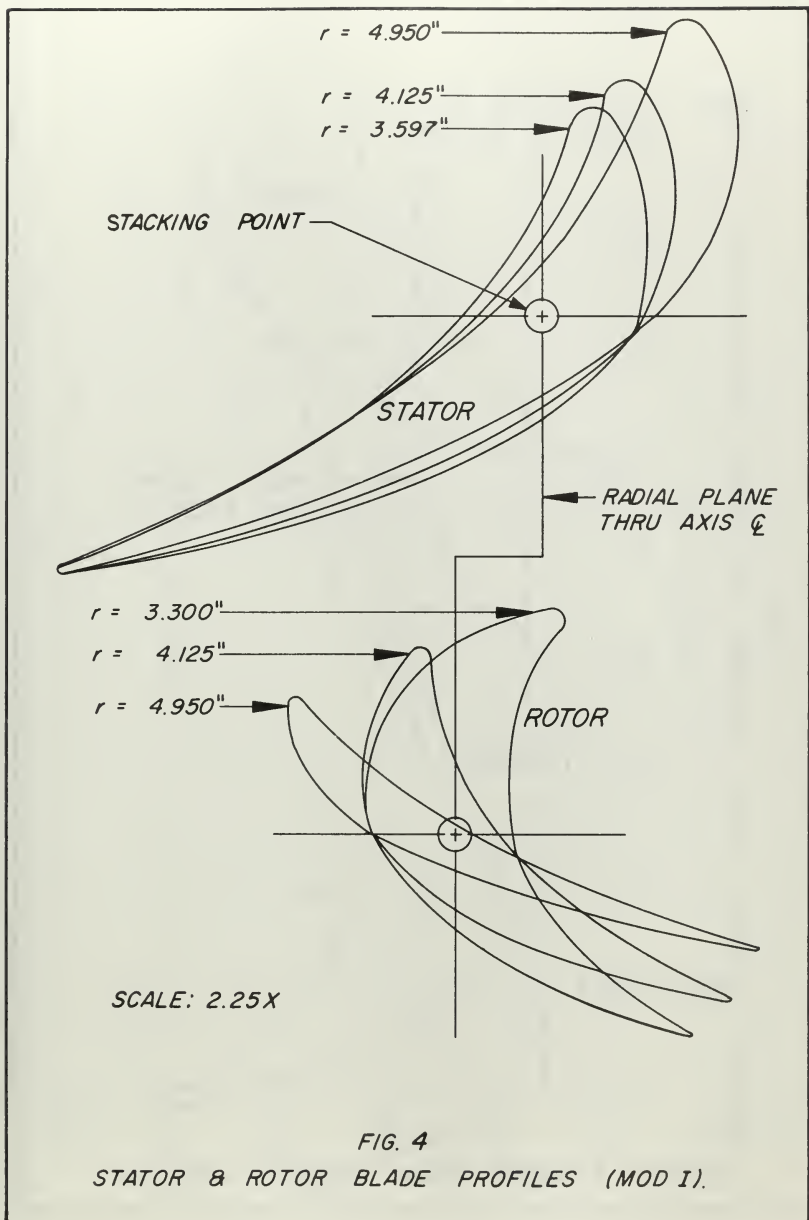
FIG. 1

TURBINE THERMODYNAMIC PROCESS



COORDINATES AND STREAMLINES
FIG. 2





NOTE: BLADES ARE OF
CONSTANT SECTION.

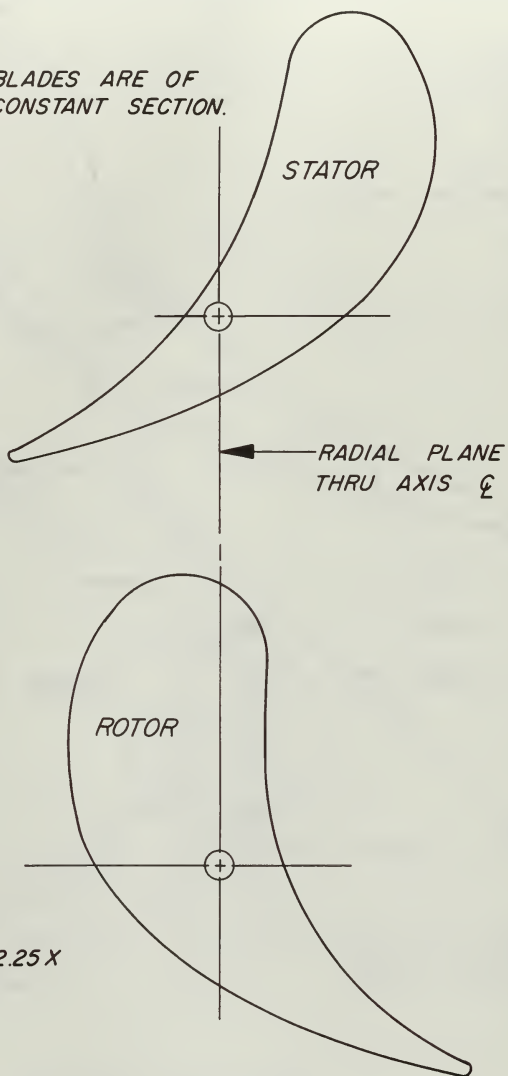
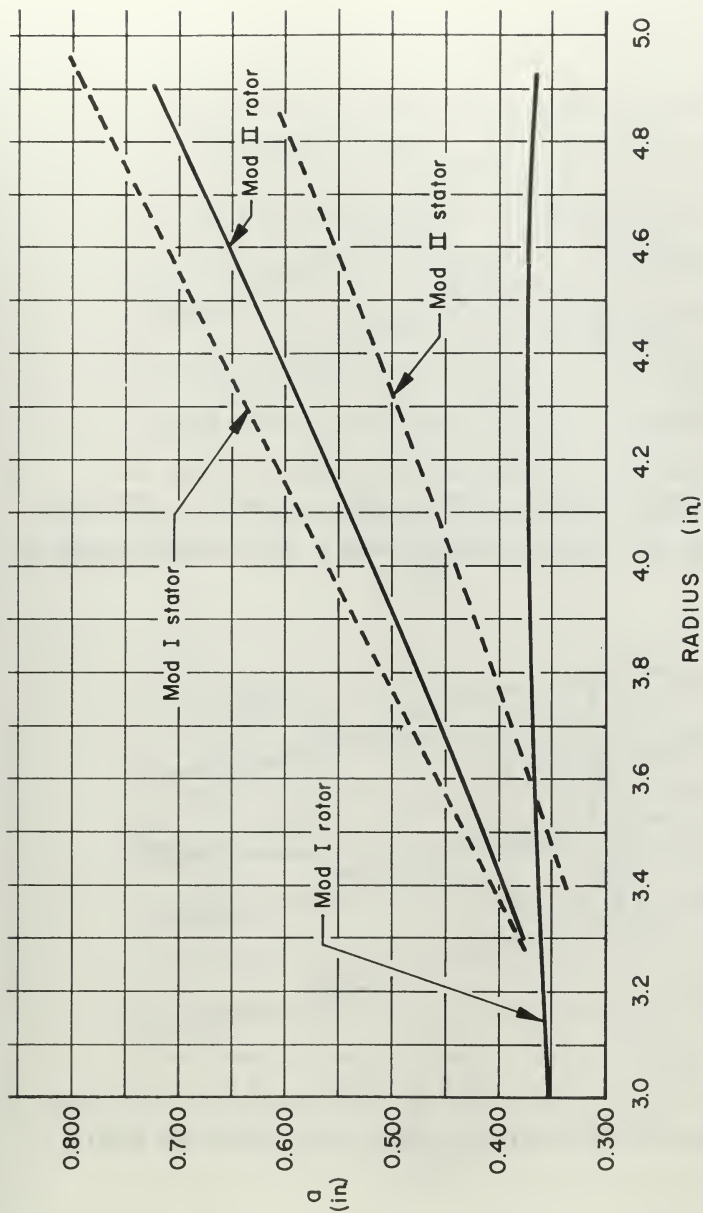
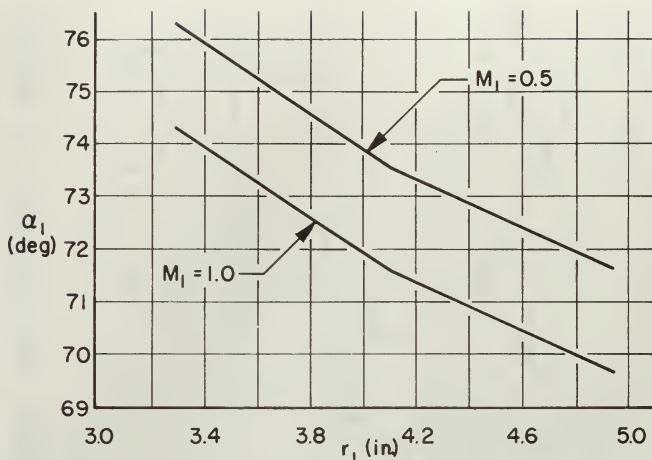


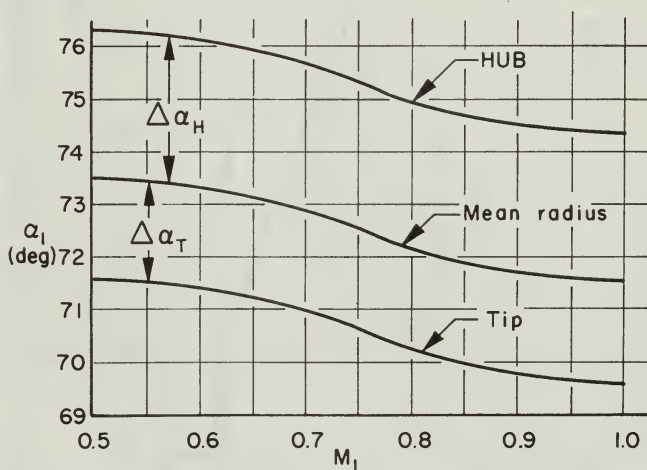
FIG. 5
STATOR & ROTOR BLADE PROFILES (MOD II).



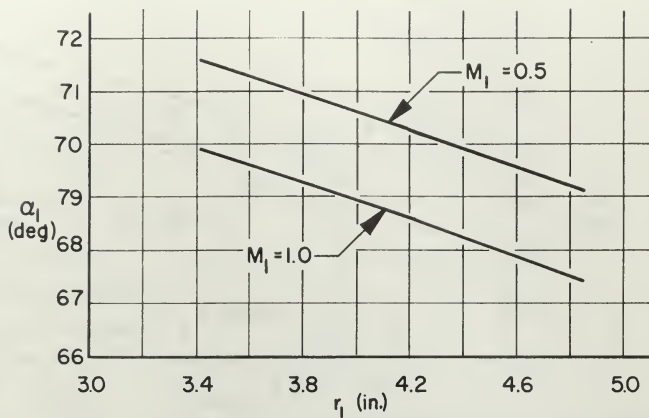
STATOR & ROTOR THROAT OPENINGS VS RADIAL POSITION (MOD I & MOD II)
 FIG. 6



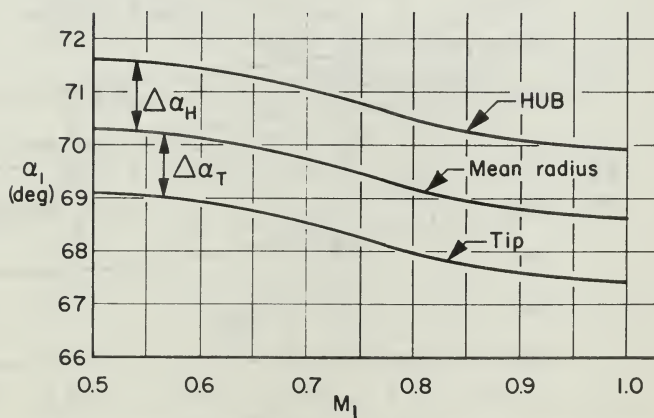
VARIATION OF STATOR OUTLET ANGLE WITH RADIUS (MOD I)
FIG. 7



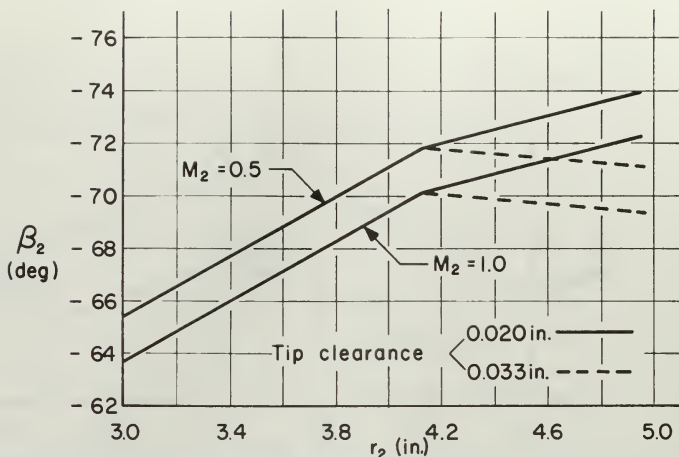
VARIATION OF STATOR OUTLET ANGLE WITH MACH NO. (MOD I)
FIG. 8



VARIATION OF STATOR OUTLET ANGLE WITH RADIUS (MOD II)
FIG. 9

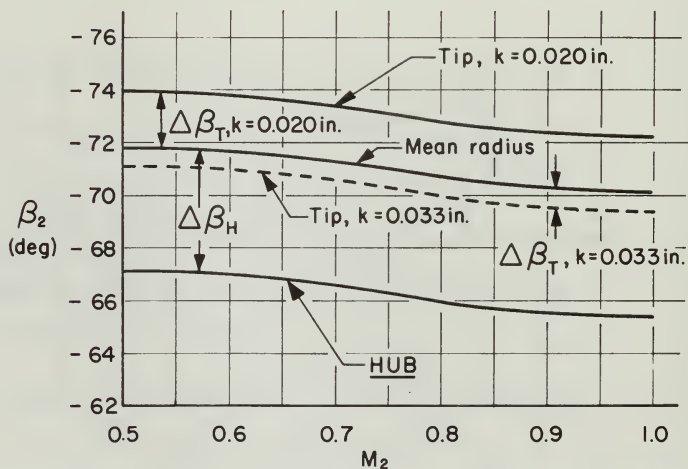


VARIATION OF STATOR OUTLET ANGLE WITH MACH NO. (MOD II)
FIG. 10



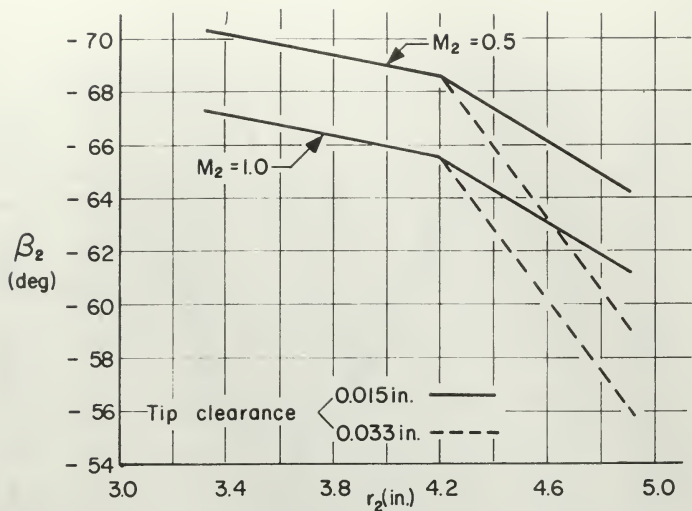
VARIATION OF ROTOR OUTLET ANGLE WITH RADIUS (MOD I)

FIG. 11

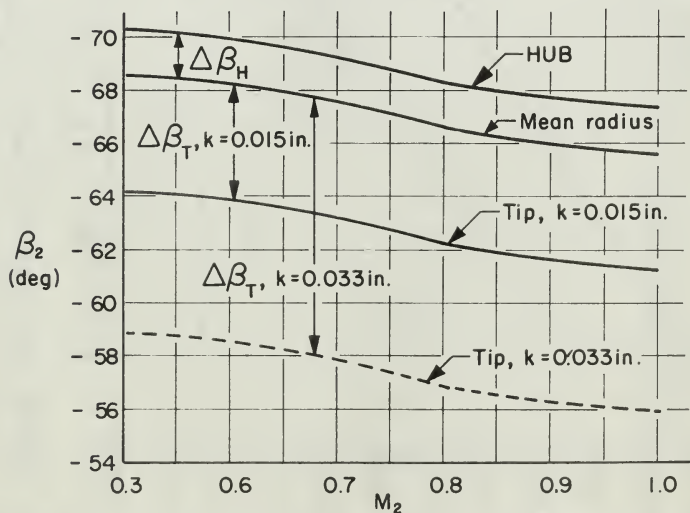


VARIATION OF ROTOR OUTLET ANGLE WITH MACH NO. (MOD I)

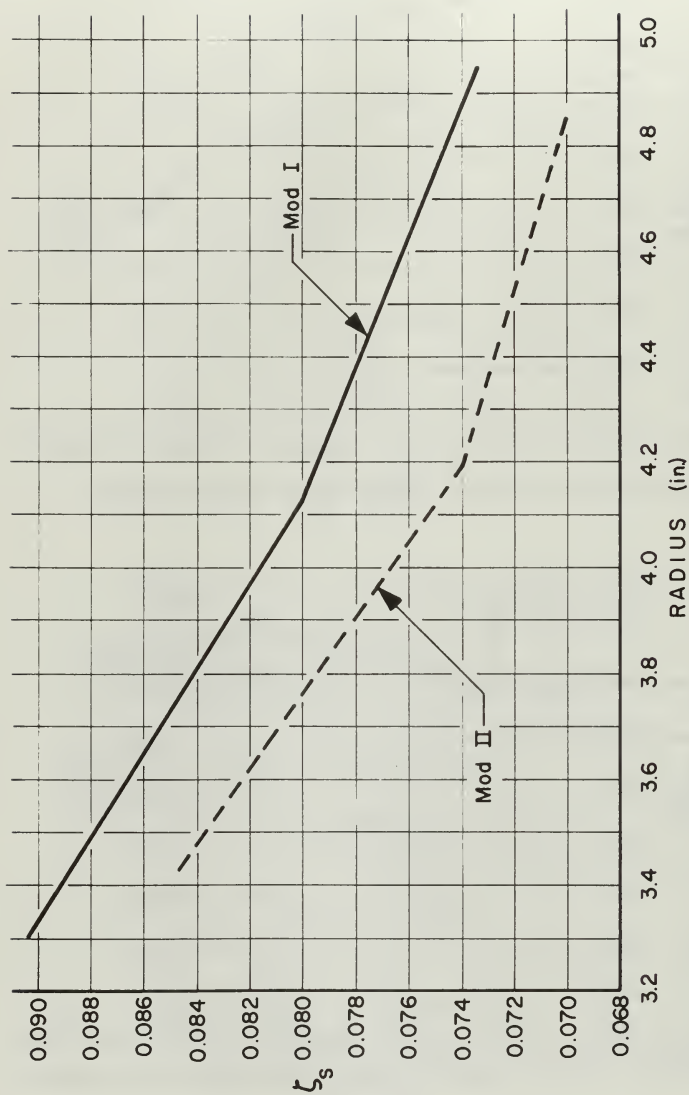
FIG. 12



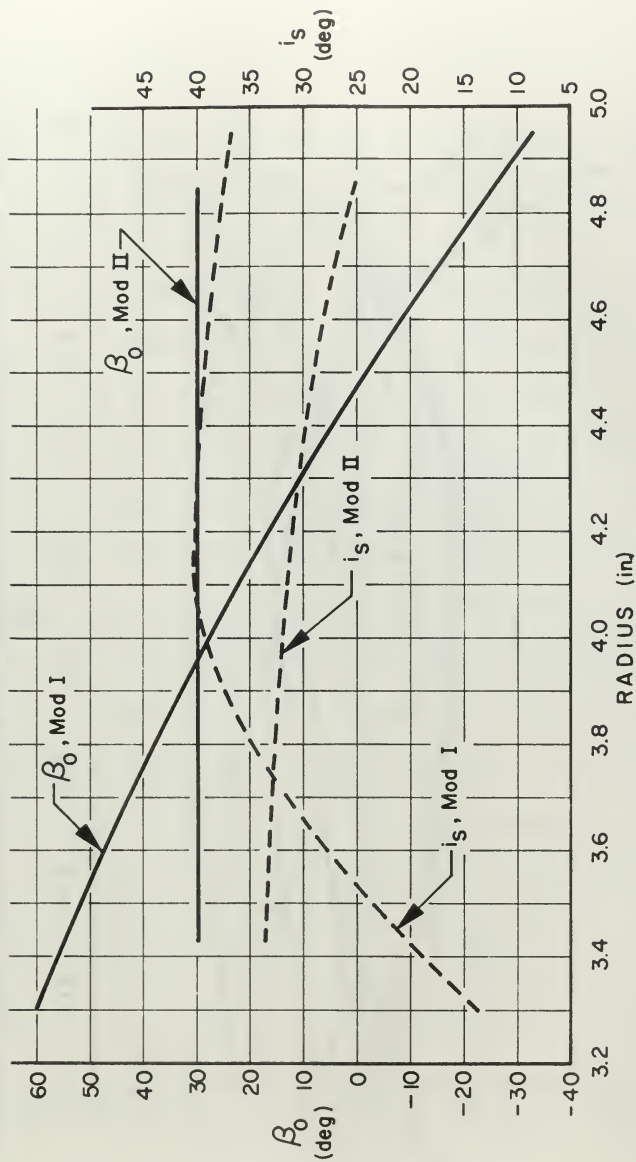
VARIATION OF ROTOR OUTLET ANGLE WITH RADIUS (MOD II)
FIG. 13



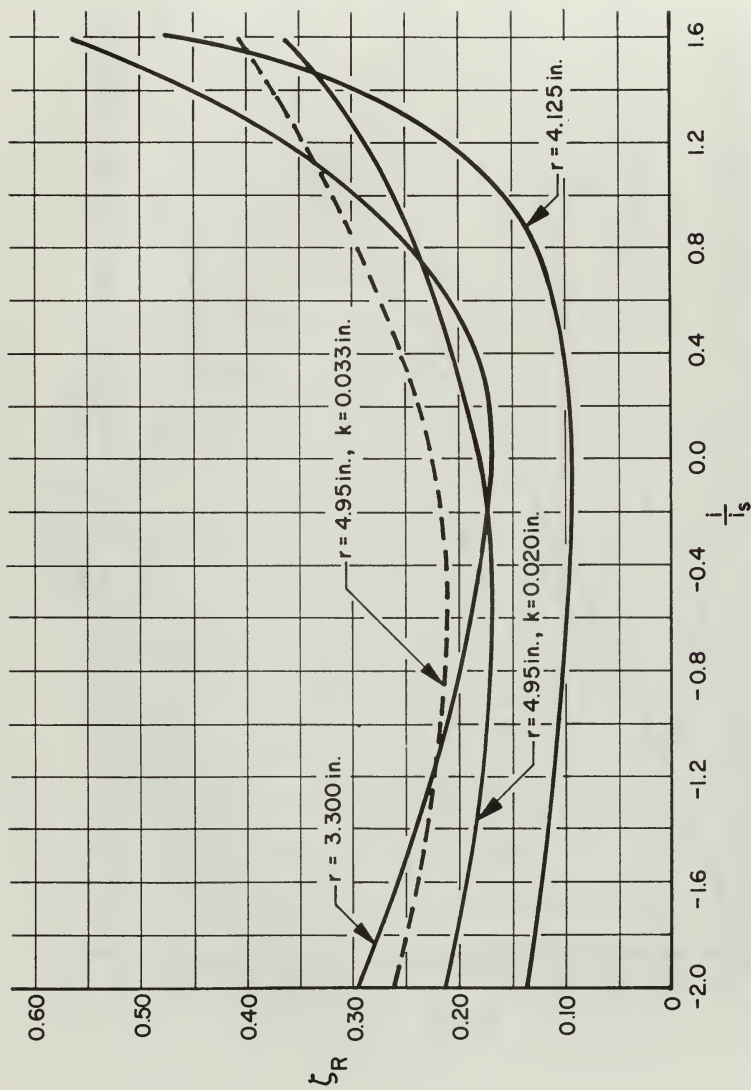
VARIATION OF ROTOR OUTLET ANGLE WITH MACH NO. (MOD II)
FIG. 14



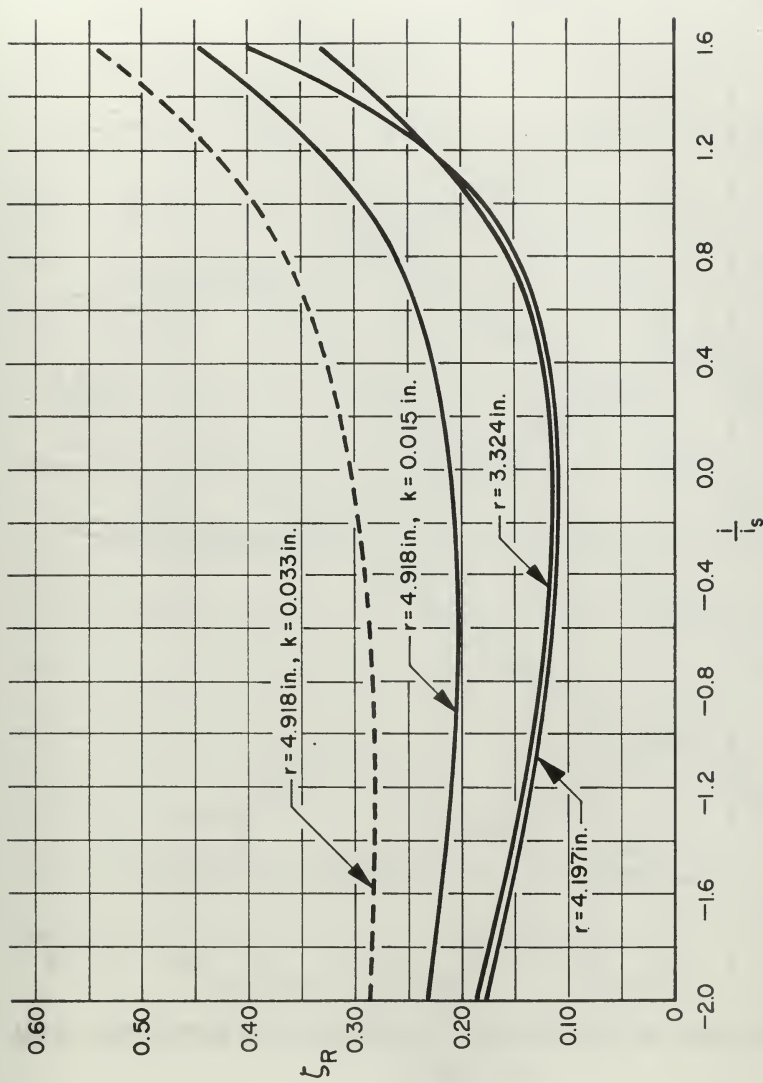
STATOR LOSS COEFFICIENTS AS FUNCTION OF RADIUS (MOD I & II)
FIG. 15



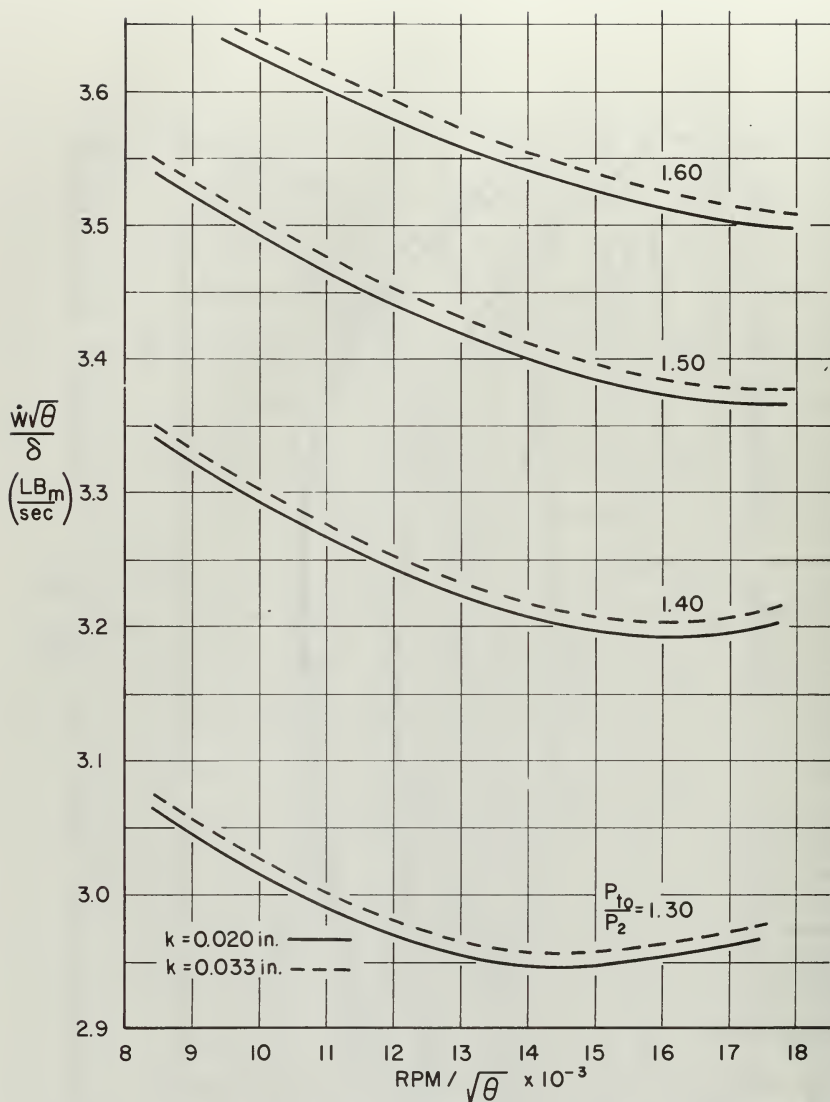
VARIATION OF BLADE INLET & STALL INCIDENCE ANGLES WITH RADIUS
(MOD I & MOD II)
FIG. 16



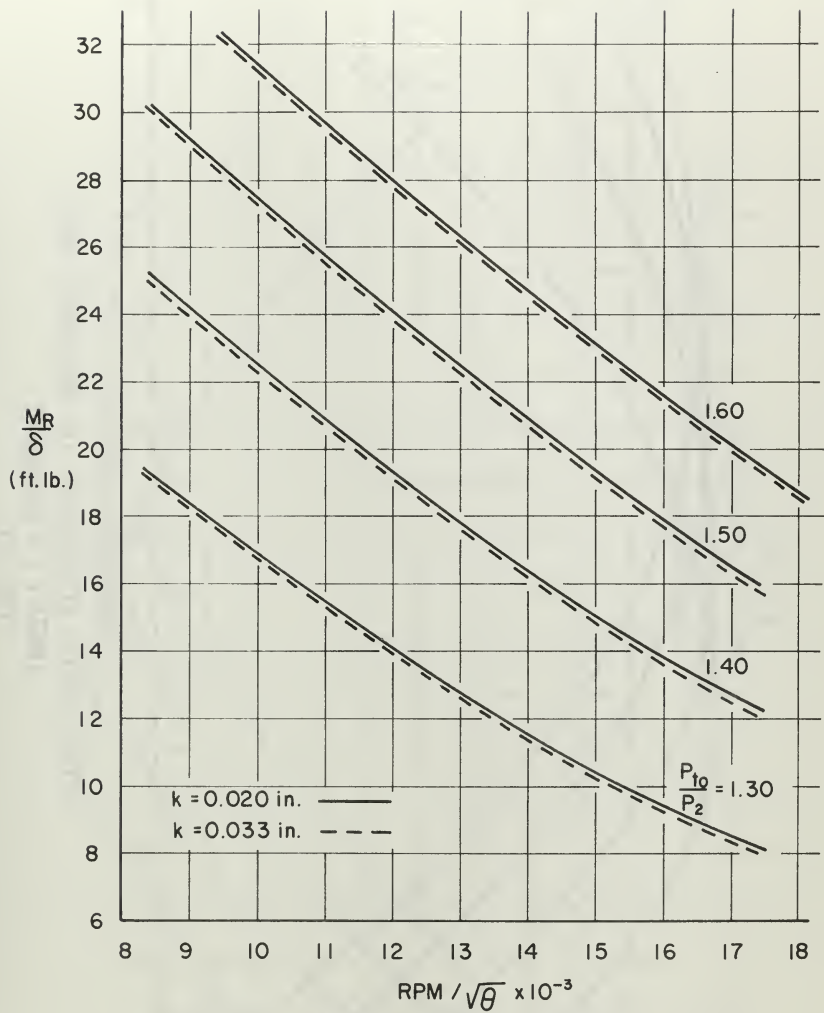
ROTOR LOSS COEFFICIENTS AS FUNCTION OF INCIDENCE RATIO (MOD I)
FIG. 17



ROTOR LOSS COEFFICIENTS AS FUNCTION OF INCIDENCE RATIO (MOD II)
 FIG. 18

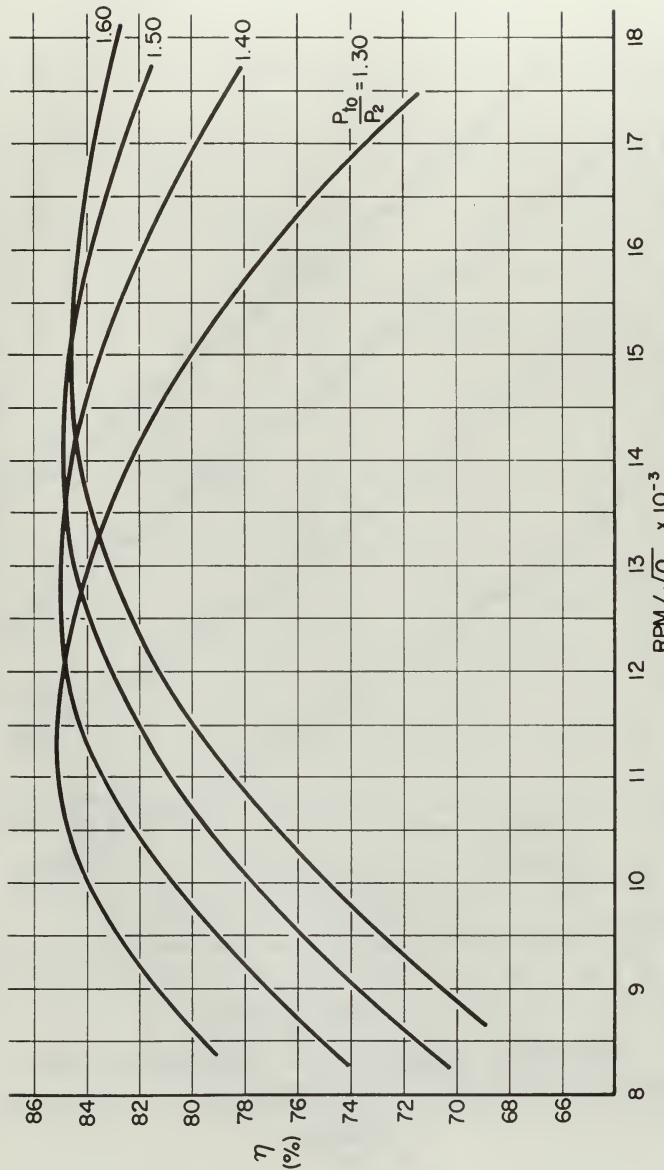


VARIATION OF REFERRED FLOWRATE WITH REFERRED RPM
 (MOD I)
 FIG. 19



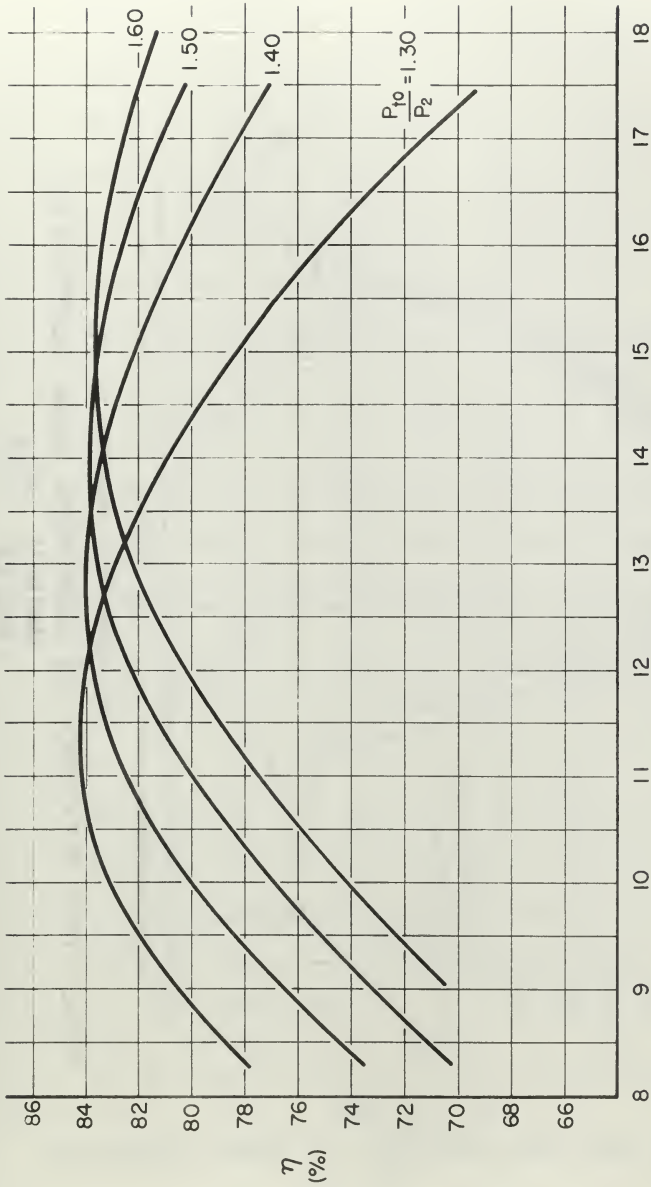
REFERRED MOMENT VS REFERRED RPM
(MOD I)

FIG. 20



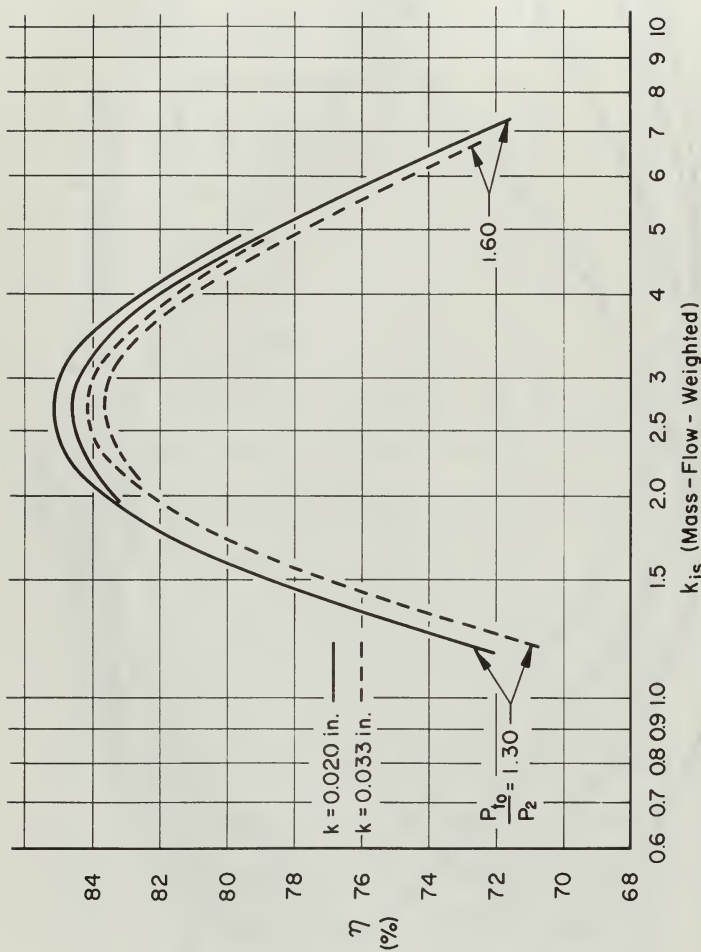
TOTAL-STATIC EFFICIENCY VS REFERRED RPM
(MOD I, $k = 0.020$ in.)

FIG. 21

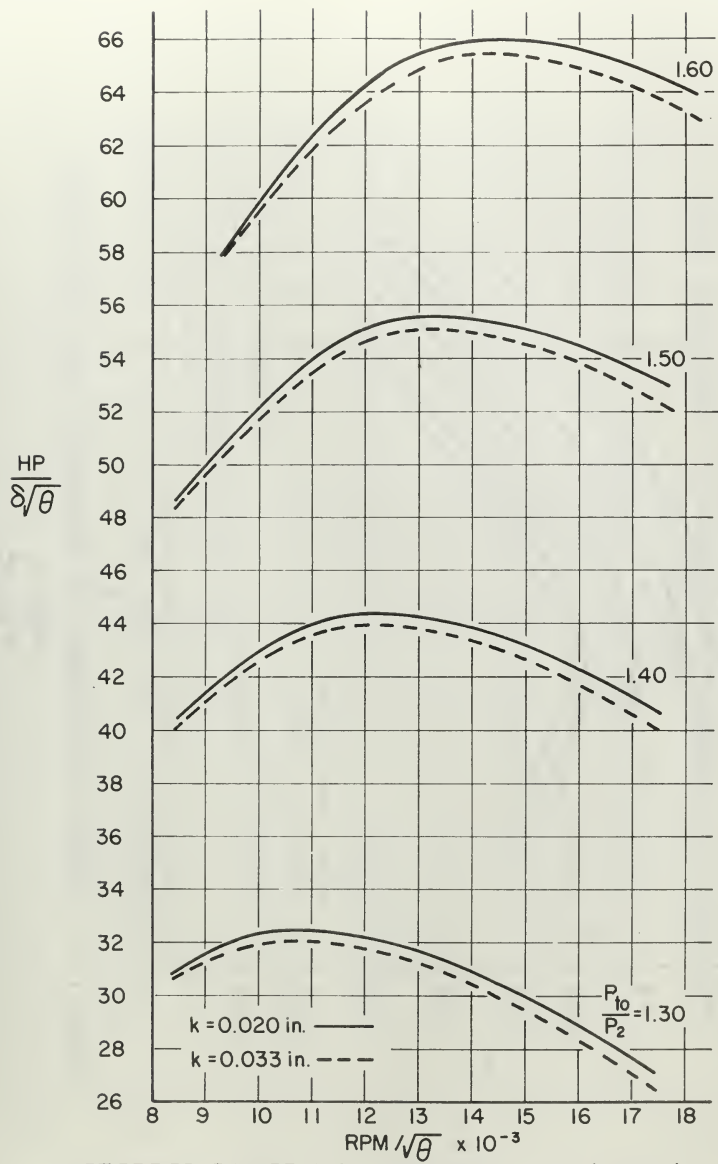


TOTAL - STATIC EFFICIENCY VS REFERRED RPM
 (MOD I , k = 0.033 in.)

FIG. 22

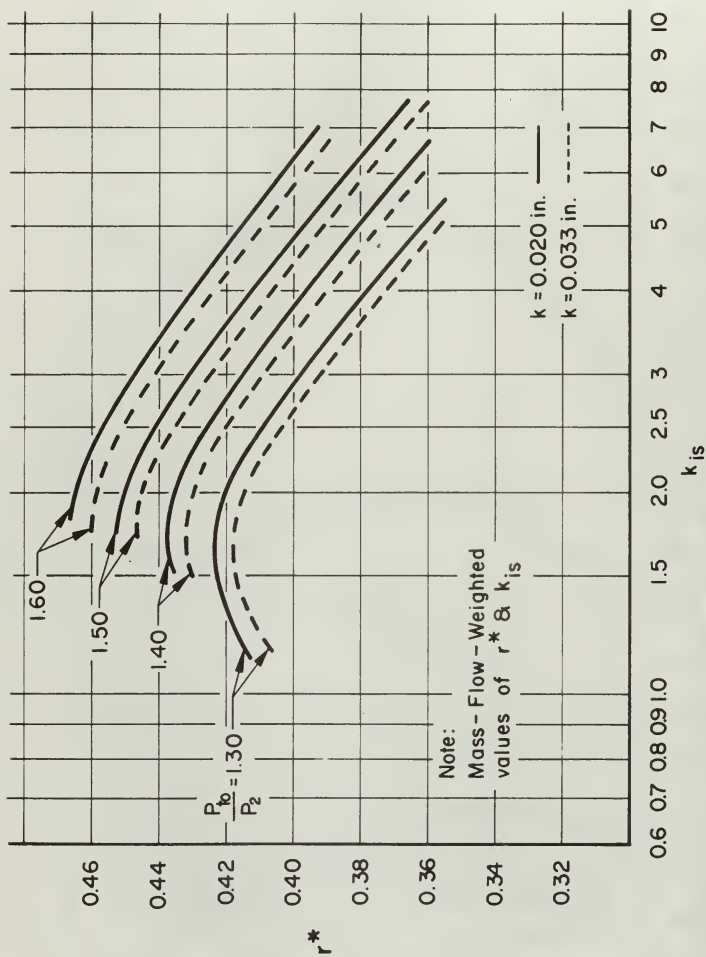


TOTAL-STATIC EFFICIENCY VS ISENTROPIC HEAD COEFFICIENT
 (MOD I)
 FIG. 23



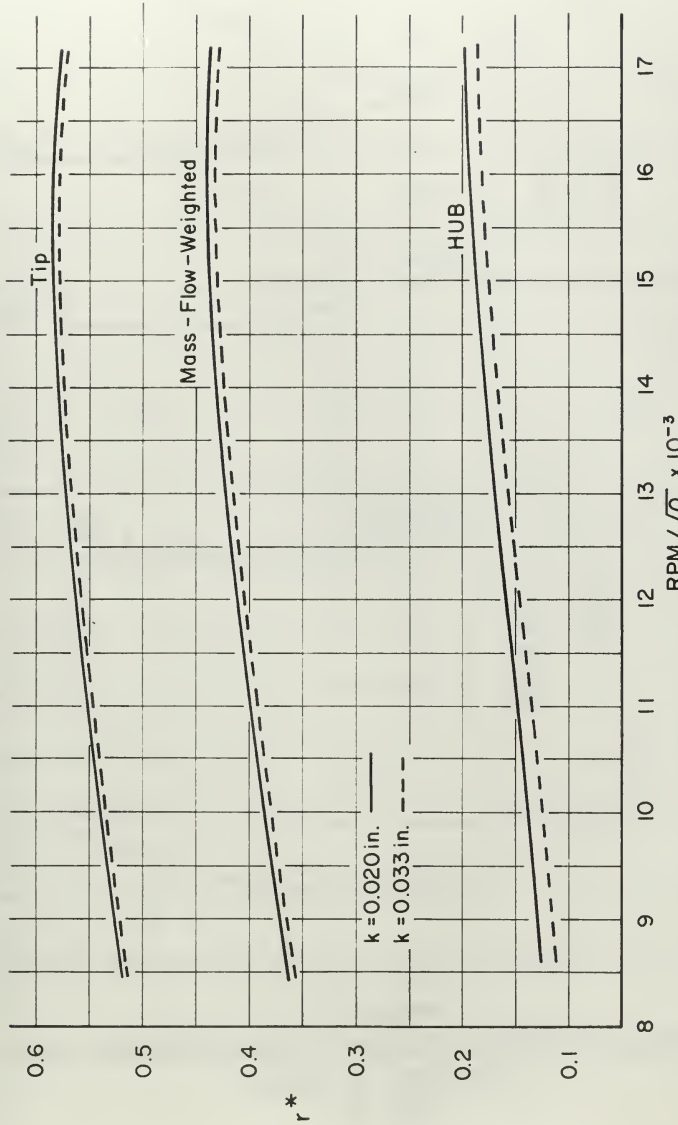
REFERRED POWER VS REFERRED RPM (MOD 1)

FIG. 24

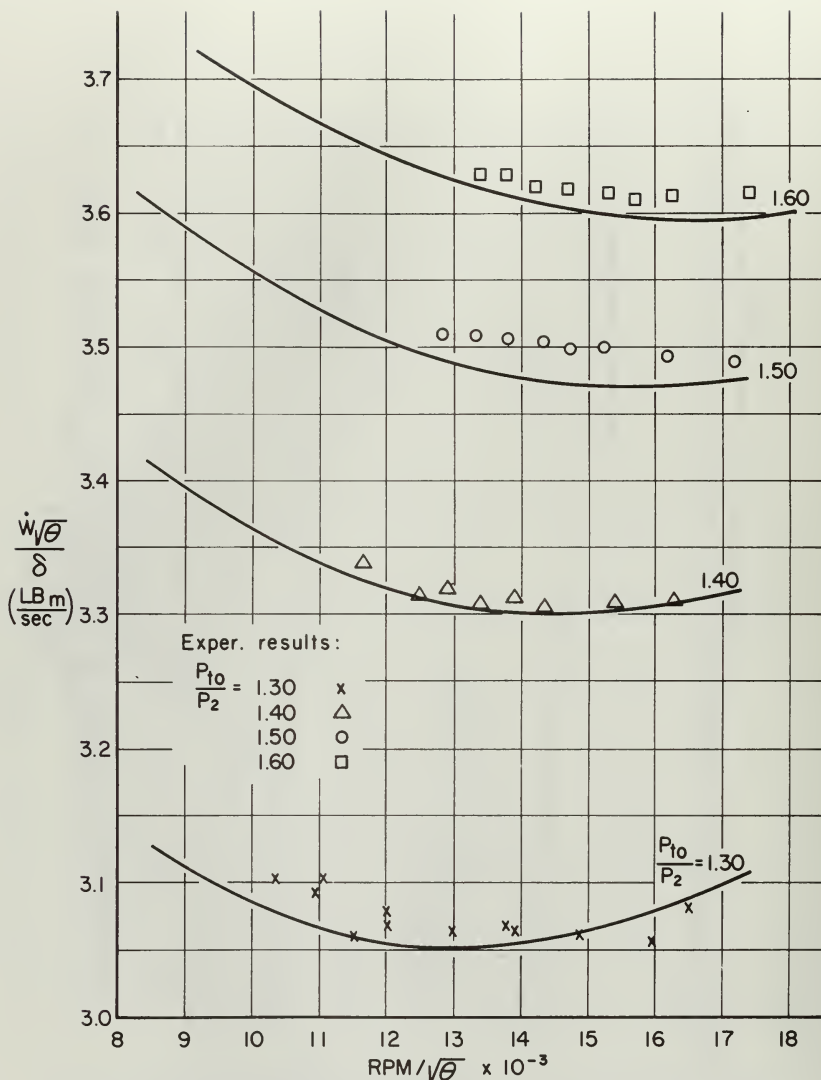


THEORETICAL DEGREE OF REACTION VS ISENTROPIC HEAD COEFFICIENT
(MOD I)

FIG. 25

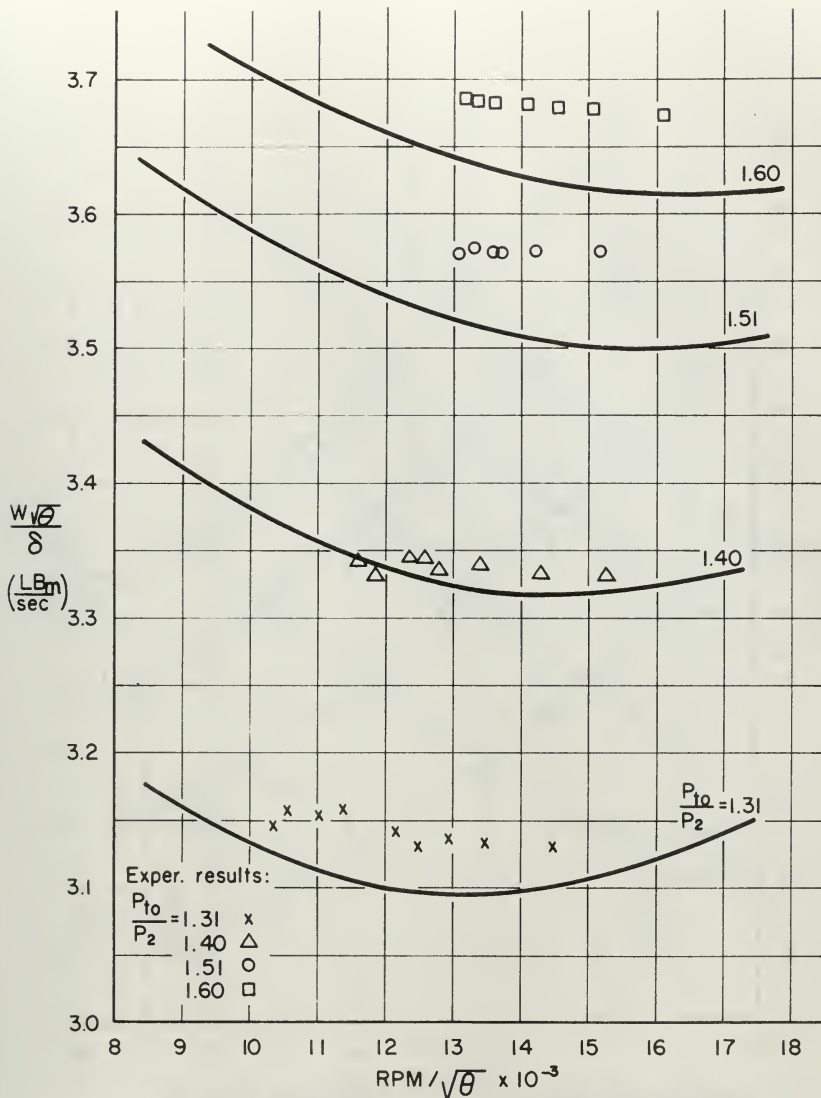


THEORETICAL DEGREE OF REACTION VS REFERRED RPM
 (MOD I, $P_{10}/P_2 = 1.40$)
 FIG. 26



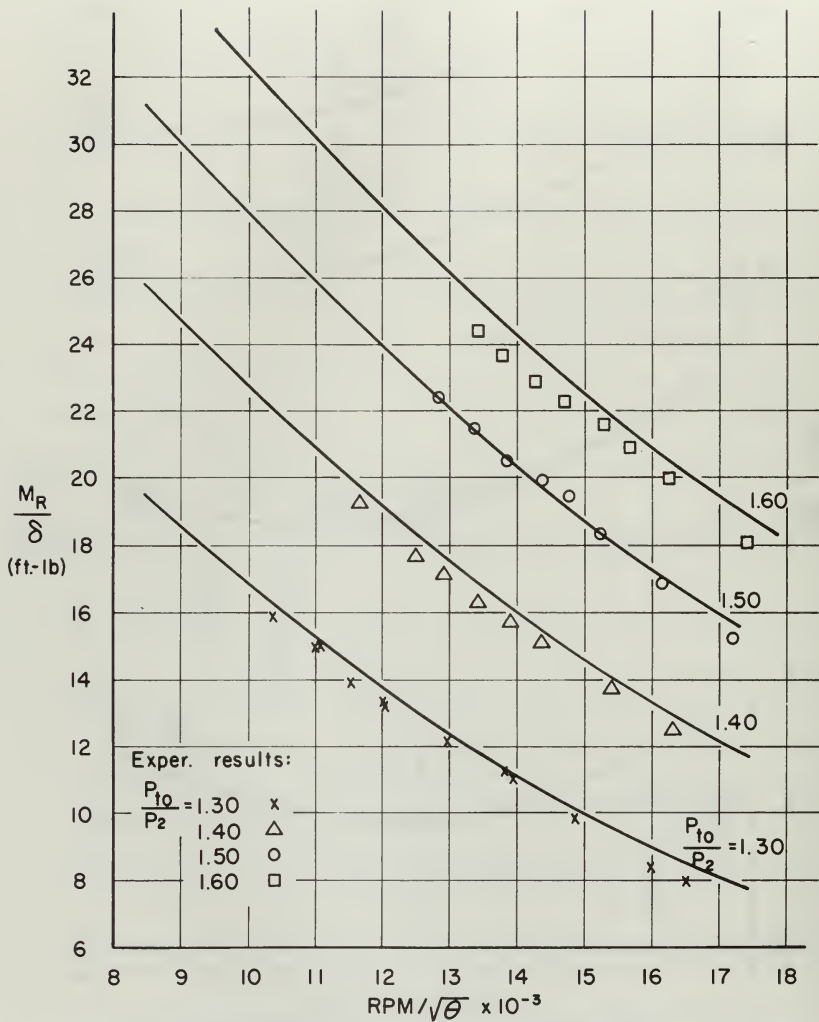
VARIATION OF REFERRED FLOWRATE WITH REFERRED RPM
(MOD II, $k=0.015$ in.)

FIG. 27



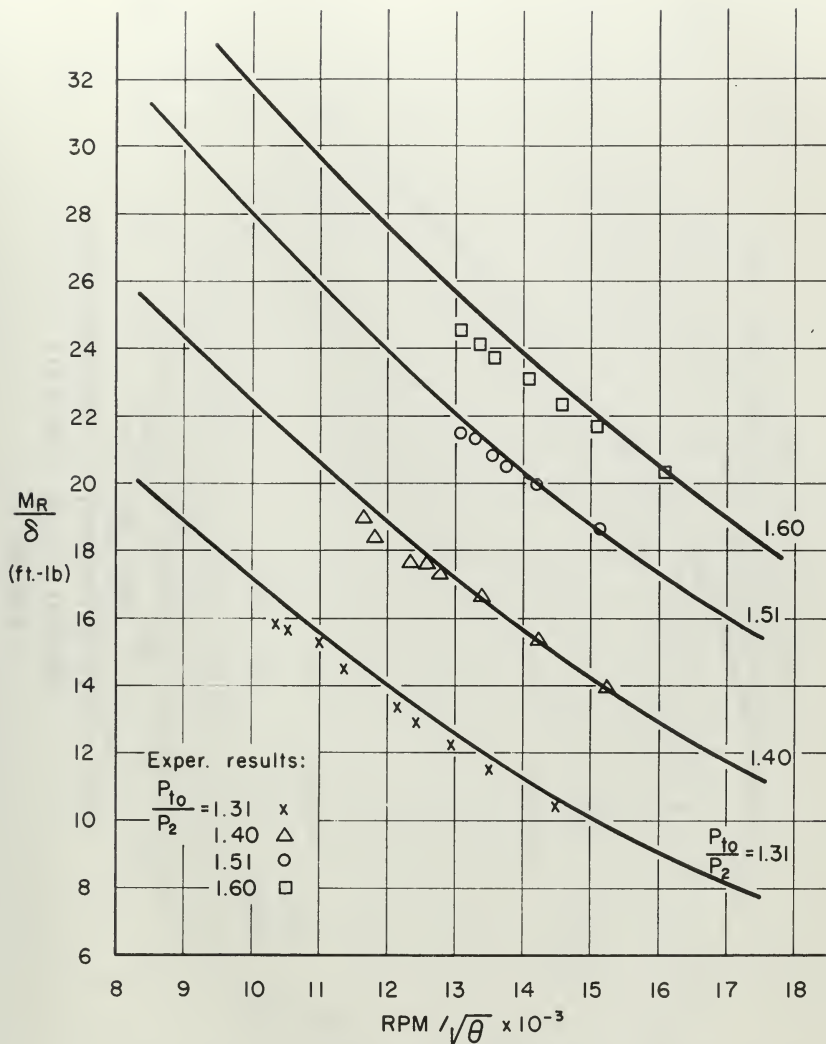
VARIATION OF REFERRED FLOWRATE WITH REFERRED RPM
(MOD II, $k=0.033$ in.)

FIG. 28



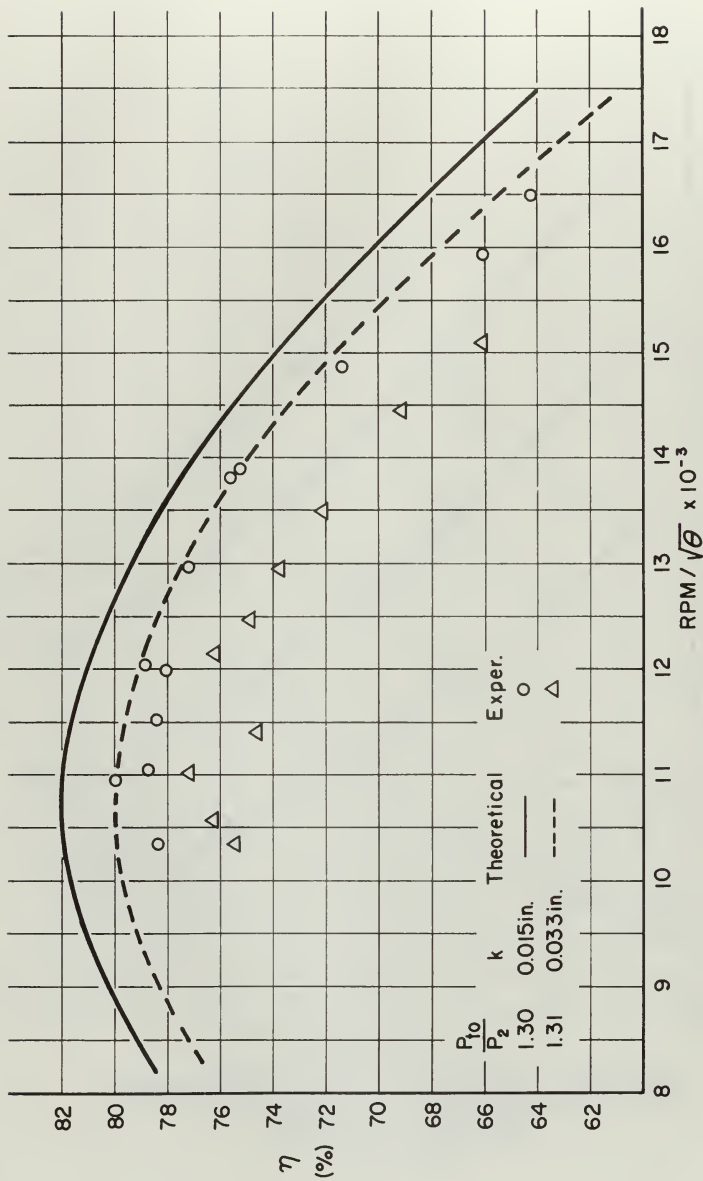
REFERRED MOMENT VS REFERRED RPM
(MOD II, $k=0.015$ in.)

FIG. 29



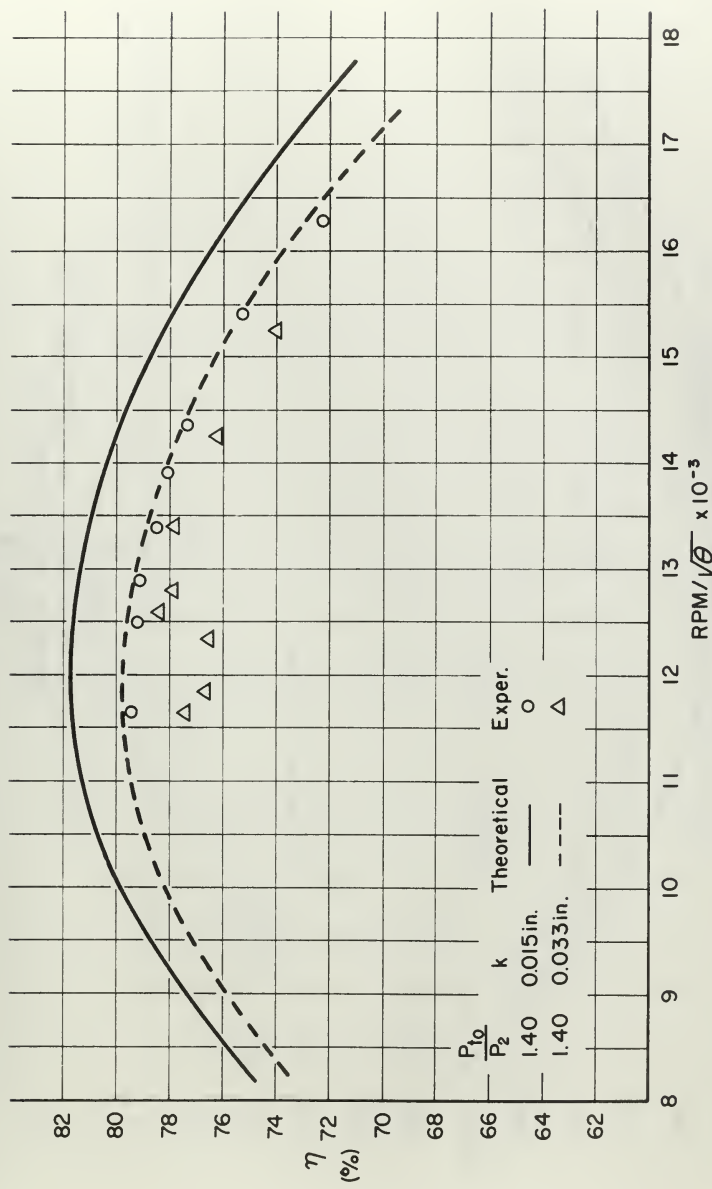
REFERRED MOMENT VS REFERRED RPM
(MOD II, $k=0.033$ in.)

FIG. 30

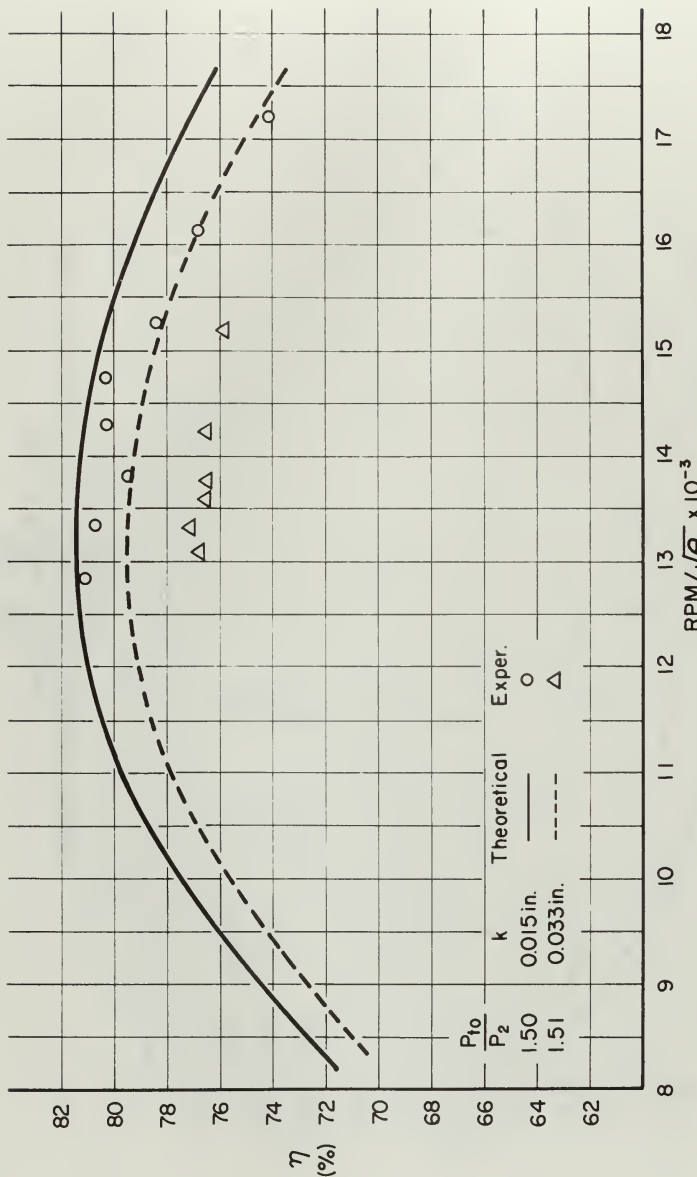


TOTAL-STATIC EFFICIENCY VS REFERRED RPM
 (MOD II, $P_{t0}/P_2 = 1.30, 1.31$)

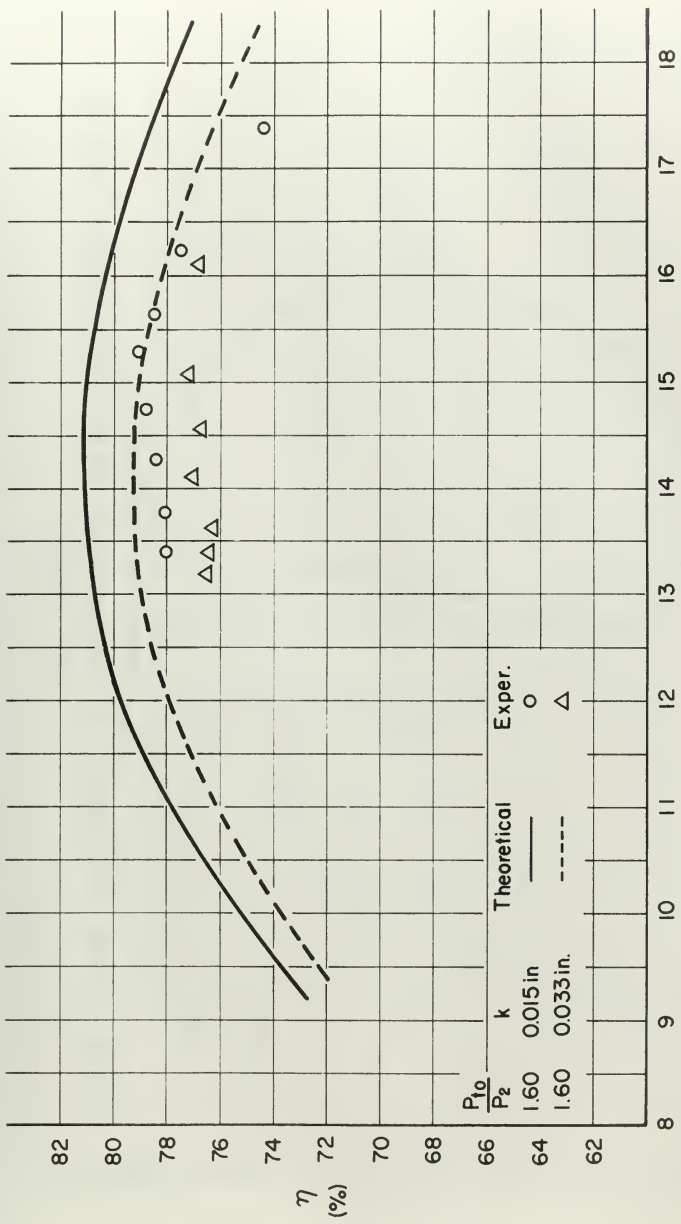
FIG. 31



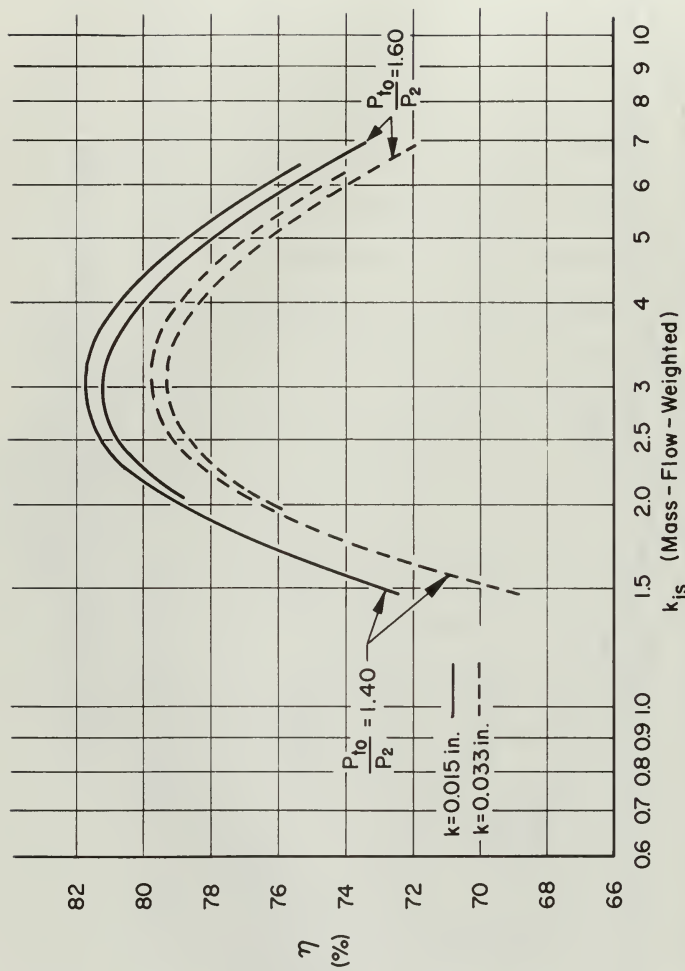
TOTAL-STATIC EFFICIENCY VS REFERRED RPM
 (MOD II $P_{10}/P_2 = 1.40$)
 FIG. 32



TOTAL-STATIC EFFICIENCY VS REFERRED RPM
 (MOD II, $P_1/P_2=1.50$, 1.51)
 FIG. 33

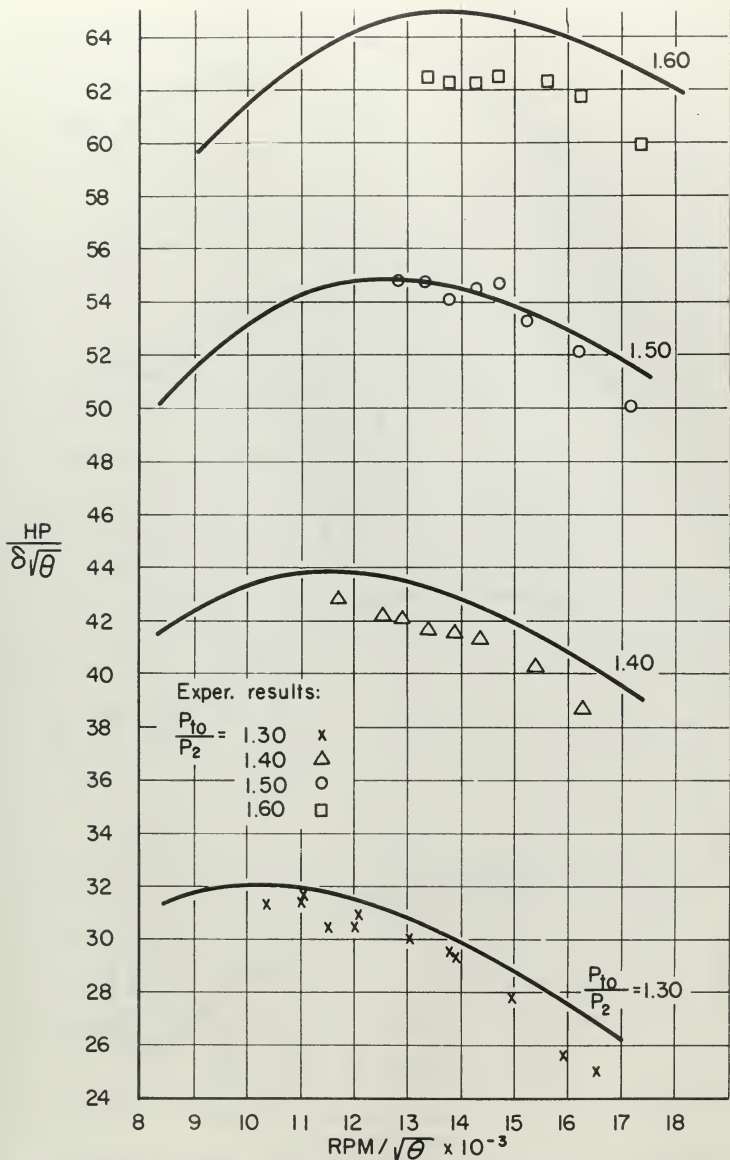


TOTAL-STATIC EFFICIENCY VS REFERRED RPM
 (MOD II, $P_{10}/P_2 = 1.60$)
 FIG. 34



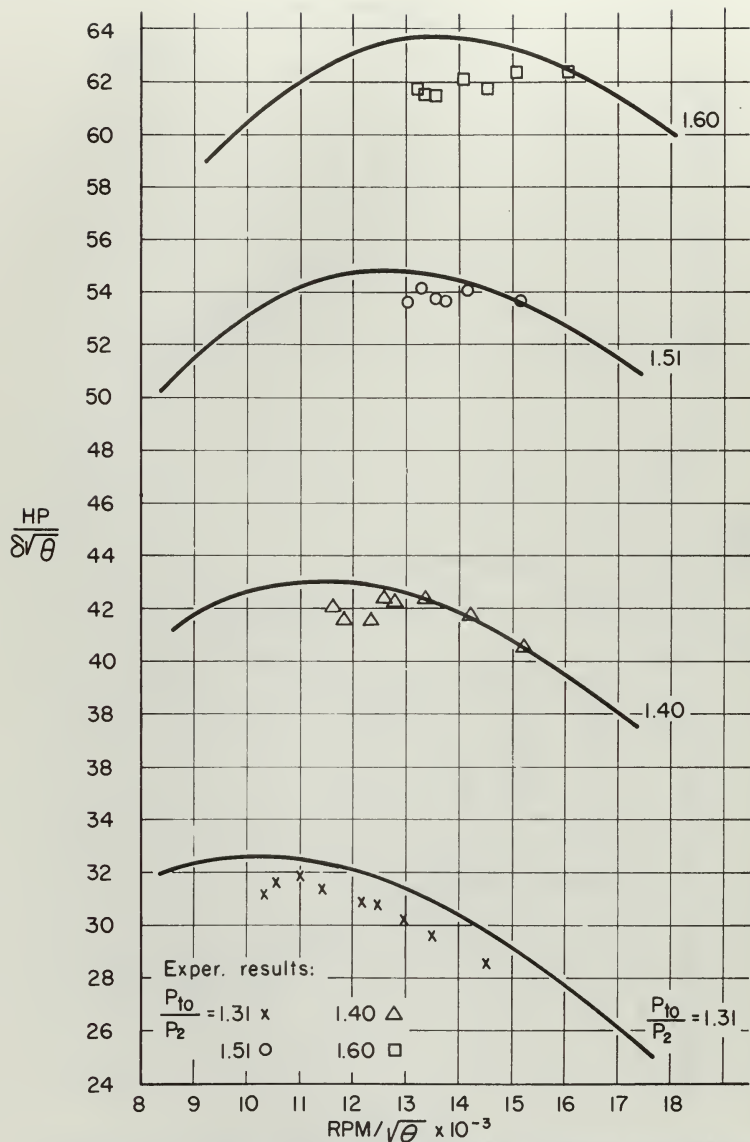
TOTAL-STATIC EFFICIENCY VS ISENTROPIC HEAD COEFFICIENT (MOD II)

FIG. 35

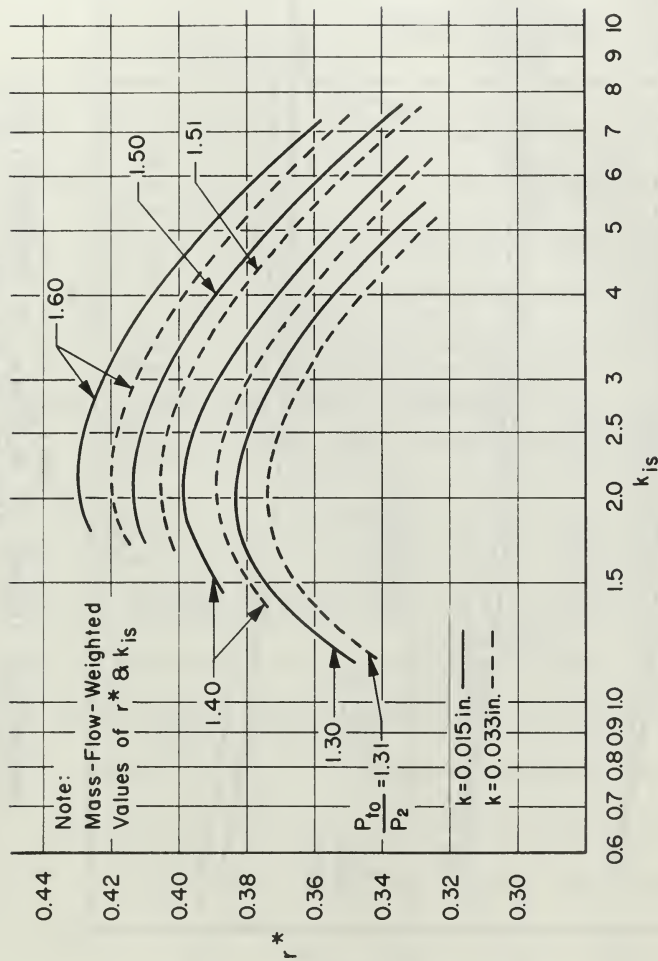


REFERRED POWER VS REFERRED RPM (MOD II, k=0.015in.)

FIG. 36

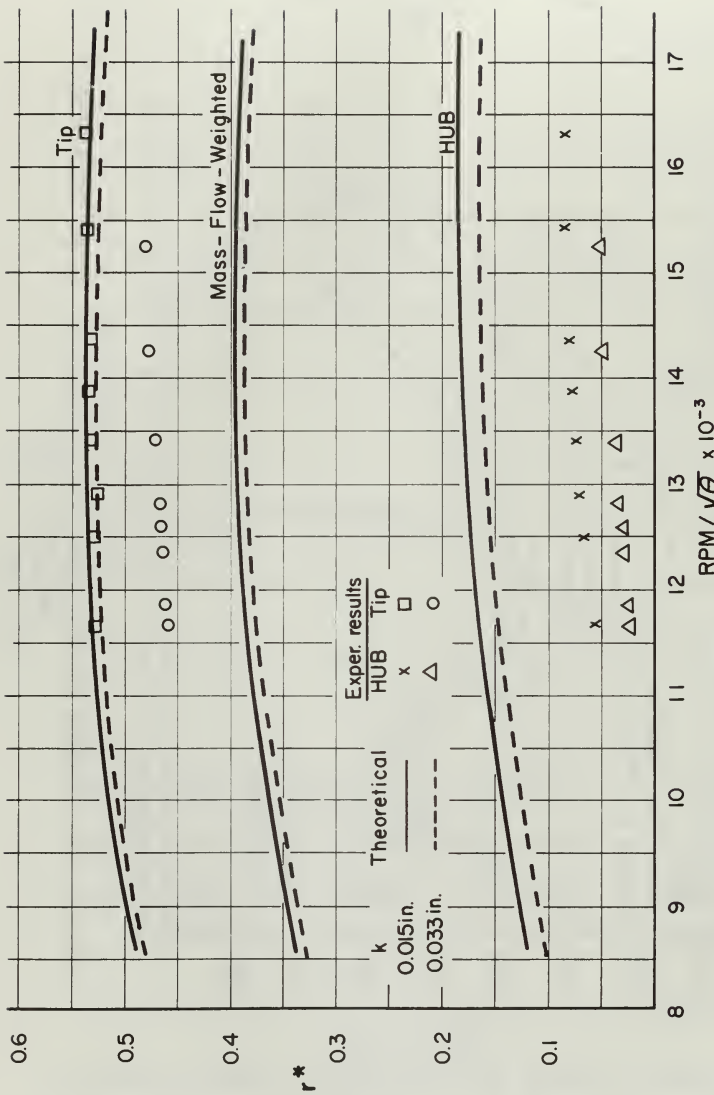


REFERRED POWER VS REFERRED RPM (MOD II, $k=0.033in.$)
 FIG. 37



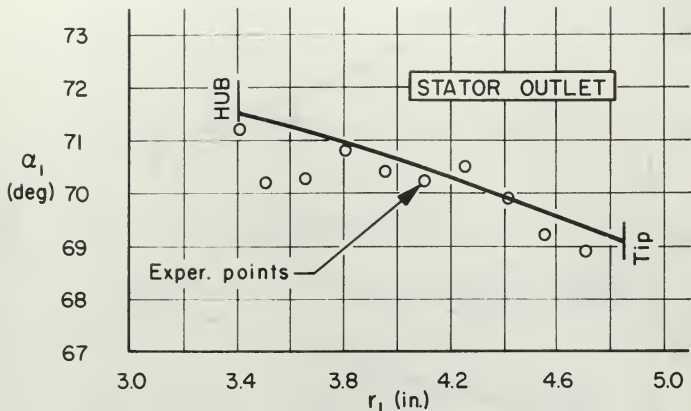
THEORETICAL DEGREE OF REACTION VS ISENTROPIC HEAD COEFFICIENT
(MOD II)

FIG. 38



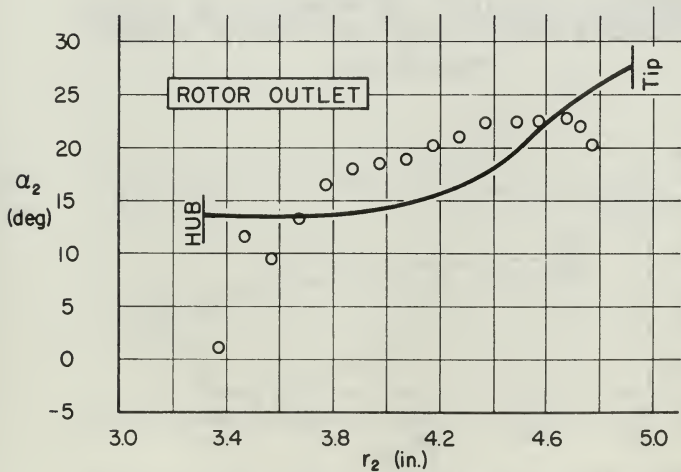
THEORETICAL DEGREE OF REACTION VS REFERRED RPM
(MOD II, $R_0/P_2 = 1.40$)

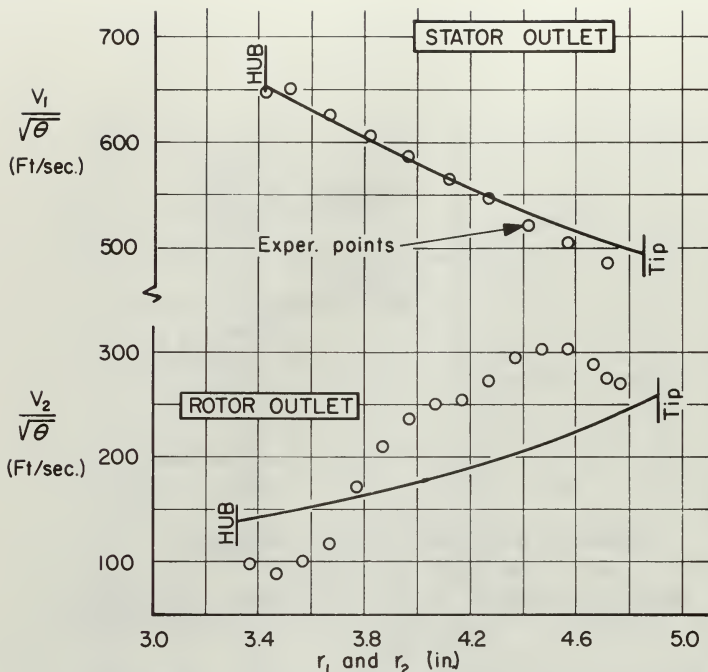
FIG. 39



ABSOLUTE FLOW OUTLET ANGLES
AS FUNCTION OF RADIUS
(MOD II, $k=0.015$ in., $P_{t0}/P_2=1.40$, $\text{RPM}/\sqrt{\theta} = 13,934$)

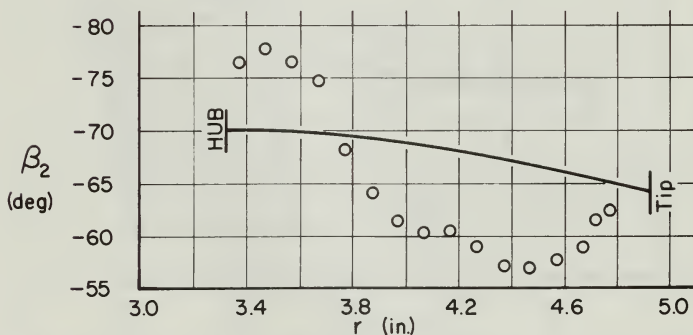
FIG. 40



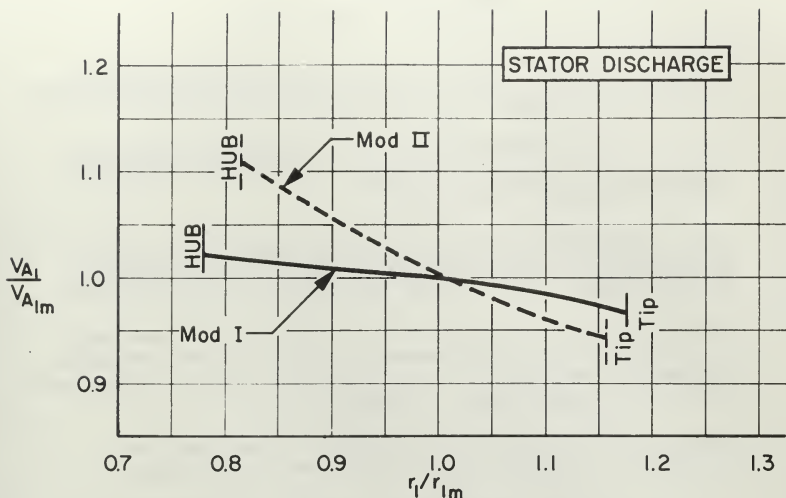


REFERRED VELOCITIES AS FUNCTION OF RADIUS
(MOD II, $k=0.015$ in. $P_{10}/P_2=1.40$, $RPM/\sqrt{\theta}=13,934$)

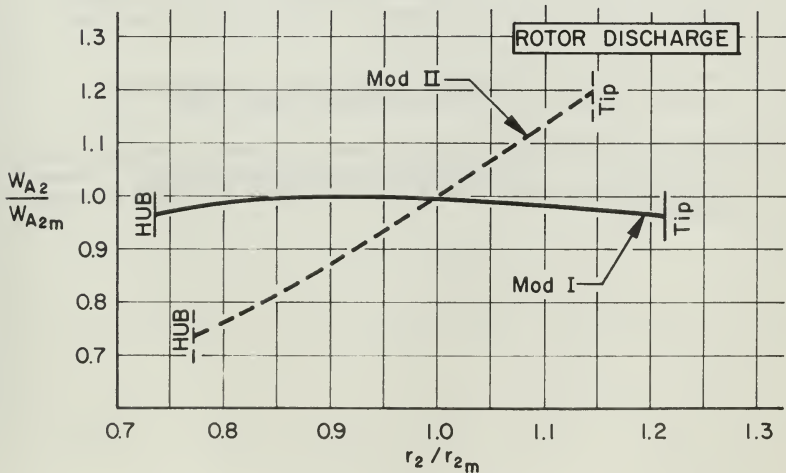
FIG. 41



RELATIVE ROTOR FLOW OUTLET ANGLE AS FUNCTION
OF RADIUS (MOD II, $k=0.015$ in. $P_{10}/P_2=1.40$, $RPM/\sqrt{\theta}=13,934$)



PLOTS OF AXIAL VELOCITY RATIOS VS RADIUS RATIOS AT PEAK EFFICIENCY (MOD I & II, $P_{10}/P_2 = 1.40$)
 FIG. 43



BIBLIOGRAPHY

1. Ainley, D. G. and Mathieson, G. C. R. An Examination of the Flow and Pressure Losses in Blade Rows of Axial-Flow Turbines. Aeronautical Research Council, R & M No. 2891, 1955.
2. Ainley, D. G. and Mathieson, G. C. R. A Method of Performance Estimation for Axial-Flow Turbines. Aeronautical Research Council, R & M No. 2974, 1967.
3. Beer, R. Aerodynamic Design and Estimated Performance of a Two-Stage Curtis Turbine for the Liquid Oxygen Turbopump of the M-1 Engine. NASA CR 54764 (AGC8800-12), Nov. 19, 1965.
4. Commons, P. M. Instrumentation of the Transonic Turbine Test Rig to Determine the Performance of Turbine Inlet Guide Vanes Through the Application of the Momentum and Moment of Momentum Equations. USNPGS Thesis, September 1967.
5. Eckert, H. E. Performance Analysis and Initial Tests of a Transonic Turbine Test Rig. USNPGS Thesis, May 1966.
6. Messegee, J. A. Influence of Axial and Radial Clearances on Performance of a Turbine Stage With Blunt Edge Non-Twisted Blades. USNPGS Thesis, September 1967.
7. Riley, M. W. The Effects of Axial Clearance on the Performance of a Dual Discharge Radial Turbine. USNPGS Thesis, December 1966.
8. Vavra, M. H. Aero-Thermodynamics and Flow in Turbomachines. New York, London: John Wiley and Sons, Inc., 1960.
9. Vavra, M. H. Problems of Fluid Mechanics in Radial Turbomachines, Pts. III and IV. Von Karman Institute Course Note 55b. Rhode-Saint-Genese, Belgium: Von Kármán Institute for Fluid Dynamics, March 1965.

APPENDIX A
DEVELOPEMENT OF EQUATIONS

1. Equation of Motion¹¹

The equation of motion for relative flow is

$$\nabla H_R = \bar{W} \times (\nabla \times \bar{W} + 2\bar{\omega}) + T \nabla s \quad (2)$$

In cylindrical coordinates:

$$\nabla H_F = \bar{i}_\theta \frac{\partial H_F}{\partial \theta} + \bar{i}_z \frac{\partial H_F}{\partial z} + \bar{i}_r \frac{\partial H_F}{\partial r} \quad (87)$$

$$\bar{W} \cdot (\nabla \times \bar{W}) =$$

$$\begin{aligned} & \bar{i}_\theta \left\{ W_r \left[\frac{\partial W_\theta}{\partial \theta} - \frac{\partial(rW_\theta)}{\partial z} \right] - W_z \frac{1}{r} \left[\frac{\partial(rW_\theta)}{\partial r} - \frac{\partial W_r}{\partial \theta} \right] \right\} \\ & + \bar{i}_z \left\{ W_r \left[\frac{\partial W_r}{\partial z} - \frac{\partial W_A}{\partial r} \right] - W_\theta \frac{1}{r} \left[\frac{\partial W_r}{\partial \theta} - \frac{\partial(rW_\theta)}{\partial z} \right] \right\} \\ & + \bar{i}_r \left\{ W_\theta \frac{1}{r} \left[\frac{\partial(rW_\theta)}{\partial r} - \frac{\partial W_r}{\partial \theta} \right] - W_A \left[\frac{\partial W_r}{\partial z} - \frac{\partial W_A}{\partial r} \right] \right\} \quad (88) \end{aligned}$$

$$\bar{W} \times 2\bar{\omega} = \bar{i}_r (2\omega W_\theta) - \bar{i}_\theta (2\omega W_r) \quad (89)$$

$$T \nabla s = T \left(\bar{i}_\theta \frac{1}{r} \frac{\partial s}{\partial \theta} + \bar{i}_z \frac{\partial s}{\partial z} + \bar{i}_r \frac{\partial s}{\partial r} \right) \quad (90)$$

Equating Eq. 87 to the components in Eqs. 88-90,

$$\bar{i}_\theta \cdot \frac{1}{r} \frac{\partial H_F}{\partial \theta} = \frac{W_\theta}{r} \left[\frac{\partial W_r}{\partial \theta} - \frac{\partial(rW_\theta)}{\partial z} \right] - \frac{W_r}{r} \left[\frac{\partial(rW_\theta)}{\partial r} - \frac{\partial W_r}{\partial \theta} \right] - 2\omega W_r + \frac{T}{r} \frac{\partial s}{\partial \theta} \quad (91)$$

$$\bar{i}_z \cdot \frac{\partial H_F}{\partial z} = W_r \left[\frac{\partial W_r}{\partial z} - \frac{\partial W_A}{\partial r} \right] - \frac{W_\theta}{r} \left[\frac{\partial W_r}{\partial \theta} - \frac{\partial(rW_\theta)}{\partial z} \right] - T \frac{\partial s}{\partial z} \quad (92)$$

$$\bar{i}_r \cdot \frac{\partial H_F}{\partial r} = \frac{W_\theta}{r} \left[\frac{\partial(rW_\theta)}{\partial r} - \frac{\partial W_r}{\partial \theta} \right] - W_A \left[\frac{\partial W_r}{\partial z} - \frac{\partial W_A}{\partial r} \right] + 2\omega W_\theta + T \frac{\partial s}{\partial r} \quad (93)$$

¹¹Eckert, op. cit., pp. 149-155.

For assumed axisymmetric flow, $\frac{\partial(\quad)}{\partial\theta} = 0$,

$$\overline{t}_z: 0 = -\frac{W_A}{r} \frac{\partial(rW_z)}{\partial z} - \frac{W_r}{r} \frac{\partial(rW_\theta)}{\partial r} - 2\omega W_r \quad (94)$$

$$\overline{t}_z: \frac{\partial H_R}{\partial z} = W_r \frac{\partial W_r}{\partial z} - W_r \frac{\partial V_A}{\partial r} + \frac{W_z}{r} \frac{\partial(rW_\theta)}{\partial z} + T \frac{\partial s}{\partial z} \quad (95)$$

$$\overline{t}_r: \frac{\partial H_R}{\partial r} = \frac{W_z}{r} \frac{\partial(rW_\theta)}{\partial r} - W_A \frac{\partial W_r}{\partial z} + W_A \frac{\partial W_A}{\partial r} + 2\omega W_\theta + T \frac{\partial s}{\partial r} \quad (96)$$

Equation 94 can be written

$$\frac{\partial(rW_\theta)}{\partial z} = -\frac{W_r}{W_A} \frac{\partial(rW_\theta)}{\partial r} - 2\omega r \frac{W_r}{W_A} \quad (97)$$

Replacing $\frac{\partial(rW_\theta)}{\partial z}$ in Eq. 95 by its equivalent in Eq. 97,

$$\frac{\partial H_R}{\partial z} = W_r \frac{\partial W_r}{\partial z} - V_A \frac{\partial W_A}{\partial r} + \frac{W_z}{r} \left(-\frac{W_r}{W_A} \frac{\partial(rW_\theta)}{\partial r} \right) - 2\omega \frac{W_z W_r}{W_A} + T \frac{\partial s}{\partial z} \quad (98)$$

or

$$\frac{\partial H_R}{\partial z} = -\frac{W_z V_A}{r W_A} \frac{\partial(rW_\theta)}{\partial r} + W_r \frac{\partial W_r}{\partial z} - W_r \frac{\partial V_A}{\partial r} - 2\omega \frac{W_z V_A}{W_A} + T \frac{\partial s}{\partial z} \quad (99)$$

Multiplying Eq. 96 by W_r and Eq. 99 by W_A ,

$$W_r \frac{\partial H_R}{\partial r} = \frac{W_r W_r}{r} \frac{\partial(rW_\theta)}{\partial r} - W_A W_r \frac{\partial W_r}{\partial z} + V_A W_r \frac{\partial V_A}{\partial r} - 2\omega W_z W_r + W_r T \frac{\partial s}{\partial r} \quad (100)$$

$$W_A \frac{\partial H_R}{\partial z} = -\frac{W_z V_A}{r} \frac{\partial(rW_\theta)}{\partial r} + W_r W_r \frac{\partial W_r}{\partial z} - W_A W_r \frac{\partial V_A}{\partial r} - 2\omega W_z W_r + V_A T \frac{\partial s}{\partial z} \quad (101)$$

Adding Eqs. 100 and 101,

$$W_r \frac{\partial H_R}{\partial r} + V_A \frac{\partial H_R}{\partial z} = T \left(W_r \frac{\partial s}{\partial r} + W_A \frac{\partial s}{\partial z} \right) \quad (102)$$

For adiabatic flow H_R is constant along a streamline, therefore,

$$\overline{W} dt + \nabla H_R = 0 \quad (103)$$

For axisymmetric flow,

$$\overline{W} dt + \nabla H_R = 0 = V_A \frac{\partial H_R}{\partial z} + W_r \frac{\partial H_R}{\partial r} \quad (104)$$

From Eq. 104,

$$\frac{\partial H_R}{\partial z} = -\frac{W_r}{V_A} \frac{\partial H_R}{\partial r} \quad (105)$$

Substituting Eq. 105 into Eq. 102,

$$W_r \frac{\partial H_R}{\partial r} + V_A \left(-\frac{W_r}{V_A} \frac{\partial H_R}{\partial r} \right) = T \left(W_r \frac{\partial s}{\partial r} + W_A \frac{\partial s}{\partial z} \right) \quad (106)$$

or

$$\frac{\partial s}{\partial z} = -\frac{W_r}{V_A} \frac{\partial s}{\partial r} \quad (107)$$

Using Eqs. 105 and 107, Eq. 99 becomes

$$-\frac{W_r}{W_A} \frac{\partial H_E}{\partial r} = -\frac{V_r W_r}{r W_A} \frac{\partial(r W_r)}{\partial r} - W_r \frac{\partial W_r}{\partial z} - W_r \frac{\partial W_A}{\partial r} - 2\omega \frac{W_r W_A}{V_A} - \frac{W_r}{W_A} T \frac{\partial S}{\partial r} \quad (108)$$

Multiplying Eq. 108 by $(-\frac{W_A}{V_A})$, gives

$$\frac{\partial H_E}{\partial r} = \frac{V_r}{r} \frac{\partial(r W_r)}{\partial r} - W_A \frac{\partial W_r}{\partial z} + W_A \frac{\partial V_A}{\partial r} + 2\omega W_J + T \frac{\partial S}{\partial r} \quad (109)$$

Eq. 109 is identical with Eq. 96, therefore Eq. 109 is the equation

that must be solved. With $[W_A \frac{\partial V_A}{\partial r} = \frac{1}{2} \frac{\partial(W_A^2)}{\partial r}]$, Eq. 109 becomes

$$\frac{\partial(V_r W_r)}{\partial r} - W_A \frac{\partial W_r}{\partial z} + \frac{2 V_r W_r}{r} \frac{\partial(r W_r)}{\partial r} + 4\omega W_J - 2 \frac{\partial H_E}{\partial r} + 2T \frac{\partial S}{\partial r} = 0 \quad (110)$$

Rewriting Eq. 110 for the rotor discharge and using the substitutions

$$H_R = H_E - \frac{U_E^2}{2} \quad \text{and} \quad T_2 = \frac{H_E}{C_P} - \frac{W_{J2}^2}{2C_P}$$

$$\frac{\partial(V_r W_r)}{\partial r_2} - 2 W_{A2} \frac{\partial V_{r2}}{\partial z} + \frac{2 V_r W_r}{r_2} \frac{\partial(r_2 W_{J2})}{\partial r_2} + 4\omega W_{J2} - 2 \frac{\partial}{\partial r_2} \left(H_E - \frac{U_E^2}{2} \right) + 2 \left(\frac{H_E}{C_P} - \frac{W_{J2}^2}{2C_P} \right) \frac{\partial S}{\partial r_2} = 0 \quad (111)$$

The last term of Eq. 111 can be expressed by

$$\frac{\partial}{\partial r_2} \left[2 H_E - (V_{r2}^2 + V_{J2}^2 + V_{A2}^2) \right] = \frac{1}{C_P} \left[2 H_E - W_{J2}^2 - W_{A2}^2 \left(1 + \frac{V_{r2}^2}{V_{A2}^2} \right) \right] \quad (112)$$

With $\left(\frac{V_{r2}^2}{V_{A2}^2} = \tan^2 \lambda \right)$ and $\left(1 - \tan^2 \lambda = \frac{1}{\cos^2 \lambda} \right)$ Eq. 112 becomes

$$\frac{1}{C_P} \left[2 H_E - W_{J2}^2 \right] = \frac{1}{C_P} \left[2 H_E - W_{J2}^2 \right] - \frac{W_{A2}^2}{C_P \cos^2 \lambda_2} \quad (113)$$

Using Eq. 113, and after rearranging, Eq. 111 becomes

$$\frac{\partial(V_r W_r)}{\partial r_2} - W_{A2} \frac{\partial V_{r2}}{\partial z} - \frac{W_{A2}^2}{C_P \cos^2 \lambda_2} \frac{\partial S_2}{\partial r_2} + 2 \frac{W_{J2}}{r_2} \frac{\partial(r_2 W_{J2})}{\partial r_2} + 4\omega W_{J2} - 2 \frac{\partial H_E}{\partial r_2} + \frac{\partial(U_E^2)}{\partial r_2} + \frac{1}{C_P} \left[2 H_E - W_{J2}^2 \right] \frac{\partial S_2}{\partial r_2} = 0 \quad (114)$$

Noting that

$$\frac{\partial(U_E^2)}{\partial r_2} = \frac{\partial(U_E^2)}{\partial r} = 2\omega^2 r_2 \quad (115)$$

Eq. 114 is

$$\frac{\partial(V_r W_r)}{\partial r_2} - W_{A2} \frac{\partial V_{r2}}{\partial z} - \frac{W_{A2}^2}{C_P \cos^2 \lambda_2} \frac{\partial S_2}{\partial r_2} + 2 \frac{W_{J2}}{r_2} \frac{\partial(r_2 W_{J2})}{\partial r_2} + 4\omega W_{J2} - 2 \frac{\partial H_E}{\partial r_2} + 2\omega^2 r_2 - \frac{1}{C_P} \left[2 H_E - W_{J2}^2 \right] \frac{\partial S_2}{\partial r_2} = 0 \quad (116)$$

This equation is made non-dimensional by multiplying by $(\frac{r_m}{\sqrt{h_{m2}}})$, where the subscript m refers to the mean streamline. In the subsequent derivations the subscript 2 will be omitted. Then

$$\frac{r_m}{W_{Am}^2} \frac{\partial (W_A^2)}{\partial r} - 2 \frac{W_A}{W_{Am}^2} r_m \frac{\partial W_A}{\partial z} - \frac{W_A^2}{W_{Am}^2} \frac{r_m}{c_p \cos^2 \beta} \frac{\partial S}{\partial r} + \frac{W_A r_m}{W_{Am} r} c \left(\frac{r}{r_m} \frac{W_A}{W_{Am}} \right) + 4 \frac{W_A r_m V_{ij}}{W_{Am}^2} - 2 \frac{r_m}{W_{Am}^2} \frac{\partial H_T}{\partial r} - \frac{z \omega^2 r r_m}{W_{Am}^2} + \frac{r_m}{c_p} \left[\frac{2 H_T}{W_{Am}^2} - \frac{W_A^2}{W_{Am}^2} \right] \frac{\partial S}{\partial r} = 0 \quad (117)$$

Now let

$$Y = \frac{W_A}{W_{Am}} \quad (118)$$

$$X = \frac{r}{r_m} \quad (119)$$

$$S^* = \frac{S}{c_p} \quad (120)$$

Equation 117 then becomes

$$\frac{\partial (Y^2)}{\partial X} - 2 \frac{Y^2}{W_A} r_m \frac{\partial W_A}{\partial z} - \frac{Y^2}{\cos^2 \beta} \frac{\partial S^*}{\partial X} + 2Y \frac{\tan \beta}{X} \frac{\partial (XY \tan \beta)}{\partial X} + 4 \frac{W_{Am} Y \tan \beta}{W_{Am}} - \frac{z}{W_{Am}^2} \frac{\partial H_T}{\partial r} + \frac{z \omega^2 U}{W_{Am}^2} + \left[\frac{2 H_T}{W_{Am}^2} - Y^2 \tan^2 \beta \right] \frac{\partial S^*}{\partial X} = 0 \quad (121)$$

The fourth term in Eq. 121 can be expanded and rearranged as

$$2Y \frac{\tan \beta}{X} \left[\frac{\partial}{\partial X} (XY \tan \beta) \right] = 2Y \frac{\tan \beta}{X} \left[XY \frac{\partial \tan \beta}{\partial X} + X \tan \beta \frac{\partial Y}{\partial X} + Y \tan \beta \right] = 2Y^2 \tan \beta \frac{\partial \tan \beta}{\partial X} + 2Y \tan^2 \beta \frac{\partial Y}{\partial X} + \frac{z Y^2}{X} \tan^2 \beta \quad (122)$$

with

$$\frac{\partial \tan \beta}{\partial X} = \frac{1}{\cos^2 \beta} \frac{\partial \beta}{\partial X}$$

and

$$2Y \tan^2 \beta \frac{\partial Y}{\partial X} = \tan^2 \beta \frac{\partial (Y^2)}{\partial X}$$

Equation 122 then is

$$\frac{\partial(Y^2)}{\partial X} (1 + \tan^2 \beta) - 2 \frac{Y^2}{W_A} r_m \frac{\partial W_r}{\partial z} - \frac{Y^2}{\cos^2 \lambda} \frac{\partial s^*}{\partial X} + 2 Y^2 \frac{\tan \beta}{\cos^2 \beta} \frac{\partial \beta}{\partial X} + \frac{2 Y^2}{X} \tan^2 \beta + \frac{4 U_m Y \tan \beta}{W_{Am}} - \frac{2}{W_{Am}^2} \frac{\partial H_E}{\partial X} + 2 \frac{U_m U}{W_{Am}^2} + \left[\frac{2 H_E}{W_{Am}} - Y^2 \tan^2 \beta \right] \frac{\partial s^*}{\partial X} = 0 \quad (122a)$$

Multiplying by $(-\cos^2 \beta / Y^2)$, and with $1 + \tan^2 \beta = \frac{1}{\cos^2 \beta}$,

$$\frac{1}{Y^2} \frac{\partial(Y^2)}{\partial X} + \cos^2 \beta \left(-\frac{2 r_m}{W_A} \frac{\partial W_r}{\partial z} - \frac{1}{\cos^2 \lambda} \frac{\partial s^*}{\partial X} \right) + 2 \tan \beta \frac{\partial \beta}{\partial X} + \frac{2}{X} \sin^2 \beta + \frac{4 U_m \sin \beta \cos \beta}{W_{Am} Y} + \frac{2 U_m U \cos^2 \beta}{W_{Am}^2 Y^2} - \frac{2 \cos^2 \beta}{W_{Am}^2 Y^2} \frac{\partial H_E}{\partial X} + \left[\frac{2 H_E \cos^2 \beta}{W_{Am}^2 Y^2} - \sin^2 \beta \right] \frac{\partial s^*}{\partial X} = 0 \quad (123)$$

The terms $\cos^2 \lambda$ and $\left(\frac{-2 r_m}{W_A} \frac{\partial W_r}{\partial z} \right)$ represent the effects due to streamline curvature and can be approximated by

$$-\frac{1}{W_A} \frac{\partial W_r}{\partial z} = \pm K \frac{\delta r}{L^2} \quad ; \quad K \approx 5 \quad (124)$$

$$\cos^2 \lambda = \frac{L^2}{L^2 + \left(\frac{\Delta R}{2} \right)^2} \quad (125)$$

If the streamline curvature in meridional planes is zero, the terms represented by Eqs. 124 and 125 will take on values of zero and one, respectively. With δr positive as shown in Fig. 2, the plus sign is used for K at station 2 and the minus sign at station 1. The streamline slope as represented by Eq. 125 is the same at stations 1 and 2 since the streamline pattern is assumed to repeat itself after station 2.

Using Eqs. 124 and 125, Eq. 114 then becomes

$$\frac{d(U_m Y^2)}{dX} = -\cos^2 \beta \left[\left(2 K r_m \frac{\delta r}{L^2} \right) \left(\frac{L^2 + \left(\frac{\Delta R}{2} \right)^2}{L^2} \right) \frac{ds^*}{dX} \right] - 2 \tan \beta \frac{d\beta}{dX} - \frac{2}{X} \sin^2 \beta - \frac{4 U_m \sin \beta \cos \beta}{W_{Am} Y} - \frac{2 U_m U \cos^2 \beta}{W_{Am}^2 Y^2} + \frac{2 \cos^2 \beta}{W_{Am}^2 Y^2} \frac{dH_E}{dX} - \left[\frac{2 H_E \cos^2 \beta}{W_{Am}^2 Y^2} - \sin^2 \beta \right] \frac{ds^*}{dX} \quad (126)$$

For the enthalpy terms to be in terms of BTU/lb_m, they must be divided by 2gJ to keep the equation dimensionless. With C₁ = 2g J, Eq. 126 is

$$\frac{d(\ln Y^2)}{dX} = -\cos^2 \beta \left[2K r_m \frac{\delta r}{L^2} - \left(\frac{L^2 + \frac{\Delta R^2}{2}}{L^2} \right) \frac{ds^*}{dX} \right] - 2 \tan \beta \frac{d\beta}{dX} - \frac{2}{X} \sin^2 \beta$$

$$- \frac{4U_m \sin \beta \cos \beta}{W_{Am} Y} - \frac{2U_m U \cos^2 \beta}{W_{Am}^2 Y^2} + \frac{C_1 \cos^2 \beta}{W_{Am}^2 Y^2} \frac{dH_E}{dX} - \left[\frac{C_1 H_E \cos^2 \beta}{W_{Am}^2 Y^2} - \sin^2 \beta \right] \frac{ds^*}{dX} \quad (127)$$

Noting the corresponding terms for the absolute flow of the stator, and with U=0, the equation for station 1 is

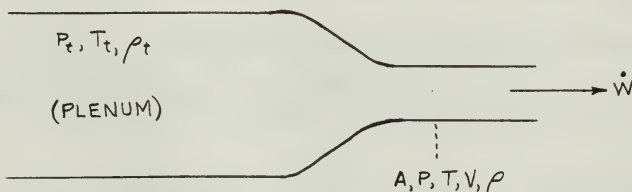
$$\frac{d(\ln Y^2)}{dX} = -\cos^2 \alpha \left[-K r_m \frac{\delta r}{L^2} - \left(\frac{L^2 + \frac{\Delta R^2}{2}}{L^2} \right) \frac{ds^*}{dX} \right] - 2 \tan \alpha \frac{d\alpha}{dX}$$

$$- \frac{2}{X} \sin^2 \alpha + \frac{C_1 \cos^2 \alpha}{Y^2 V_{Am}^2} \frac{dH}{dX} - \left[\frac{C_1 H \cos^2 \alpha}{Y^2 V_{Am}^2} - \sin^2 \alpha \right] \frac{ds^*}{dX} \quad (128)$$

2. Flow Function Φ

Flowrate in lb_m/sec for the expansion process shown in Fig. 44 can be written

$$\dot{W} = \rho A V \quad (129)$$



Expansion From Plenum

Fig. 44

Assuming an isentropic expansion,

$$\frac{T}{T_t} = \left(\frac{P}{P_t} \right)^{\frac{\gamma-1}{\gamma}} \quad (130)$$

and,

$$T_t - T = T_t \left(1 - \frac{T}{T_t} \right) = T_t \left[1 - \left(\frac{P}{P_t} \right)^{\frac{\gamma-1}{\gamma}} \right] \quad (131)$$

then using the thermodynamic relations

$$\frac{V^2}{2gJc_p} = T_t - T \quad \text{and} \quad c_p = \frac{R}{J} \frac{\gamma}{\gamma-1} \quad (132)$$

the discharge velocity can be expressed by

$$V = \left\{ 2gR \frac{\gamma}{\gamma-1} T_t \left[1 - \left(\frac{P}{P_t} \right)^{\frac{\gamma-1}{\gamma}} \right] \right\}^{\frac{1}{2}} \quad (133)$$

The density ρ is found with the isentropic assumption by

$$\frac{P_t}{\rho_t^\gamma} = \frac{P}{\rho^\gamma} \quad (134)$$

or

$$\rho = \left(\frac{P}{P_t} \right)^{\frac{1}{\gamma}} \rho_t = \left(\frac{P}{P_t} \right)^{\frac{1}{\gamma}} \frac{P_t}{RT_t} \quad (135)$$

Using Eqs. 133 and 135, Eq. 129 becomes

$$\dot{W} = A \frac{P_t}{RT_t} \left(\frac{P}{P_t} \right)^{\frac{1}{\gamma}} \left\{ 2gR \frac{\gamma}{\gamma-1} T_t \left[1 - \left(\frac{P}{P_t} \right)^{\frac{\gamma-1}{\gamma}} \right] \right\}^{\frac{1}{2}} \quad (136)$$

This can be rearranged to give

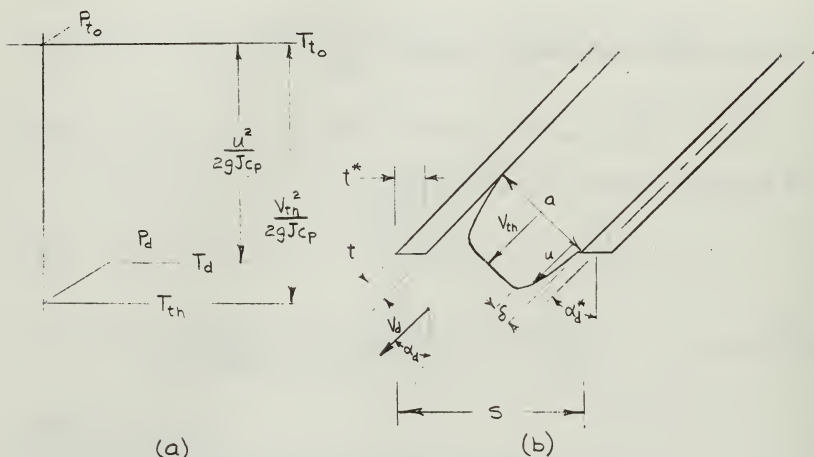
$$\dot{W} = \frac{AP_t}{\left(\frac{P}{P_t} \right)^{\frac{1}{\gamma}} RT_t} \left\{ \frac{2\gamma}{\gamma-1} \left[\left(\frac{P}{P_t} \right)^{\frac{2}{\gamma}} - \left(\frac{P}{P_t} \right)^{\frac{\gamma+1}{\gamma}} \right] \right\}^{\frac{1}{2}} \quad (137)$$

or

$$\frac{\dot{W} \sqrt{T_t}}{4 P_t} \sqrt{\frac{R}{g}} = \left\{ \frac{2\gamma}{\gamma-1} \left[\left(\frac{P}{P_t} \right)^{\frac{2}{\gamma}} - \left(\frac{P}{P_t} \right)^{\frac{\gamma+1}{\gamma}} \right] \right\}^{\frac{1}{2}} \equiv \Phi \quad (138)$$

3. Restriction Factor ¹²

The expansion process through a blade row is shown in Fig. 45 (a). The letter u represents the velocity at some point within the boundary layer and V_{th} represents the velocity for an isentropic expansion. The various dimensions, angles, and velocities for the throat location are shown in Fig. 45(b).



Conditions at Exit of Blade Row

Fig. 45

The mass flowrate per unit blade height can be written

$$\dot{m} = \rho_{th} V_{th} \cos \alpha_d \left[s - \frac{t}{\cos \alpha_d^*} - \frac{\sum \delta}{\cos \alpha_d} \right] + \sum_0^s \int u \rho dy \quad (139)$$

where:

- ρ_{th} = density at P_d for isentropic expansion (slugs/ft³)
- ρ = density corresponding to the velocity u (slugs/ft³)
- α_d^* = blade angle
- δ = boundary layer thickness

¹²Vavra, M. H., Problems of Fluid Mechanics in Radial Turbomachines (Rhode-Saint-Genese, Belgium: Von Kármán Institutefor Fluid Dynamics, 1965) VKI Course Note 55b, pp. G46-50.

For Mach numbers of 0.8 or less, the discharge angle can be calculated quite accurately by

$$\alpha_d = \cos^{-1} \left[\frac{a}{s - \frac{t}{\cos \alpha_d^*}} \right] \quad (140)$$

where:

a = minimum throat width

t = blade thickness

then with $\eta = \frac{y}{\delta}$ and using Eq. 140 in Eq. 139,

$$\dot{m} = \rho_{th} V_{th} \frac{a \cos \alpha_d^*}{s \cos \alpha_d^* - t} \left[\frac{s \cos \alpha_d^* - t}{\cos \alpha_d^*} - \sum \delta \left(\frac{s \cos \alpha_d^* - t}{a \cos \alpha_d^*} \right) \right] + \sum \rho_{th} V_{th} \delta \int_0^1 \frac{\rho}{\rho_{th}} \frac{u}{V_{th}} d\eta \quad (141)$$

which can be expressed as

$$\dot{m} = \rho_{th} V_{th} a \left\{ 1 - \sum \frac{\delta}{a} \left(1 - \int_0^1 \frac{\rho}{\rho_{th}} \frac{u}{V_{th}} d\eta \right) \right\} \quad (142)$$

Assuming constant pressure at the throat,

$$f = \frac{P_d}{P^*}$$

and

$$\frac{\rho}{\rho_{th}} = \frac{T_{th}}{T} \quad (143)$$

where

$$\frac{T_{th}}{T} = \frac{T_{t0} - \frac{V_{th}^2}{2gJc_p}}{T_{t0} - \frac{u^2}{2gJc_p}} = \frac{T_{t0} - \frac{V_{th}^2}{2gJc_p}}{T_{t0} - \left(\frac{V_{th}^2}{2gJc_p} \right) \left(\frac{u}{V_{th}} \right)^2} = \frac{1 - X_e}{1 - X_e \left(\frac{u}{V_{th}} \right)^2} \quad (144)$$

In Eq. 144 the term X_e is

$$X_e = 1 - \frac{T_{th}}{T_{t0}} = 1 - \left(\frac{P_d}{P_{t0}} \right)^{\frac{\gamma-1}{\gamma}} \quad (145)$$

The boundary layer is assumed to be turbulent and the profile can therefore be expressed by

$$\frac{u}{V_{th}} = \left(\frac{y}{\delta} \right)^m = \eta^m \quad (146)$$

Then with the displacement thickness of the boundary layer defined as

$$\delta^* \equiv \delta \left[1 - (1 - X_e) \int_0^1 \frac{\eta^m}{1 - X_e \eta^{2m}} d\eta \right] \quad (147)$$

Eq. 142 can be written

$$\dot{m} = \rho_{th} V_{th} a \left[1 - \frac{\Sigma \delta^*}{a} \right] \quad (148)$$

The loss coefficient to the throat is

$$y = 1 - \frac{V_d^2}{V_{th}^2} \quad (149)$$

The loss coefficient can also be expressed in terms of the kinetic energy lost, by

$$y = \frac{\Delta \dot{E}}{\dot{m} \frac{V_d^2}{2}} = 1 - \frac{\dot{E}}{\dot{m} \frac{V_{th}^2}{2}} \quad (150)$$

where \dot{E} represents energy rate at the discharge due to the average velocity V_d , or

$$\dot{E} = \rho_{th} V_{th} \left[a - \Sigma \delta \right] \frac{V_{th}^2}{2} + \Sigma \int_0^{\delta} \left(u \rho \frac{u^2}{2} \right) dy \quad (151)$$

Equation 151 can be rewritten to give

$$\dot{E} = \rho_{th} \frac{V_{th}^3}{2} a \left\{ 1 - \Sigma \frac{\delta}{a} \left[1 - (1 - X_e) \int_0^1 \frac{\eta^{3m}}{(1 - X_e \eta^{2m})} d\eta \right] \right\} \quad (152)$$

Then using the energy thickness which is defined as

$$\delta^{***} \equiv \delta \left[1 - (1 - X_e) \int_0^1 \frac{\eta^{3m}}{(1 - X_e \eta^{2m})} d\eta \right] \quad (153)$$

the loss coefficient can be expressed by

$$y = 1 - \frac{\rho_{th} \frac{V_{th}^3}{2} a \left[1 - \Sigma \frac{\delta^{***}}{a} \right]}{\dot{m} \frac{V_d^2}{2}} = 1 - \frac{\rho_{th} \frac{V_{th}^3}{2} a \left[1 - \Sigma \frac{\delta^{***}}{a} \right]}{\rho \frac{V_{th}^3}{2} a \left[1 - \Sigma \frac{\delta^*}{a} \right]}$$

or

$$y = 1 - \frac{1 - \Sigma \frac{\delta^{***}}{a}}{1 - \Sigma \frac{\delta^*}{a}} \quad (154)$$

The restriction factor ξ represents that part of the throat opening in which would occur the uniform theoretical velocity, therefore

$$\xi = 1 - \sum \frac{\delta^*}{a} \quad (155)$$

Now defining an energy parameter H^{***} by

$$H^{***} \equiv \frac{\delta^{***}}{\delta^*} \quad (156)$$

Eq. 155 becomes

$$\xi = \frac{H^{***} - 1}{H^{***} - 1 + \frac{y_t}{z}} \quad (157)$$

The loss coefficient y in Eq. 157 accounts for the losses that occur from the inlet to the throat of the blade channel. No means exists for predicting this loss coefficient. Half the total loss coefficient for the blade row $\frac{y_t}{z}$ will be used to represent these losses. Eq. 157 then becomes

$$\xi = \frac{H^{***} - 1}{H^{***} - 1 + \frac{y_t}{z}} \quad (158)$$

4. Method of Evaluating H^{***} ¹³

By use of the binomial theorem, the denominator of the integral part of Eqs. 147 and 153 can be expanded, yielding

$$(1 - X_e \eta^{2m})^{-1} = 1 + X_e \eta^{2m} + X_e^2 \eta^{4m} + X_e^3 \eta^{6m} + X_e^4 \eta^{8m} + \dots$$

The integral of Eq. 153 is then

$$\int_0^1 \left[\eta^{3m} + X_e \eta^{5m} + X_e^2 \eta^{7m} + X_e^3 \eta^{9m} + X_e^4 \eta^{11m} + \dots \right] d\eta$$

Then, integrating and evaluating gives

$$\int_0^1 \frac{\eta^{3m}}{1 - X_e \eta^{2m}} d\eta = \frac{1}{3m+1} + \frac{X_e}{5m+1} + \frac{X_e^2}{7m+1} + \frac{X_e^3}{9m+1} + \frac{X_e^4}{11m+1} + \dots$$

Equation 153 can now be expressed as

$$\frac{\delta^{***}}{\delta} = 1 - \left(\frac{1}{3m+1} + \frac{X_e}{5m+1} + \frac{X_e^2}{7m+1} + \frac{X_e^3}{9m+1} + \frac{X_e^4}{11m+1} + \dots \right) + \frac{X_e}{3m+1} + \frac{X_e^2}{5m+1} + \frac{X_e^3}{7m+1} + \dots$$

¹³Eckert, op. cit., pp. 159-160.

or,

$$\frac{\delta^{***}}{\delta} = 1 + (\chi_e - 1) \left(\frac{1}{3m+1} + \frac{\chi_e}{5m+1} + \frac{\chi_e^2}{7m+1} + \frac{\chi_e^3}{9m+1} + \frac{\chi_e^4}{11m+1} + \dots \right)$$

also,

$$\frac{\delta^{***}}{\delta} = (\chi_e - 1) \left(\frac{1}{\chi_e - 1} + \frac{1}{3m+1} + \frac{\chi_e}{5m+1} + \frac{\chi_e^2}{7m+1} + \frac{\chi_e^3}{9m+1} + \frac{\chi_e^4}{11m+1} + \dots \right)$$

In a similar manner, the expression for Eq. 147 is

$$\frac{\delta^*}{\delta} = (\chi_e - 1) \left(\frac{1}{\chi_e - 1} + \frac{1}{m+1} + \frac{\chi_e}{3m+1} + \frac{\chi_e^2}{5m+1} + \frac{\chi_e^3}{7m+1} + \frac{\chi_e^4}{9m+1} + \dots \right)$$

The energy parameter can now be expressed by

$$H^{***} = \frac{\frac{1}{\chi_e - 1} + \frac{1}{3m+1} + \frac{\chi_e}{5m+1} + \frac{\chi_e^2}{7m+1} + \frac{\chi_e^3}{9m+1} + \frac{\chi_e^4}{11m+1}}{\frac{1}{\chi_e - 1} + \frac{1}{m+1} + \frac{\chi_e}{3m+1} + \frac{\chi_e^2}{5m+1} + \frac{\chi_e^3}{7m+1} + \frac{\chi_e^4}{9m+1}} \quad (159)$$

The number of terms in the numerator and denominator of Eq. 159 is considered sufficient to give good convergence for H^{***} .

Although the exponent m for the turbulent boundary layer is dependent on Reynolds number, it is taken to be a constant for this analysis.

APPENDIX B

COMPUTATION OF OUTLET ANGLES AND LOSS COEFFICIENTS

1. Outlet Angles

The absolute discharge angles for the stator and the relative discharge angles for the rotor are computed by using the same methods. For these calculations, the assumption is made that the outlet angles are not influenced by the flow incidence angles. The factors which do affect the discharge angles are:

1. Blade geometry; this results in the angles being a function of the radius since spacing and possibly profiles change from hub to tip.

2. Radial tip clearance; the effects of tip clearance are assumed to influence the rotor flow from the mean streamline out to the tip, with the largest effect being near the tip.

3. Exit Mach number; in accordance with the experimental results surveyed by Ainley, the outlet angles are a function of Mach number. Values of the angles are calculated for Mach numbers M of 0.5 and 1.0. Then a smooth curve of outlet angle versus M is drawn between these points with an inflection point at $M=0.75$. Below $M=0.5$, the flow angles are assumed to be equal to the value computed for $M=0.5$.

Vavra's formula is used for the first approximation of the stator outlet angles for $M \leq 0.5$.

$$\alpha^* = \cos^{-1} \left(\frac{a/s}{K_t} \right) \quad (160)$$

where

$$K_t = 1 - \frac{2.7}{10^3} \left(\frac{t}{s} 100 \right)^{3.3} \frac{a}{s} \quad (161)$$

The effects of blade curvature are next taken into account by using the method given by Ainley,¹⁴

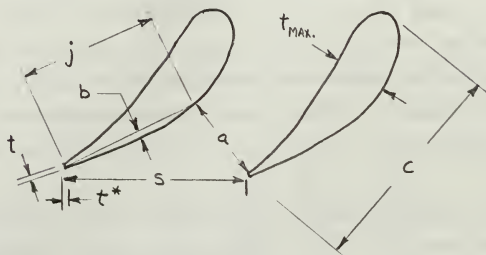
$$\alpha = \alpha^* + 4 \left(\frac{s}{e} \right) \quad (162)$$

¹⁴Ainley, op. cit., pp. 3-4.

In Eq. 162, "e" is the mean radius of curvature of the upper surface of the blade profile between the passage throat and the trailing edge. This quantity is approximated by

$$e = \frac{j^2}{8b} \quad (163)$$

where j and b are shown in Fig. 46.



Blade Geometry

Fig. 46

The discharge angle for $M=1.0$ is found in a manner similar to that described by Ainley,

$$\alpha_{(M_1=1.0)} = \cos^{-1} \left(\frac{a}{s-t^*} \right) \quad (164)$$

The change in α due to the increase in local Mach number from 0.5 to 1.0 is assumed to be constant along the blade height and equal to that computed for the mean radius.

$$\delta \alpha_T = \delta \alpha_H = \alpha_{m(M_1=0.5)} - \alpha_{m(M_1=1.0)} \quad (165)$$

Relative discharge angles for the hub and mean radii of the rotor are found by the same method as used for the stator. The effects of tip clearance are accounted for in the computation of β_2 for the tip position. With Ainley's formula, the flow angle β_2 for the tip is

$$\beta_2 = \tan^{-1} \left\{ \left[1 - X \left(\frac{k}{h} \right) \left(\frac{\cos \beta_0}{\cos \beta_2'} \right) \right] \tan \beta_2' + X \left(\frac{k}{h} \right) \left(\frac{\cos \beta_0}{\cos \beta_2'} \right) \tan \beta_0 \right\} \quad (166)$$

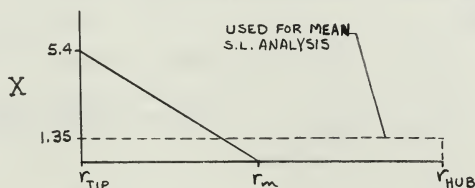
The new terms in Eq. 166 are:

h - blade height

β_2' - discharge angle before tip clearance is accounted for

X - factor which depends on the type of shroud

Ainley suggests that X be set equal to 1.35 if no shroud is arranged at the rotor tips. However, Ainley's value has been determined with a mean streamline analysis. To localize the effects of tip clearance, X has been changed to 5.4, a value which gives about the same overall tip clearance effect as if the value of $X=1.35$ were used for the mean streamline. Fig. 47 shows that the areas under the two lines representing X as a function of radius are approximately equal. The slope of the solid line representing X for this method is obtained because of the assumed linear variation of outlet angle with radius between the mean radius and the tip.



Tip Clearance Factor X as
Function of Radius

Fig. 47

Sample calculations for stator outlet angles are shown in Table I. A sample of rotor outlet angle computations can be seen in Table II.

TABLE I

SAMPLE CALCULATIONS FOR STATOR OUTLET ANGLES

MOD I turbine

$M_1 \leq 0.5$

radius - in.	3.597	4.125	4.950
spacing (s) - in.	1.738	1.994	2.392
throat opening (a) - in.	0.455	0.590	0.804
trailing edge thickness (t) - in.	-----	0.044	-----
$\frac{a}{s}$	0.2619	0.2960	0.3360
$(\frac{t}{s} 100)^{3.3} = A$	21.4	13.6	7.48
$K_t = 1 - (0.0027) (A) (\frac{a}{s})$	0.9849	0.9891	0.9932
$\frac{a}{sK_t}$	0.2658	0.2991	0.3384
$\alpha^* = \cos^{-1} (\frac{a}{sK_t})$	74.6°	72.6°	70.2°
$4 (\frac{s}{e})$	0.703	0.9106	1.37
$\alpha = \alpha^* + 4 (\frac{s}{e})$	<u>75.3°</u>	<u>73.5°</u>	<u>71.6°</u>

$M_1 = 1.0$

Use 4.125 in. from centerline as representative radius.

Projected trailing edge thickness (t*)-in.	0.13		
$\alpha_{1m} = \cos^{-1} (\frac{a}{s-t^*}) - \text{deg.}$	71.5°		
$\delta\alpha = 73.5 - 71.5 = 2.0$			
α	<u>73.3°</u>	<u>71.5°</u>	<u>69.6°</u>

TABLE II
SAMPLE CALCULATIONS FOR ROTOR OUTLET ANGLES

MOD II turbine

tip clearance = 0.033 in.

$M \leq 0.5$

radius - in.	3.3235	4.197	4.918
spacing (s) - in.	1.595	1.4643	1.7158
throat opening (a) - in.	0.382	0.560	0.721
trailing edge thickness (t) - in.	-----	0.048	-----
$\frac{a}{s}$	0.3295	0.3824	0.4202
$(\frac{t}{s})(100)$	4.1397	3.278	2.7975
$(\frac{t}{s}100)^{3.3} = A$	109.0	50.3	29.8
$K_t = 1 - (0.0027)(A)(\frac{a}{s})$	0.9030	0.9481	0.9662
$\frac{a}{sK_t}$	0.3649	0.4033	0.4349
$\beta^* = \cos^{-1}(\frac{a}{sK_t})$	-68.5°	-66.2°	-64.2°
$4(\frac{s}{e})$	1.75	2.37	3.04
$\beta = \beta^* - 4(\frac{s}{e})$	<u>-70.3°</u>	<u>-68.6°</u>	-67.2°
k - in.			0.033
k/h			0.0207
X=(4) (1.35)=type shroud factor			5.4
$\cos \beta_0, \beta_0 = 30^\circ$			0.86603
$\cos \beta_2', \beta_2' = -67.2^\circ$			0.38268
$(X)(\frac{k}{h}) \frac{\cos \beta_0}{\cos \beta_2'} = B$			0.25297
$\tan \beta_2'$			-2.4142
(1-B)tan β_2'			-1.8035
$\tan \beta_0$			0.57735
(1-B)tan β_2' + B TAN $\beta_0 = C$			-1.6574
$\beta_2 = \tan^{-1}(C)$			<u>-58.9°</u>

TABLE II (continued)
 SAMPLE CALCULATIONS FOR ROTOR ANGLE

$$M_2 = 1.0$$

Use radius = 4.197 in. as representative radius.

Projected trailing edge thickness (t*)-in. 0.108

$$\beta_{2m} = \cos^{-1}\left(\frac{a}{s-t^*}\right) \quad -65.6^\circ$$

$$\Delta\beta = -68.6 + 65.6 = -3.0$$

radius - in.

3.3235 4.197 4.918

β_z

-67.3° -65.6° -62.6°

2. Loss Coefficients

Loss coefficients were predicted using Ainley's methods. The techniques used are completely described in Refs. 1 and 2. The assumptions, definitions, and equations which are necessary for a basic understanding of the method are described below.

It is assumed that loss coefficients are independent of Mach number and, for a given glade geometry, are a function of the flow incidence on the blade. Losses are divided into profile losses, secondary losses, and losses due to tip clearance. Mixing losses are not accounted for separately but are included in profile and secondary losses.

A parameter Y is defined by

$$Y = \frac{\text{Loss in total pressure}}{\text{Total pressure at outlet} - \text{outlet static pressure}} \quad (167)$$

For incompressible flow, which is assumed for these calculations, the loss coefficient is

$$C_p = \frac{\sum Y_i}{1 + \sum Y_i} \quad (168)$$

The subscript i on Y in Eq. 168 indicates the type loss represented; i.e., Y_p would be the profile loss.

For zero incidence, the Y for profile losses is

$$Y_{P(i=0)} = \left\{ Y_{P(\beta_o=0)} + \left(\frac{\beta_o}{\beta_d'} \right)^2 \left[Y_{P(\beta_o=-\beta_d')} - Y_{P(\beta_o=0)} \right] \right\} \left(\frac{t_m/c}{0.2} \right)^{-\beta_o/\beta_d'} \quad (169)$$

where:

- β_d' - blade discharge angle not accounting for tip clearance
- t_m - maximum blade thickness
- c - blade chord

Equation 169 is applicable to both the stator and rotor. However, for stator use the blade inlet angle β_o is zero. The quantities $Y_{P(\beta_o=-\beta_d')}$ and $Y_{P(\beta_o=0)}$ are taken from Fig. 4 in Ref. 2 where these quantities are plotted as a function of blade solidity. The maximum value of t_m/c is set equal to 0.25 for thick blades.

To determine profile losses for incidences other than zero, Fig. 6 in Ref. 2 shows $\frac{Y_p}{Y_{P(i=0)}}$ versus $\frac{i}{i_s}$ where i_s is defined as that incidence where the losses are twice the minimum losses.

Secondary and tip clearance losses are computed by

$$Y_s + Y_k = \left[\lambda + B \frac{k}{h} \right] \left[\frac{C_L}{s/c} \right]^2 \frac{\cos^2 \beta_d'}{\cos^3 \beta_m} \quad (170)$$

where:

β_m - the mean of the gas inlet and exit angles of the blade row

B - factor representing type shroud, similar to X

$$\frac{C_L}{s/c} = 2 (\tan \beta_o - \tan \beta_d') \cos \beta_m = f(i)$$

$$\lambda = f \left[\frac{(A_d/A_i)^2}{(1 + \frac{I.D.}{O.D.})} \right] \quad (171)$$

in Eq. 171:

$$A_d = (\text{annulus area at discharge}) (\cos \beta_d')$$

$$A_i = (\text{annulus area at inlet}) (\cos \beta_o)$$

I.D. and O.D. - inner and outer diameters, respectively, at the blade exit

Values of λ are obtained from Fig. 8 in Ref. 2. Ainley suggests a value of 0.5 for B for the type shroud used. With the same reasoning as previously used for the effect of tip clearance on discharge angles, B is set equal to 2.0 for the losses at the tip and zero for the mean radius and hub locations.

Sample calculations for the prediction of stator loss coefficients are shown in Table III. Sample calculations for prediction of stalling incidence and rotor loss coefficients are shown in Table IV.

TABLE III

SAMPLE CALCULATIONS FOR STATOR LOSS COEFFICIENT

MOD I turbine

radius = 3.597 in.

pitch (s) = 1.738 in.

inlet angle (α_0) = 0outlet angle (α_1) = 75.3°

chord (c) = 2.691 in.

All figures referred to are in Ref. 2.

$$Y_{P(i=0)} = \left\{ Y_{P(\alpha_1=0)} + \left(\frac{\alpha_0}{\alpha_1} \right)^2 \left[Y_{P(\alpha_0=-\alpha_1)} - Y_{P(\alpha_0=0)} \right] \right\} \left(\frac{t/c}{0.2} \right)^{-\alpha_0/\alpha_1}$$

$$\alpha_0 = 0 \quad \frac{\text{PITCH}}{\text{CHORD}} = \frac{1.738}{2.691} = 0.6459$$

$$Y_{P(i=0)} = 0.047$$

$$Y_s = \left[\lambda + B \frac{k}{h} \right] \left[\frac{C_L}{s/c} \right]^2 \left[\frac{\cos^2 \alpha_1}{\cos^3 \alpha_m} \right] \quad k=0$$

$$\lambda = f \left[\left(\frac{A_2/A_1} \right)^2 / \left(1 + \frac{I.D.}{0.D.} \right) \right] = f \left\{ (\cos 75.3^\circ)^2 / \left(1 + \frac{6.6}{9.898} \right) \right\} \quad \begin{array}{l} I.D. = 6.6 \text{ in.} \\ 0.D. = 9.898 \text{ in.} \end{array}$$

$$\lambda = f(0.0386) \quad \lambda = 0.0056 \quad (\text{Fig. 8})$$

$$\alpha_m = \tan^{-1} \left(\frac{\tan 75.3^\circ}{2} \right) = \tan^{-1}(1.906) = 62.3^\circ$$

$$\frac{C_L}{s/c} = 2 \left[\tan \alpha_0 - \tan \alpha_1 \right] \cos \alpha_m = 2 \left[-(\tan 75.3^\circ) \right] \cos 62.3^\circ$$

$$\frac{C_L}{s/c} = 3.5438$$

$$Y_s = [0.0056] [3.5438]^2 \left[\frac{\cos^2 75.3^\circ}{\cos^3 62.3^\circ} \right] = 0.0451$$

$$Y_s + Y_p = 0.0929$$

CORRECTION FACTOR FOR TRAILING EDGE THICKNESS, $F = 1.03$
(Fig. 9)

$$(1.03)(0.0929) = 0.0949$$

$$\psi = \frac{0.0949}{1+0.0949} = \underline{0.0866}$$

TABLE IV

SAMPLE CALCULATIONS FOR STALLING INCIDENCE AND ROTOR LOSS COEFFICIENTS

MOD II turbine	$s = 1.7158$ in.	$\beta_0 = 30^\circ$
radius = 4.918	$k = 0.033$ in.	$\beta_2' = -67.2^\circ$
$t_{\max} = 0.728$ in.	$c = 1.967$ in.	blade height(h) = 1.595 in.

Figures referred to are in Ref. 2.

$$Y_{P(i=0)} = \left\{ Y_{P(\beta_0=0)} + \left(\frac{\beta_0}{\beta_2'} \right)^2 \left[Y_{P(\beta_0=-\beta_2')} - Y_{P(\beta_0=0)} \right] \right\} \left(\frac{t/c}{0.2} \right)^{-\beta_0/\beta_2'}$$

$$\frac{t}{c} = \frac{0.728}{1.967} \text{ (USE 0.25)}, \quad -\frac{\beta_0}{\beta_2'} = 0.446, \quad \left(\frac{\beta_0}{\beta_2'} \right)^2 = 0.1993$$

$$\frac{s}{c} = \frac{1.7158}{1.967} = 0.8723, \quad Y_{P(\beta_0=0)} = 0.0365, \quad Y_{P(\beta_0=-\beta_2')} = 0.154 \quad (\text{Fig. 4})$$

$$Y_{P(i=0)} = \left\{ 0.0365 + (0.1993)(0.154 - 0.0365) \right\} (1.25)^{0.446} = 0.0662$$

$$\frac{\beta_2'}{\beta_2 \left(\frac{s}{c} = 0.75 \right)} = 0.955 \text{ (Fig. 7)}, \quad \beta_2 \left(\frac{s}{c} = 0.75 \right) = -70.4^\circ, \quad \frac{\beta_0}{\beta_2 \left(\frac{s}{c} = 0.75 \right)} = 0.426$$

$$i_s \left(\frac{s}{c} = 0.75 \right) = 32.5^\circ, \quad \Delta i_s = -7^\circ \text{ (Fig. 7)}, \quad i_s = 32.5^\circ - 7^\circ = \underline{\underline{25.5^\circ}}$$

$$Y_s + Y_K = \left[\lambda + B \left(\frac{k}{h} \right) \right] \left[\frac{C_L/s/c}{\cos^3 \beta_m} \right]^2 \frac{\cos^2 \beta_2'}{\cos^3 \beta_m} \quad B = 2.0 \quad B \frac{k}{h} = 0.01881$$

$$\cos \beta_2' = 0.38752$$

$$\cos^2 \beta_2' = 0.15017$$

$$\lambda = f \left[\left(\frac{A_2/A_1}{1 + \frac{\text{I.D.}}{\text{O.D.}}} \right)^2 \right]$$

$$\text{I.D. OUTLET} = 3.3235 \text{ in.}$$

$$\text{O.D. OUTLET} = 4.918 \text{ in.}$$

$$\text{I.D. INLET} = 3.3245 \text{ in.}$$

$$\text{O.D. INLET} = 4.8505 \text{ in.}$$

$$\beta_{2m}' = 70.3^\circ$$

$$\frac{A_2}{A_1} = \frac{\pi(4.918^2 - 3.3235^2)}{\pi(4.8505^2 - 3.3245^2)} \frac{\cos 70.3^\circ}{\cos 30^\circ}$$

$$\lambda = f(0.148), \quad \lambda = 0.0072 \quad (\text{Fig. 8})$$

$$Y_s + Y_K = \left[0.0072 + 0.01881 \right] \left[\frac{C_L/s/c}{\cos^3 \beta_m} \right]^2 \frac{0.15017}{\cos^3 \beta_m}$$

$$Y_s + Y_K = (0.003906) \left[\frac{C_L/s/c}{\cos^3 \beta_m} \right]^2 \frac{1}{\cos^3 \beta_m}$$

TABLE IV (continued)
 SAMPLE CALCULATIONS FOR ROTOR LOSS COEFFICIENT

	<u>-1.5</u>	<u>0.0</u>	<u>1.5</u>
i/i_s			
$i = (i/i_s) i_s$	-38.25	0	38.25
$\beta_1 = i + \beta_0$	-8.25	30	68.25
$TAN \beta_1$	-0.1450	0.5774	2.5065
$\frac{TAN \beta_1 + TAN \beta_2'}{2} = A$	-1.2619	-0.9008	0.0638
$\beta_m = TAN^{-1}(A)$	-51.6	-42.0	3.6
$\cos \beta_m$	0.6212	0.7430	0.9980
$TAN \beta_1 - TAN \beta_2' = B$	2.2339	2.9563	4.8854
$C_L/s/c = 2(B) \cos \beta_m$	2.7752	4.3928	9.7510
$[C_L/s/c]^2$	7.7016	19.2964	95.0813
$1/\cos^3 \beta_m$	4.1726	2.4385	1.0061
$Y_s + Y_K = (0.003906) \left[\frac{C_L}{s/c} \right]^2 \frac{1}{\cos^3 \beta_m}$	0.2345	0.3434	0.6980
$Y_P/Y_{P(L=0)}$ (Fig. 6)	2.1	1.0	4.5
$Y_P = [Y_P/Y_{P(L=0)}] Y_{P(L=0)}$	0.1390	0.0662	0.2979
$Y_P + Y_s + Y_K$	0.3735	0.4096	0.9959
(CORRECTION FACTOR)(ΣY) = C (Fig. 9)	0.3922	0.4301	1.0457
$\frac{u}{1+C}$	<u>0.2817</u>	<u>0.3007</u>	<u>0.5112</u>

APPENDIX C

COMPUTER PROGRAM

A computer program using Fortran IV was written for use with the performance analysis. The program was used to predict performance values for the MOD I and MOD II turbines. However, an attempt was made to keep the program general. If the methods of this thesis are utilized for expressing turbine characteristics, this program can be used for other single stage axial turbines.

Input for the program consists of information representing the turbine characteristics, an indicator specifying the detail of output desired, and the conditions for which performance values are to be obtained.

Twenty input cards are used to introduce the turbine characteristics. The information contained on each of these cards, with required dimensions, is listed below.

1. Stator mean streamline gas outlet angles (ALFAM-radians) for mean streamline exit Mach numbers of 0.5, 0.7, 0.75, 0.8 and 1.0.

2. Relative rotor mean streamline gas outlet angles (BETAM-radians) for the same Mach numbers listed in (1.).

3. Radii ahead of the stator (RC-in.) for the five streamlines, such that the flow area is divided into four equal parts.

4. Assumed radii of the five streamlines at the stator exit (RS-in.).

5. Same as (4.), only for the rotor exit plane (RR-in.).

6. The predicted stator loss coefficients (ZETAS) for the hub, mean radius, and tip.

7. Ten values of incidence ratio (RINC) ranging from -2.0 to 1.6, in increments of 0.4.

8. Ten values of rotor loss coefficients (ZETAR1) for the hub corresponding to the incidence ratios of (7.).

9. Same as (8.), only for the mean radius (ZETAR3).

10. Same as (8.), only for the tip (ZETAR5).

11. Length L shown in Fig. 2 (CL-in.) and the curvature factor K (CK).
 12. Differences in stator gas outlet angles (DALF-radians) from the angle for the mean streamline, for streamlines 1, 3, and 5.
 13. Same as (12.), only for the relative rotor outlet angles (DBET).
 14. Ten radii for the stator exit plane, equally spaced or approximately equally spaced, ranging from the radius of the hub to the radius of the tip (R1-in.).
 15. Ten values of stator throat opening (A1-in.) corresponding to the radii of (14.).
 16. Same as (14.), only for the rotor exit plane (R2-in.).
 17. Ten values of rotor throat opening (A2-in.) corresponding to the radii of (16.).
 18. Inlet blade angles for the rotor (BETO-degrees) for the hub, mean radius, and tip.
 19. Ten stall incidence angles (STALI-degrees) corresponding to the radii in (14.).
 20. The radial tip clearance of the rotor (TIPC-in.), the number of stator blades (ZS), and the number of rotor blades (ZR).
- Input card number 21 specifies the output to be printed, and its use will be described later. The remaining input specifies the conditions for which performance values are to be found, and enters the estimations of the flow Mach numbers used for the first approximations in the iteration process. Input card number 22 specifies the number of sets (NSETS) of operating conditions for which solutions are to be found. A card containing the following information is used for each point specified by NSETS:
- a. Estimated Mach number of the flow ahead of the stator (AMC).
 - b. Estimated Mach number of the mean streamline flow after the stator (AMS).
 - c. Total inlet pressure (PTO-psi.).
 - d. Total inlet temperature (TTO-⁰R).

- e. Estimated relative Mach number of the mean streamline flow at the rotor exit (AMR).
- f. The rotor speed (RPM).
- g. The ratio of total inlet to static discharge pressure (PR).

There are eight subroutines in addition to the main or executive part of the program. The subroutines and their main functions are listed below:

1. Subroutine PARAB is used to determine the coefficients of the parabolic equations used to approximate curves.
2. Subroutine LSQPOL determines by the method of least squares the coefficients of the fourth order polynomials used to approximate curves.
3. Subroutine CHAN computes the flowrate and the reference flowrate from conditions ahead of the stator.
4. Subroutine STATOR determines the axial velocity ratios that satisfy the equation of motion at station 1.
5. Subroutine FLOWREF computes the reference flowrate at the stator exit and the rotor exit, and adjusts the axial velocity of the mean streamline flow at these locations to satisfy overall continuity.
6. Subroutine SLINE checks streamline continuity for the stator exit and the rotor exit, and determines new streamline radii to satisfy streamline continuity.
7. Subroutine ROTOR1 converts the absolute flow properties ahead of the rotor to relative flow properties.
8. Subroutine ROTOR2 determines the axial velocity ratios at station 2 that satisfy the equation of motion.

The main program computes the mass-flow-weighted value of total inlet to static discharge pressure ratio, and adjusts the Mach number of the flow ahead of the stator to obtain the pressure ratio specified. The overall turbine performance values of η , M_R , H.P., r^* , and k_{18} are also computed in the main program.

Computer output representing the solution for each set of conditions is printed on two pages. The flow properties at the stator exit plane are printed on one page. A sample of this output can

be seen in Table V. The second page contains the flow properties for the rotor as well as the overall turbine performance values. A sample of the second page of output is in Table VI. Most of the output quantities are self-explanatory. However, the following symbols may not be readily recognized and are defined as:

SLINE - streamline

ZETAP - one-half the total loss coefficient, used for calculating ξ

A - throat opening of the blade channel

W-FRAC - fraction of the flowrate \dot{w} between the hub and the indicated streamline

BO - rotor blade inlet angle

INCID - rotor flow incidence angle

PSIR - relative flow velocity coefficient $\frac{W_2}{W_{2th}}$

In addition to the main output there are additional WRITE statements in the program. The additional output allows the user to follow more closely the intermediate steps of the solution process. This output is also helpful when program changes are made which require debugging. The extra output is not desirable for production runs because of the large amounts of computer running time and printout that result. When the additional output is wanted, 1 is read into the computer on input card number 21 for the indicator IND. If 0 is read into the computer for IND, only the main output representing the final solution will be printed.

The statements of the program are listed on the following pages.

```

0001 RFAL*3 RINC,ZETAR1,Y3,93,T10,C10,A10,R1,A1,Y1,B1,R2,A2,Y2,B2,
0002 1ZETAR3,Y4,B4,ZETAR5,Y5,B5,STALI,Y6,R6
DIMENSION ALFAM(10),BETAM(10),RS(10),RR(10),ZETAR(10),ZETAPR(10),
1DALF(10),DBET(10),ASL(10),ARL(10),X(10),X2(10),YSL(10),BETA2(10),
2TL(10),PL(10),VL(10),VAL(10),ZETAPS(10),WAL(10),VA2(10),WPER1(10),
3SDSX1(10),VU1(10),HELI(10),TELI(10),PTEL(10),WXR(10),PUL(10),R12(10),
4SDSX2(10),WU2(10),WU1(10),VU2(10),VU1(10),SR2(10),SR1(10),R12SR(10),
5R13(10),R14(10),R15(10),PRAT1(10),PRAT2(10),WPER2(10),DMDX(10),U2(10),Y1SR(10),
6P2(10),Y2(10),PRAT3(10),SS(10),ALFAZ2(10)
8 DIMENSION DELH(10),TIR(10),RSTAR(10),PTI(10),T2S(10)
9ZETAI(10),ETAS(10),BETALI(10),PBI(10),RSTAR(10),DELRI(10),WPER(10),ETAR(10),
10ALFA(10),BETAL(10),AMSL(10),ZETAS(20),BETAD(10),MPE(10),RO(10),ZETAS(10),
11ZETARNS(20),ZETAR3(20),ZETAR5(20),BETAD(10),STAL(10)
DIMENSION STL(20),C10(20),A1(20),WGI(20),Y1(20),DELY1(20),B1(20),SB(20),
1TL0(20),S1(20),B2(20),Y3(20),CTI(20),A10(30,30),R2(20),DELY1(20),Y2(20),
2DELY2(20),S1(20),Y3(20),Y4(20),DELY3(20),B3(20),Y4(20),DELY4(20),R4(20),
3Y5(20),DELY5(20),B5(20),Y6(20),DELY6(20),R6(20),RINC(20),DR(10),
4BETALI(10),STALI(10),RINCI(10),AMR2(10),ALFAZ2(10),BETA22(10),
5ALFAM(10),BETALI(10),ZETAI(10),AREAL(10),AREA2(10)
COMMON IND
G=32,174
CJ=778,16
CP=0,24
GAM=1,24
EXPI=GAM/(GAM-1.)
EXP2=1/EXPI
1 READ(5,1) (ALFAM(I),I=1,5)
FORMAL(5,F8.4) (BETAM(I),I=1,5)
2 READ(5,1) (RC(I),I=1,5)
READ(5,1) (RS(I),I=1,5)
0016 READ(5,1) (RA(I),I=1,5)
0017 READ(5,2) (ZETAS(I),I=1,5,2)
783 FORMAT(2F8.4)
0019 READ(5,784) (RINC(I),I=1,10)
0020 FORMAT(5D8.4)
0021 READ(5,3) (ZETAR1(I),I=1,5)
0022 READ(5,3) (ZETAR3(I),I=6,10)
0023 READ(5,3) (ZETAR5(I),I=1,5)
0024 READ(5,3) (ZETAR3(I),I=6,10)
0025 READ(5,3) (ZETAR5(I),I=1,5)
0026 READ(5,3) (ZETAR5(I),I=6,10)
0027 READ(5,783) (CLCK)
0028 READ(5,2) (DALF(I),I=1,5,2)
0029 READ(5,3) (DBET(I),I=1,5,2)
0030 FORMAT(5,2)
0031 READ(5,2) (DBET(I),I=1,5,2)

```

```

0032 READ(5,764)(F1(I),I=1,10)
0033 READ(5,3)(A1(I),I=1,5)
0034 READ(5,3)(A1(I),I=6,10)
0035 READ(5,784)(R2(I),I=1,10)
0036 READ(5,3)(A2(I),I=1,5)
0037 READ(5,3)(A2(I),I=6,10)
0038 FORMAT(10D5.2)
0039 READ(5,764)(BETAQ(I),I=1,5,?)
0040 READ(5,784)(STALI(I),I=1,10)
0041 READ(5,2)I,PC,ZS,ZR
0042 READ(5,4)INDFAM,1,2,3,AA1,BA1,CAL,0.5,0.7,0.8,1.0)
0043 CALL PARAB(ALFAM,3,4,5,AA2,BA2,CA2,0.75,0.8,1.0)
0044 CALL PARAB(BETAM,3,4,5,AB1,CB1,0.5,0.7,0.8,1.0)
0045 CALL PARAB(BETAM,3,4,5,AB2,CB2,0.75,0.8,1.0)
0046 DO 10 I=1,5
0047 X1(I)=RS(I)/RR(3)
0048 X2(I)=RR(I)/RR(3)
0049 RROLDD3=RR(3)
0050 RROLDD4=RR(4)
0051 RROLDD2=RR(2)
0052 RROLDD3=RS(3)
0053 RROLDD4=RS(4)
0054 RROLDD2=RS(2)
0055 RROLDD3=RS(1)
0056 RROLDD4=RS(5)
0057 RROLDD2=RS(4)
0058 RROLDD3=RS(5)
0059 RROLDD4=RS(1)
0060 RROLDD2=RR(3)
0061 RROLDD3=RR(4)
0062 CALL LSQPOLLIC,4,0,0,0,SIGMA,R1,AL,WGT,Y1,DELY1,B1,SB,T10,ST1,
1C10,CT1,A10)
0063 CALL LSQPOLLIC,4,0,0,0,SIGMA,R2,A2,WGT,Y2,DELY2,B2,SB,T10,ST1,
1C10,CT1,A10)
0064 ASFB1(1)+B1(2)*RS(3)+B1(3)*RR(3)**2+B1(4)*RS(3)**3+B1(5)*RS(3)**4
0065 ARFB2(1)+B2(2)*RR(3)+B2(3)*RR(3)**2+B2(4)*RR(3)**3+B2(5)*RR(3)**4
0066 ASFE=ASE
0067 ARFE=ARE
0068 RSE=RR(3)
0069 RREF=RR(3)
0070 ARFE=ARE
0071 XS1=X1(1)
0072 XS2=X1(3)
0073 XS3=X1(5)
0074 XR1=X2(1)
0075 XR2=X2(3)
0076 XR3=X2(5)

```

```

0078 CALL PARAB(BETA0,1,3,5,BR1,RR2,9R3,XS1,XS3,XS5)
0079 CALL LSQPOL(IC,4,0,0,0,SIGMA,RINC,ZETAR1,WGT,Y3,DELY3,R3,SB,TIO,
0080 I,STL,CIO,CY1,AIO)
0081 CALL LSQPOL(IIO,4,0,0,0,SIGMA,RINC,ZETAR3,WGT,Y4,DELY4,R4,SB,TIO,
0082 I,STL,CIO,CY1,AIO)
0083 CALL LSQPOL(IIO,4,0,0,0,SIGMA,RINC,ZETAR5,WGT,Y5,DELY5,R5,SB,TIO,
0084 I,STL,CIO,CY1,AIO)
0085 CALL LSQPOL(III,4,0,0,0,SIGMA,R1,STALI,WGT,Y6,DELY6,R6,SB,TIO,STI,
0086 I,STL,CIO,CY1,AIO)
0087 READ (15,4) NSETS
0088 4 FORMAT (I5)
0089 DO 400 J=1,NSETS
0090 READ (5,5) AMC,AMS,pTO,TTO,AMR,RPM,PR
0091 5 FORMAT (7F8.4)
0092 750 N9=N9+1
0093 IF(N9-10)290,290,223
0094 IF(AMS-0.75)30,40,50
0095 30 ALFAI(3)=AA1+BA1*AMS+CA1*AMS**2
0096 40 ALFAI(3)=ALFAM(3)
0097 50 IF (AMS-1.)280,270,270
0098 270 ALFAI(3)=ALFAM(5)
0099 GO TO 60
0100 280 ALFAI(3)=AA2+BA2*AMS+CA2*AMS**2
0101 90 IF(AMR-0.75)70,80,90
0102 70 BETA2(3)=AB1+BB1*AMR+CB1*AMR**2
0103 GO TO 100
0104 80 BETA2(3)=BETAM(3)
0105 GO TO 100
0106 90 BETA2(3)=AB2+BB2*AMR+CB2*AMR**2
0107 100 RS(2)=RSOLD3
0108 RS(3)=RSOLD3
0109 RS(4)=RSOLD4
0110 DO 530 I=1,5
0111 XI(I)=RS(I)/RS(3)
0112 ASF=ASFE0
0113 RSF=RSFE0
0114 ES2=1.0
0115 VAL(I)=185.0
0116 YS(1)=1.08
0117 YS(2)=1.095
0118 YS(3)=1.973
0119 YS(4)=1.973
0120 YS(5)=.95

```

```

0132 CALL CHAN (TTC,AVC,PTO,RC,WLBM,XCHAN,WPERO)
0133 NS=0
0134 DO R01,K=1,15
0125 CALL STATOR(ALFA1,X1,ITO,PTO,AMS,TI,PI,VI,VA1,S11,SI2,YS,S1,
1DSDX1,VU1,PRAT1,TIIS,SS,DALF,AA1,BA1,CAL,AA2,RA2,CA2,ALFAM,RSF,
2DFLR,C,CK,ZETAPS,RS,RS1,RS3,RS5,ZETAS,DR,ZETA1,NS)
DO I20,I=1,5
PTE(I)=PTO
TTE(I)=TTO
120 CALL FLOWR(PRATI,ZETAPS,X1,WI1,PTF,PTO,TTE,ITD,ASF,ZS,RSF,ASF,
1ZR,RSF,1,WCHAN,VAL,WPER1,CODE,WLAM,B1,RS,TIPC,AREAI)
IF (CODE=20.)R01,8C2,801
801 CONTINUE
802 CALL SLINE (RS,X1,DWD,X,WPER1,WPERO,HE,U2,DHEDX,S1,DSDX1,ASF,PSF,
1FS1,FS2,CODE,I,B1)
IF (CODE=4C.)R10,300,R10
300 VA2(3)=1.85.
YR(1)=1.0
YR(2)=1.0
YR(3)=1.0
YR(4)=1.0
YR(5)=1.0
FC1=1.
FC2=FC1**2
ARF=ARF0
RRF=RROLD3
RR(2)=RROLD2
RR(3)=RRF
RR(4)=RROLD4
DO I71,I=1,5
AMS1(I)=VI(I)/(49.01*SQRT(TI(I)))
X2(I)=OR(I)/RR(I)
71 CONTINUE
0CALL ROTOR1(VU1,VA1,BPM,I1,BETA1,HF,TTE,PTE,X2,PI,T1,W1,WU1,X1,
1RS,ZETAR,ZETAPR,RR,DHEDX,DSDX1,S1,U2,OMEG,BR1,BR2,BR3,FSL,FS2,
2B3,B4,B5,B6,RS1,RS3,RS5,BEID,STALI,TRINCI)
CODE=1.
DO I200,K=1,14
201 CALL ROTOR2 (BETA2,HF,DHEDX,DSDX1,D5X2,VA2,WJ2,W2,VU2,X2,U2,
1YR,ZETAR,R11,R12,R13,R14,RI,SRI,SR2,AA,SR,TTE,PTE,T2,P2,PRAT2,
3RR1,RR3,RR5,AS)
IF (INDS-1)210320,310
320 WRITE (6,36) (AA(I),I=1,5)
36 FORMAT (/35H ENTROPY INDETERMINATE,PRINT AA 1-5, 5F8.3)
GO TO 400
310 CALL FLOWR(PRAT2,ZETAPR,X2,WI1,PTF,PTO,TTE,ITD,ASF,ZS,RSF,ARF,ZR,
1RRF,2,WCHAN,VA2,WPER2,CODE,WLAM,B2,RR,TIPC,AREA2)

```

```

0160 IF (CODE-20.) 20C,13C,200
0161 CONT INUE
0162 CALL SLINE (RR,X2,DWDX,WPER2,WPER0,HE,U2,DHEDX,S1,DSDX1,
1ARF,RRF,FC1,FC2,CODE-2,R2)
IF (CODE-40.) 201,220,201
0163 220 DO 221 I=1,5
0164 DELR(I)=RS(I)-(RC(I)+RR(I))/2.
0165 221 DR(I)=RC(I)-RR(I)
0166 NS=1
0167 DO 881 K=1,15
0168 CALL STATOR(ALFA1,X1,TTO,PTO,AMS,TI,PI,VI,VAL,S11,SI2,YS,S1,
1DSDX1,VU1,PRAT1,TIIS,SS,DALF,AA1,BAL,CAL,AA2,RA2,CA2,ALFAM,RSF,
2DELRC,CL,CK,ZETAPS,RS,RS1,RS3,RS5,ZETAS,DR,ZETA1,NS)
DO 860 I=1,5
PTE(I)=PTO
860 CALL FLOWR(PRAT1,ZETAPS,X1,W11,PTE,PTO,TFE,TTJ,ASF,ZS,RSF,ASF,
1ZR,RSF,1,WCHAN,VAL,WPER1,CODE,WLBM,RI,RS,TIPC,AREA1)
IF (CODE-20.)881,822,881
0174 881 CONT INUE
0175 822 CALL SLINE (RS,X1,DWDX,WPER1,WPER0,HE,U2,DHEDX,S1,DSDX1,ASF,RSF,
1FS1,FS2,CODE-1,81)
IF (CODE-40.) 880,861,880
0177 861 CALL ROTR1(VU1,VAL,RDM,U,BETA1,HE,TFE,PTE,X2,PI,TI,W1,WU1,X1,
2RS,ZETAP,ZETAP2,RR,DHEDX,DSDX1,S1,U2,OMEG,ORI,BR2,OR3,FS1,FS2,
282,84,85,86,RS1,RS3,RS5,BETA,STALI,PRINCI)
CODE=1.
894 DO 896 K=1,10
CALL ROTR2 (BETA2,HE,DHEDX,DSDX1,DSDX2,VA2,WJ2,W2,VU2,V2,X2,U2,
1YR,ZETAR,RI1,RI2,RI3,RI4,RI,SRI,SR2,AA,SR,TFE,PTET2,P2,PRAT2,
3RR1,RR3,RR5,NS)
IF (INDS-1)895,32C,895
895 CALL FLOWR(PRAT2,ZETAPR,X2,W11,PTE,PTO,TFE,TTJ,ASF,ZS,RSF,ARF,ZR,
1RRF,2,WCHAN,VA2,WPER2,CODE,WLBM,B2,RR,TIPC,AREA2)
IF (CODE-20.)896,897,896
896 CONT INUE
897 CALL SLINE (RR,X2,DWDX,WPER2,WPER0,HE,U2,DHEDX,S1,DSDX1,
1ARF,RRF,FC1,FC2,CODE-2,82)
IF (CODE-40.)894,226,894
226 DO 227 I=1,5
227 PRAT3(I)=PIG/P2(I)
PRAT5=(PRAT3(I)+2. * (PRAT3(2)+PRAT3(3)+PRAT3(4) +PRAT3(5)))/8.
DIFF=ABS(PR-PRAT5)
IF (.0003-DIFF)G1C,920,920
910 N11=0
920 N11=1

```

```

0196 GU TO 223
0197 IF (PR,PRAT) 5) 712, 712, 712, 714
0198 AMC=AND-01FF/18.
0199 IF (IND-1) 750, 223, 223
0200 AMC=AMC+DIFF/18.
0201 IF (IND-1) 750, 223, 223
0202 WRITE (6, 999)
0203 FORMAT (1H1)
0204 WRITE (6, 9)
0205 FORMAT (43H
0206 WRITE (6, 7)
0207 FORMAT (/52H
0208 WRITE (6, 8)
0209 J, PTC, TIO, RPM, PR
0210 FORMAT (16X,
0211 15, F8.2, F8.2, F9.0, F6.2)
0212 WRITE (6, 11)
0213 SLINE PI X1 ZETAS ZETAPS Y A)
0214 FORMAT (/47H
0215 50 500, I=1, 5
0216 WRITE (6, 12) I, RS(I), X1(I), ZFTAL(I), ZETAPS(I), YS(I), AREAL(I)
0217 FORMAT (14, 2F8.3, 3F8.3, F8.4)
0218 WRITE (6, 13)
0219 130 FORMAT (/60H
0220 SLINE TI PI ALFAI BETAI UI W-FRAC
0221 IPTO/PI)
0222 DO 510 I=1, 5
0223 AMSL(I)=V1(I)/(49.01*SQRT(TI(I)))
0224 PRATI(I)=V1(I)
0225 PRINCI(I)=RINC(I)*57.3
0226 ALFALL(I)=ALFAI(I)*57.3
0227 BETALL(I)=BETAI(I)*57.3
0228 WRITE (6, 14) I, V1(I), PI(I), ALFALL(I), BETALL(I), U(I), WPERI(I), PRATI(
0229 I)
0230 FORMAT (14, F9.2, F7.2, 2F8.2, F8.2, 2F8.4)
0231 WRITE (6, 15)
0232 FORMAT (751H
0233 SLINE VAI VUI V1 WUI WI MI)
0234 DO 520 I=1, 5
0235 WRITE (6, 16) I, VAL(I), VUI(I), WUI(I), WI(I), AMSI(I)
0236 FORMAT (14, 5F8.1, F8.3)
0237 WRITE (6, 999)
0238 WRITE (6, 17)
0239 ROTOR SOLUTION)
0240 FORMAT (43H
0241 WRITE (6, 7)
0242 J, PTO, TIO, RPM, PR
0243 WRITE (6, 8)
0244 180 FORMAT (/68H
0245 SLINE R2 X2 TTE PTE ZETAR ZETAPR
0246 IPTO/Y
0247 DO 170 I=1, 5
0248 AMR2(I)=W2(I)/(49.01*SQRT(I2(I)))
0249 FORMAT (14, 2F8.3, 2F8.2, 2F8.5, F8.4, FR.1)
0250 WRITE (6, 19) I, RR(I), X2(I), ITE(I), PTE(I), ZETAR(I), ZETAPR(I),

```

```

0241 IYR(I),VA2(I)
0242 WRITE (6,23)
0243 W-FRAC
0244 DO 190 I=1,5
0245 ALFA2(I)=ATAN(WU2(I)/VA2(I))
0246 V2(I)=VA2(I)/COS(ALFA2(I))
0247 ALFA2(I)=ALFA2(I)*.57*3
0248 DELTA2(I)=BETA2(I)*.57*3
0249 FORMAT(I4,F9.2,I7.2,3F8.3,F8.2,F8.5,F8.4)
190 WRITE(6,24)I,I2(I),P2(I),PRAT3(I),ALFA22(I),BETA22(I),U2(I),
WPER2(I),AREA2(I)
0250 WRITE (6,25)
0251 FORMAT (/6RH,SLINE M2 VU2 V2 WU2 W2 R0
ISTAL1
INCID)
0252 DO 210 I=1,5
0253 FORMAT(I4,F8.3,4F8.1,3F8.2)
210 WRITE(6,26)I,AMR2(I),VU2(I),V2(I),WU2(I),W2(I),BETA(I),STAL1(I),
IRINCI(I)
DO 230 I=1,5
0255 DELH(I)=(U(I)*VU1(I)-U2(I)*VU2(I))/(G*CJ)
0256 T12(I)=T10-DELH(I)/CP
0257 T2(I)=P2(I)*((T10-T1(I))/T2(I))*EXP1
0258 PT1(I)=P1(I)*((T10-T1(I))*EXP1
0259 T21S(I)=T10*(P2(I)/PT0)*EXP2
0260 T2S(I)=T10*(P2(I)/PT0)*EXP2
0261 ETAS(I)=(T10-T1(I))/(T10-T2S(I))
0262 ETAS(I)=(T10-T1(I))/(T10-T2S(I))
0263 ETAR(I)=(T10-T1(I)-T2(I))/(T10-T1S(I))
0264 AKSTAR(I)=(T1S(I)-T2(I))/(T10-T2S(I))
0265 AKS(I)=.2*.G*CJ*CP*((T10-T2IS(I))/U(I))*2
0266 PSR(I)=SQRT(ETAR(I))
0267 DELH(I)=0.
0268 DO 240 I=1,4
0269 L=I+1
0270 DELH(I)=DELH(I)+.5*(WPER2(L)-WPER2(L-1))*DELH(I)
0271 HP=DELH(I0)*CJ*WLBW/550.
0272 AMOM=HP*550./OMEG
0273 THETA=SQRT(T0/518.4)
0274 DELTA=PT0/14.7
0275 HPI=HP/(THETA*DELTA)
0276 AMOM1=AMOM/DELTA
0277 RPM1=RPM/THETA
0278 WLBW1=WLBW/THETA/DELTA
0279 WRITE (6,27)
0280 FORMAT (I7,5H,SLINE DELH PT1 TT2 PT2 T2IS T2S)
0281 DO 250 I=1,5
0282 FORMAT (I4,6F,P.2)

```



```

0284 WRITE (6,28) I,DELH(I),PT1(I),TT2(I),PT2(I),T2S(I),T2S(I)
0285 WRITE (6,29)
0286 FORMAT (/59H SLINE ETAI ETAS FTAR PSIR RSTAP AKIS
1 DELH)
0287 DO 260 I=1,5
0288 WRITE (14,29.4,F7.4,2F8.4,F8.5,F8.3,F9.5)
0289 WRITE (6,31) I,ETA1(I),ETAS(I),ETAR(I),PSIR(I),RSTAR(I),AKIS(I),
1 DELH(I)
0290 WRITE (6,32)
0291 FORMAT (/71H HORSE MOMENT FLORATE REF HORSE REF MOMENT
1 WRITE (6,34)
0292 FORMAT (6,34)
0293 WRITE (6,34)
1 RPM LBM/SEC POWER FT-LB LRM/SEC POWER FT-LB RFF
0294 WRITE (6,33) HP,AMOM,WLBM,HPI,AMOM1,RPML,WLBM1
0295 ETAS=(ETAI(1)+ETAI(5))+2.*(ETAI(2)+ETAI(3)+ETAI(4)))/8.
0296 AKIS5=(AKIS(1)+AKIS(5))+2.*(AKIS(2)+AKIS(3)+AKIS(4)))/8.
0297 RSTAR5=(RSTAR(1)+RSTAR(5))+2.*(RSTAR(2)+RSTAR(3)+RSTAR(4)))/8.
0298 WRITE (6,95)
0299 FORMAT (/59H
1 STAP)
0300 WRITE (6,96)ETA5,PRAT5,AMC,AKIS5,RSTAR5
0301 FORMAT(1X,3F6.4,F11.4,F11.5,F10.3,F10.5)
0302 IF(INO-1)400,930,930
0303 IF(NTL-1)750,400,400
0304 CONTINUE
0305 END
0306

```

```

0001 SUBROUTINE PARAB (V,I,J,K,A,B,C,VA21,VAR2,VAP3)
0002 DIMENSION V(10)
0003 COMMON IND
0004 VAR1=VAR1**2
0005 VAR2=VAR2**2
0006 VAR3=VAR3**2
0007 D=VAR2*VAR32-VAR3*VAR22+VAR1*(VAR22-VAR32)+VAR12*(VAR3-VAR2)
0008 L + VAR12*(V(I)*VAR3-V(K)*VAR2)
0009 DB=V(J)*VAR32-V(K)*VAR22+V(I)*(VAR22-VAR32)+VAR12*(V(K)-V(J))
0010 DC=VAR2*V(K)-VAR3*V(J)+VAR1*(V(J)-V(K))+V(I)*(VAR3-VAR2)
0011 A=DA/D
0012 B=DB/D
0013 C=DC/D
0014 RETURN
0015 END

```

```

0001 SUBROUTINE LSQPL(M,KM,IW,ISW,LP,SIGMA,X,F2,K,Y,DELY,B,SB,I,ST,C,
0002 REAL*8 X,F2,Y,B,I,C,A,5,P,BM,D,FBAR,XBAR,PDF,XP,XPXP,XPXPM,XP,
0003 DIMENSION S(20),X(1),F2(1),ST(1),SB(1),F(100),PM(100),P(100),R(1),
0004 COMMON IND
0005 DC 7 I=1,11
0006 DO 4 J=1,11
0007 D(I,J)=0.0D0
0008 CONTINUE
0009 LL=0
0010 SUMEV2=0.0
0011 A(1,1)=1.0
0012 A(2,2)=1.0
0013 FBAR=0.0
0014 XBAR=0.0
0015 D(1,1)=1.0
0016 D(1,1009)=1010,1009
0017 W(1)=1.0
0018 GOT(1011)
0019 W2=SQRT(W(I))
0020 FM=FM+W(I)
0021 F(I)=W2*F2(I)
0022 PM(I)=W2
0023 FBAR=FBAR+F(I)*PM(I)
0024 XBAR=XBAR+F(I)*PM(I)**2
0025 T(1)=FBAR/FM
0026 A(2,1)=XBAR
0027 PDF=0.0
0028 D(20)=1.0
0029 P(I)=(X(I)-XBAR)*PM(I)
0030 PDF=PDF+P(I)*F(I)
0031 P(2)=PDF/PXP
0032 PMXPM=FM
0033 S(1)=PMXPM
0034 KM=KM+1
0035 B(1)=T(1)*A(1,1)+T(2)*A(2,1)
0036 B(2)=T(1)*A(2,2)
0037 D(190K)=2.0*KM
0038 IF(K-2)50,165,65
0039 WRITE(6,4000)
0040
0041
0042
0043
0044
0045

```

```

0046 4000 FOR MAT (7HSTOP 40)
0047      S(0,0) = 0.0
0048      65  XPXB = 0.0
0049      XPXP = 0.0
0050      B(K) = 0.0
0051      D(70) = 1.0 * M
0052      XP = X(J) * P * (J)
0053      XPXD = XPXP + XP * PM(J)
0054      XPXP = XPXP + XP * PM(J)
0055      ALPHA = XPXP / PMXP
0056      BETA = XPXP / PMXP
0057      PPXF = 0.0
0058      PPXP = 0.0
0059      D(90) = 1.0 * M
0060      PT = P(I)
0061      P(I) = X(I) * PT - ALPHA * PT - BETA * PM(I)
0062      PPXF = PPXF + P(I) * F(I)
0063      PPXP = PPXP + P(I) * P(I)
0064      90  PM(I) = PT
0065      I(K) = PPXF / PPXP
0066      PM(X) = PXP
0067      PXP = PPXP
0068      A(K,1) = -ALPHA * A(K-1,1) - BETA * A(K-2,1)
0069      A(K,K-1) = A(K-1,K-2) - A(K-1,K-1) * ALPHA
0070      A(K,K) = 1.0
0071      IF (K-3) 150,150,110
0072      110  K1 = K-2
0073      D(120) = 2.0 * K1
0074      A(K,1) = A(K-1,1) - ALPHA * A(K-1,1) - BETA * A(K-2,1)
0075      150  D(160) = 1.0 * K
0076      160  B(I) = 9(I) + T(K) * A(K,1)
0077      165  SIG3 = 0.0
0078      D(180) = 1.0 * M
0079      Y(I) = POLY(YE(I), X(I), K, B)
0080      DELY(I) = Y(I) - F2(I)
0081      SIG3 = SIG3 + (DELY(I)) ** 2 * W(I)
0082      SIG3 = SIG3 * F2(M)
0083      SIG2 = SIG3 * FLUCAT(M) / FLOAT(M-K)
0084      IF (K-2) 140, 1650, 1651
0085      FLEV2 = 0.0
0086      1650  GO TO 1652
0087      1651  FLEV2 = SUM(V2 - SIG3) / SIG2
0088      SUMV2 = SIG3
0089      SIGMA = SQRT (SIG2)
0090      S(K) = PXP
0091      D(499) = 1.0 * K
0092      ST(I) = SIGMA / SQRT(S(I))
0093      499  D(501) = 1.0 * K

```



```

0142 D(L1,1)=-53.00C/256.00D
0143 DO700 I=1,K
0144 J=K-I+1
0145 VARA=0.0
0146 I1=K-J
0147 IF(I1)702,7C1,7C2
0148 DO703 JJ=1,I1
0149 JK=K-JJ+1
0150 VARA=VARA+D(JK,J)*BM(K,JK)
0151 BM(K,J)=A(K,J)-VARA/D(J,J)
0152 IF(K-2)700,7C4,7C0
0153 BM(1,1)=A(1,1)/D(1,1)
0154 CONTINUE
0155 DO708 I=1,K
0156 C(I)=0.0
0157 DO707 J=1,K
0158 C(J)=C(J)+BM(J,I)*I(J)
0159 SC(I)=SC(I)+(BM(J,I)*ST(J))**2
0160 SC(I)=SQRT(SC(I))
0161 CONTINUE
0162 IF(IND-1)190,192,192
0163 WRITE(6,600)
0164 WRITE(6,1) (I,B(I),SB(I),I=1,K)
0165 WRITE(6,186) SIGMA,FLEV,SUMV2
0166 IF(LP)187,67C,187
0167 WRITE(6,188)
0168 WRITE(6,602) (I,C(I),SC(I),I=1,K)
0169 CONTINUE
0170 WRITE(6,603) (I,X(I),F2(I),Y(I),DELY(I),W(I),I=1,M)
0171 CONTINUE
0172 IF(IND-1)220,211,211
0173 IF(LSH)210,220,210
0174 DO215 I=2,KM
0175 WRITE(6,5) I,(A(I),J),J=1,I)
0176 KM=KM-1
0177 RETURN
0178
0180 1 FORMAT(3H B(OP12,2H)=IPE15.7,6H ERRB=E10.3,3H B(OP12,2H)=IPE15.7,
0181 6H ERRE=E10.3)
0182 2 FORMAT(4H I,1LX 4HX(I),1LX 4HY(I),1LX 7HDELY(I),10X 4HW(I)/)
0183 3 FORMAT(4H O,1LX 4HX(I),1LX 4HY(I),1LX 7HDELY(I),10X 4HW(I),6I)
0184 4 FORMAT(4H O,1LX 4HX(I),1LX 4HY(I),1LX 7HDELY(I),10X 4HW(I),6I)
0185 5 FORMAT(7HOSIGMA=IPE16.7,9H F LEVEL=IPE16.7,12H SUM SQ DEVI=IPE16.7LSQ
0186 * // 45H COEFFICIENTS OF Y=I1*P1+I2*P2+ETC ANDLSQ
0187 1 ERRORS/)
0188 188 FORMAT(23HO LEGENDRE POLYNOMIALS/45H COEFFICIENTS OF Y=C1*U1+C2*U2LSQ
0189 12+ETC AND ERRORS/)
0190 600 FORMAT(41HCCEFFICIENTS OF Y=B1+B2*X+ETC AND ERRORS/)

```

```

0186   FORMAT(3H, T(I2,2H)=1PEI5.7,6H,ERRI=EI1.3,3H, T(OPI2,2H)=1PEI5.7,6H
LSQ
0187   IERRI=EIO.3,3H, T(OPI2,2H)=1PEI5.7,6H,ERRI=EIO.3)
LSQ
0188   IERRC=EIO.3,3H, C(I2,2H)=1PEI5.7,6H,ERRC=EIO.3,3H, C(OPI2,2H)=1PEI5.7,6H
LSQ
0189   IERRM=EIO.3,3H, C(OPI2,2H)=1PEI5.7,6H,ERRC=EIO.3)
LSQ
END

```

```

0001   REAL FUNCTION POLYE1*(X,K,B)
LSQ
0002   DIMENSION B(30)
LSQ
0003   S=B(K)
LSQ
0004   KK=K-1
LSQ
0005   DO 40 I=1,KK
LSQ
0006     S=S*B(IK)
LSQ
0007   END DO
LSQ
0008   POLYE1=S
LSQ
0009   RETURN
LSQ
0010   END
LSQ

```

```

0001 SUBROUTINE CHAN (TT0,AMC,PT0,RC,WLBM,WCHAN,WPERO)
0002 DIMENSION RC(10),WPERO(10)
0003 COMMON /IND /,2*AMC**2)
0004 VC=49.01*SQRT(TC)*AMC
0005 PC=PT0/(1.+2*AMG**2)**3.5-
0006 RHO=PC/(53.35*TC)
0007 AREA= 3.1416*(RC(5)**2-RC(1)**2)
0008 WLBM=RHO*AREA*VC
0009 WCHAN=WLBM/(PT0*SQRT(32.174/(53.35*TT0)))
0010 WPERO(1)=0.
0011 WPERO(2)=.25
0012 WPERO(3)=.5
0013 WPERO(4)=.75
0014 WPERO(5)=1.
0015 RETURN
0016 END
0017

```



```

0001 SUBROUTINE STATOR (ALFAL,X,TTO,PTO,AM,T,P,AVL,VAL,SIL,SIZ,Y,S,DSDX,
0002 1VUL,CK,ZETAPS,R,RS1,RS3,RS5,ZETA,DR,ZETAS,NS)
0003 2DIMENSION ALFAL(10),X(10),T(10),P(10),V(10),VAL(10),SIL(10),
0004 3SIZ(10),Y(10),S(10),DSDX(10),VUL(10),PRAT(10),TUS(10),SS(10),
0005 4DALDX(10),ALFA(10),DALFDX(10),ALFAM(10),AMS(10),DALFDX(10),DELR(10)
0006 5ZETAS(10),ETA(10),ZETAPS(10),R(10),ZETA(10),DR(10)
0007 COMMON IND
0008 CR=0.0
0009 C9=0.0
0010 C1=2.*32.174*778.16*.24
0011 C2=VAL(3)*2/(CI*TI0)
0012 C3=VAL(3)*1.5
0013 IF(R(1)-RS3)C0,301,C2
0014 ZETAS(1)=ZETA(1)+(R(1)-RS1)*(ZETA(3)-ZETA(1))
0015 ALFAL(1)=ALFAL(3)+(R(1)-RS1)/(RS1-RS3)*DALF(1)
0016 GO TO 303
0017 300 ZETAS(4)=ZETA(4)
0018 ALFAL(4)=ALFAL(4)
0019 GO TO 303
0020 301 ZETAS(5)=ZETA(5)
0021 ALFAL(5)=ALFAL(5)
0022 GO TO 303
0023 302 ZETAS(11)=ZETA(3)+(R(1)-RS3)/(RS5-RS3)*(ZETA(5)-ZETA(3))
0024 ALFAL(11)=ALFAL(3)+(R(1)-RS3)/(RS5-RS3)*DALF(5)
0025 ZETAPS(1)=ZETAS(1)/2.0
0026 ETA(1)=1.15
0027 M=1+
0028 IF(I-1)307,307,309
0029 DALFDX(1)=(ALFAL(2)-ALFAL(1))/(X(2)-X(1))
0030 GO TO 315
0031 IF(I-2)311,312,313
0032 DALFDX(1)=.5*((ALFAL(N)-ALFAL(1))/(X(N)-X(1))+(ALFAL(1)-ALFAL(M))/
0033 1(X(1)-X(M)))
0034 GO TO 315
0035 DALFOX(5)=(ALFAL(5)-ALFAL(4))/(X(5)-X(4))
0036 TANL=2.*TAN(ALFAL(1))
0037 PROD=TANL*DALFOX(1)
0038 SINSQ=2.*SIN(ALFAL(1))*2/*X(I)
0039 SIL(1)=MUE
0040 CON(1)=MUE
0041 DO 332 J=1,5
0042 IF(J-1)306,306,310
0043 IF(NS-1)317,310,310
0044 DO 308 I=1,5
0045 SS(I)=0
0046 SI2(I)=SIL(I)
0047 GO TO 518
0048 310 DO 312 I=1,5

```

```

0043 AA=C*Y(I)**2/COS(ALFA(I))**2
0044 AB=(1-AA)/(1.-AA/ETA(I))
0045 S(I)=ALCG(AB)
0046 DSDX(1)=(S(2)/(X(2)-X(1))
0047 DSDX(2)=0.5*(DSDX(1)+(S(3)-S(2))/(X(3)-X(2)))
0048 DSDX(3)=0.5*(S(4)-S(3))/(X(4)-X(3))+(S(3)-S(2))/(X(3)-X(2)))
0049 DSDX(4)=0.5*(S(5)-S(4))/(X(5)-X(4))
0050 DSDX(5)=(S(5)-S(4))/(X(5)-X(4))
0051 DO 316 I=1,5
0052 TF(NS=1)319,321
0053 SS(I)=1.-COS(ALFA(I))**2/(C2*Y(I)**2)*DSDX(I)
0054 CO I=1,6
0055 SS(I)=1.-COS(ALFA(I))**2/(C2*Y(I)**2),SIN(ALFA(I))**2+COS(AL
312 1FAI(I))**2*(CL**2+DR(I)/2.0)**2/CL**2*DSDX(I)+COS(ALFA(I))**2*
314 2CK**2.*RSF*DEL(I)/CL**2
0056 SS(I)+SII(I)
316 SUM1=(S(12(1)+S(12(2)))*(X(2)-X(1)))/4.
318 SUM2=(S(12(2)+S(12(3)))*(X(3)-X(2)))/4.
SUM3=(S(12(3)+S(12(4)))*(X(4)-X(3)))/4.
SUM4=(S(12(4)+S(12(5)))*(X(5)-X(4)))/4.
EN1=-SUM2
EN2=-SUM2
EN3=SUM3
EN4=SUM3+SUM4
Y(1)=1.+EN1*EN1**2/2.+EN1**3/6.+EN1**4/24.+EN1**5/120.
Y(2)=1.+EN2+EN2**2/2.+EN2**3/6.+EN2**4/24.+EN2**5/120.
Y(3)=1.+EN3+EN3**2/2.+EN3**3/6.+EN3**4/24.+EN3**5/120.
Y(4)=1.+EN4+EN4**2/2.+EN4**3/6.+EN4**4/24.+EN4**5/120.
Y(5)=1.+EN5+EN5**2/2.+EN5**3/6.+EN5**4/24.+EN5**5/120.
323 IF(I=0)323,323,323
320 IF(J=1)324,324,320
322 IF(J=5)322,324,322
324 WRITE(6,326)
326 FORMAT(7,57H SLINE C8 C9 ITERATION I,ALFA I,OSDX I,TOTAL
DO 330 I=1,5
328 FORMAT(4,F4.2,F4.2,I9,F12.4,F9.5,F9.4,2F8.4)
330 WRITE(6,328) I,C8,C9,J,SII(I),SS(I),SI2(I),Y(I),ALFA(I)
332 DO 334 I=1,5
334 VAL(I)=VAL(I)*Y(I)
VAL(I)=VAL(I)*TAN(ALFA(I))
VUI(I)=VAL(I)/COS(ALFA(I))
Y(I)=Y(I)-VUI(I)**2/CL
TII(SI)=Y(I)-TIO-TII(SI)/FIAL(I)
P(I)=PTO*(Y(I)-TII(SI)/TIO)**3.5
334 PRAT(I)=P(I)/PTO

```

```

0088
0089
0090
0091
0092
0093
0094
0095
0096
0097
0098
0099
0100
0101
0102
0103
0104
0105
0106
0107
0108
0109
0110
0111
0112
0113
0114
0115
0116
0117
0118
0119
0120
0121
0122
0123
0124
0125
0126

C9=C9+1.
IF(C9-2.) 336, 356, 356
DO(352, 1) 155
AMS(I)=V(I)/(49.01*SQRT(I(I)))
IF(AMS(I)-.5) 338, 344, 346
338 IF(AMS(I)-.5) 340, 340, 342
340 ALFA(3)=ALFAM(I)
GO TO 348
342 ALFA(3)=AA1+BA1*AMS(I)+CA1*AMS(I)**2
GO TO 348
344 ALFA(3)=ALFAM(3)
GO TO 348
346 ALFA(3)=AA2+BA2*AMS(I)+CA2*AMS(I)**2
348 IF(R(I)-RS3) 339, 350, 341
339 ALFA(1)=ALFA(3)+(R(I)-RS3)*DALF(1)
GO TO 352
350 ALFA(1)=ALFA(3)
GO TO 352
341 ALFA(1)=ALFA(3)+(R(I)-RS3)/(RS5-RS3)*DALF(5)
352 CONTINUE
DO(354, I=1, 5)
M=I-1
N=I+1
IF(I-1) 347, 347, 349
347 DALFDX(1)=(ALFA(2)-ALFA(1))/(X(2)-X(1))
GO TO 355
349 IF(I-5) 351, 353, 353
351 DALFDX(I)=.5*((ALFA(N)-ALFA(I))/(X(N)-X(I))+(ALFA(I)-ALFA(M))/
1(X(I)-X(M)))
GO TO 355
353 DALFDX(5)=(ALFA(5)-ALFA(4))/(X(5)-X(4))
355 TANL=-2.*TAN(ALFA(I))
PRND=TANL*CALFDX(I)
SIN SQ=-2.*SIN(ALFA(I))**2/X(I)
354 SIN(I)=PRND+SIN SQ
CONTINUE
GO TO 304
356 RETURN
END

```

```

0001 SUBROUTINE FLOWR(PRAT,ZETAP,X5,WI,PIE,PTO,TTE,IT0,AS,ZS,RS,AR,ZR,
0002 I,REAL*8 B,M,WCHAN,VA,WPER,CODE,WLBM,H,R,TIP,C,A)
0003 DIMENSION PRAT(10),ZETAP(10),X(10),WI(10),PIE(10),TTE(10),
0004 IVAL(10),WPER(10),B(20),A(10),R(10)
0005 COMMON IND
0006 GAM=1.4
0007 G=32.174
0008 A(3)=B(1)+B(2)*R(3)+R(3)*R(3)**2+A(4)*R(3)**3+B(5)*R(3)**4
0009 F(1)=1./(C+1.)
0010 F(2)=1./(3.*C+1.)
0011 F(3)=1./(5.*C+1.)
0012 F(4)=1./(7.*C+1.)
0013 F(5)=1./(9.*C+1.)
0014 F(6)=1./(11.*C+1.)
0015 PRATCR=1.2/(GAM+1.)**((GAM-1.))
0016 PHI=1.2/(GAM+1.)**((1.)/(GAM-1.))*SORT(2.*GAM/(GAM+1.))
0017 DD(1)=1.5
0018 I=1
0019 I=1-PRAT(I)**((GAM-1.)/GAM)
0020 GO TO 404
0021 XE=1.-PRATCR**((GAM-1.)/GAM)
0022 XE2=XE**2
0023 XE3=XE**3
0024 XE4=XE**4
0025 XEINV=1./(XE-1.)
0026 HNUM=XEINV+F2+XE*F3+XE2*F4+XE3*F5+XE4*F6
0027 HSTAR=XEINV*FI+XE*F2+XE2*F3+XE3*F4+XE4*F5
0028 XI=(HSTAR-HNUM)/HDEN
0029 IF (PRATCR-PRAT(I))406,408,408
0030 PHI=SORT(2.*GAM/(GAM-1.))*((PRAT(I)**(2./GAM))-PRAT(I))**
0031 I((GAM+1.)/GAM))
0032 GO TO 410
0033 PHI=PHICR
0034 AVI=B(1)+B(2)*R(I)+B(3)*R(I)**2+B(4)*R(I)**3+B(5)*R(I)**4
0035 ARAT=A(1)+A(3)
0036 IF(1-5)415,414,414
0037 IF(1-5)415,414,414
0038 IF(1-5)415,414,414
0039 IF(1-5)415,414,414
0040 WRITE(6,75H) XI,PHI,ARAT
0041 WTI=(PIE(I)/PTO)/SQRT(TTE(I)/TTO)*ARAT*XI*PHI
0042 SUM1=(WI(1)+WI(2))*((X(1)-X(2))/2.
0043 SUM2=(WI(2)+WI(3))*((X(2)-X(3))/2.
0044 SUM3=(WI(3)+WI(4))*((X(3)-X(4))/2.

```

```

0049 SUM4=(W1(4)+W1(5))*(X(5)-X(4))/2.
0047 YSUM=SUM1+SUM2+SUM3+SUM4
0048 IF (M-1)428,429,428
0049 WREQ=WCHAN/(AS*ZS*RS)
0050 DIFF=ABS(WREQ-WSUM)
0051 GO TO 430
0052 WREQ=WCHAN/(AR*ZR*RR)
0053 DIFF=ABS(WREQ-WSUM)
0054 IF (DIFF-.0002)432,432,434
0055 VA(3)=VA(3)
0056 CODE=20.
0057 GO TO 442
0058 IF (WSUM-WREQ)436,432,438
0059 VA(3)=VA(3)+DIFF/.00065
0060 GO TO 442
0061 VA(3)=VA(3)-DIFF/.00065
0062 WPER(1)=SUM1/WSUM
0063 WPER(2)=(SUM1+SUM2)/WSUM
0064 WPER(3)=(SUM1+SUM2+SUM3)/WSUM
0065 WPER(4)=(SUM1+SUM2+SUM3)/WSUM
0066 WPER(5)=1.450,423,423
0067 IF (IND-1)450,423,423
0068 WRITE (6,422) (W1(I),I=1,5)
0069 FORMAT (7,20H FLOW INTEGRAND 1-5, 5F10.5)
0070 WRITE (6,424) SUM1,SUM2,SUM3,SUM4,WSUM
0071 FORMAT (7,15H Sums 1-4,WSUM, 5F10.5)
0072 WRITE (6,440) WSUM,WREQ,VA(3)
0073 FORMAT (35H REF FLOWS,COMPUTED-REQUIRED,AX VE1,2F10.4,F10.2)
0074 WRITE (6,444) WCHAN,WLBM
0075 FORMAT (7,36H REF FLOW RATE CHANNEL-SQUARE INCHES,F8.5,18H FLOW RATE
0076 | LB/SEC,E8.5)
0077 WRITE (6,446) M
0078 FORMAT (7,30H STREAMLINE FLOW FRACTIONS, M=,I2)
0079 WRITE (6,448) X(2),WPER(2),X(3),WPER(3),X(4),WPER(4)
0080 FORMAT (6F10.4)
0081 RETURN
0082 END

```

```

0001 OSUBROUTINE SLINE (PR,X,DWDX,WPER2,WPER1,HE,U,DHEDX,S,DSDX1,
0002 IARR,RRF,FC1,FC2,CODE,M,B)
0003 REAL*8 B
0004 DIMENSION RR(10),X(10),DWDX(10),WI(10),WPER2(10),WPER1(10),HE(10),
0005 DHEDX(10),S(10),DSDX1(10),U(10),B(20)
0006 COMMON IND
0007 N7=0
0008 SAVE=RR(3)
0009 CODE=1.
0010 DO 700 I=1,4
0011 J=I+1
0012 DWDX(I)=(WPER2(J)-WPER2(I))/(X(J)-X(I))
0013 DO 720 I=2,4
0014 K=I+1
0015 J=I-1
0016 IF (ABS(WPER2(I)-WPER1(I))-0.02)716,716,702
0017 IF (WPER2(I)-WPER1(I))704,716,708
0018 IF (M-1)706,712,706
0019 SL=(HE(K)-HE(I))/X(K)-X(I)
0020 DEL=2.*(SL-DHEDX(I))/X(K)-X(I)
0021 DHEDX(I)=DHEDX(I)+DEL*XN-X(I)
0022 HE(I)=HE(I)+DHEDX(I)
0023 SL=(S(K)-S(I))/X(K)-X(I)
0024 DEL=2.*(SL-DSDX1(I))/X(K)-X(I)
0025 DSDX1(I)=DSDX1(I)+DEL*XN-X(I)
0026 S(I)=S(I)+DSDX1(I)
0027 GO TO 712
0028 XN=X(I)-WPER2(I)-WPER1(I)/DWDX(I)
0029 IF (M-1)710,712,710
0030 SL=(HE(I)-HE(J))/X(I)-X(J)
0031 DEL=2.*(DHEDX(I)-SL)/X(I)-X(J)
0032 DHEDX(I)=DHEDX(I)+DEL*XN-X(I)
0033 HE(I)=HE(I)+DHEDX(I)
0034 SL=(S(I)-S(J))/X(I)-X(J)
0035 DEL=2.*(DSDX1(I)-SL)/X(I)-X(J)
0036 DSDX1(I)=DSDX1(I)+DEL*XN-X(I)
0037 S(I)=S(I)+DSDX1(I)
0038 RR(I)=XM*SAVE
0039 GO TO 718
0040 N=N+1
0041 IF (N-3)720,730,720
0042 U(I)=U(I)*XN/X(I)
0043 CONTINUE
0044 DO 720 I=1,5
0045 X(I)=RR(I)/RR(3)
0046 FC1=RR(3)/SAVE

```

```

0047
0048
0049
0050
0051
0052
0053
0054
0055
0056
0057
0058
0059
0060

FCZ=FCI#2
RRZ=RR(3)
RRF=R(1),B(2)*RRF+B(3)*RRF**2+B(4)*RRF**3+B(5)*RRF**4
AKF=R(1),732,721,721
IF(IIND-1),729,732,729
IF(JM-1),724,724)
721 FORMAT (7,47H SLINE XNEW HENEW DHEDX S-NEW DSDX1)
729 WRITE (6,724)
724 DO 728 I=1,5
726 FORMAT (14,F9.4,F9.2,F9.4,F9.6,F9.5)
728 WRITE (6,726) I,X(I),HE(I),DHEDX(I),S(I),DSDX1(I)
730 CODE=40.
732 RETURN
END

```

```

0001 OSUBROUTINE RCTOR1(VUL,VAL,RPM,U,BETA1,HE,TTE,X2,P1,I,WI,WUL,
1X1,RS,ZETAPR,RR,DHEDX,DSDX,S,U2,OMEG,BP1,BR2,RR3,FS1,FS2,
2B3,B4,B5,B6,RS1,RS2,RS3,RS5,BFO,STALI,RINC)
0002 REAL*8 B3,B4,B5,B6
0003 DIMENSION VUL(10),VAL(10),U(10),BETA1(10),HE(10),TTE(10),PTE(10),
1X2(10),P1(10),WI(10),WUL(10),X1(10),RS(10),ZETAR(10),
2ZETAPR(10),RR(10),DHEDX(10),DSDX(10),S(10),U2(10),ZETA(10),
3B3(20),B4(20),B5(20),B6(20),BETO(10),STALI(10),RINC(10)
0004 COMMON IND
0005 C=2*.332-174*778-16*.24
0006 OMEG=RP/3-1416/30.
0007 DO 520 I=1,5
0008 U(I)=OMEG*RS(I)/12
0009 U2(I)=U(I)*RR(I)/RS(I)
0010 WUL(I)=U(I)-U(I)
0011 BETA1(I)=ATAN(WUL(I)/VAL(I))
0012 W(I)=VAL(I)/COS(BETA1(I))
0013 PTE(I)=1(I)+W(I)*Z/C+(U2(I)**2-U(I)**2)/C
0014 PTE(I)=PI(I)*TTE(I)/I(I)**3.5
0015 HE(I)=TTE(I)*.24
0016 BETO(I)=BR1+FS*BR2*X1(I)+FS2*BR3*X1(I)**2
0017 STALI(I)=B6(1)+B6(2)*RS(I)+B6(3)*RS(I)**2+B6(4)*RS(I)**3+B6(5)*RS
1(I)**4
0018 RINC(I)=BETA1(I)-BETO(I)/57.3
0019 BINC=BINC(I)/(STALI(I)/57.3)
0020 IF(IND-I)510,501,501
0021 IF(RINC+2.0)500,500,502
0022 500 RINC=-2.0
0023 GO TO 506
0024 IF(RINC-I+.6)510,504+504
0025 504 RINC=1.6
0026 WRITE(6,508)RINC
0027 FORMAT(15.1)
0028 ZETA(1)=B3(1)+B3(2)*RINC+B3(3)*RINC**2+B3(4)*RINC**3+B3(5)*RINC
1+*4
0029 ZETA(3)=B4(1)+B4(2)*RINC+B4(3)*RINC**2+B4(4)*RINC**3+B4(5)*RINC*
1+4
0030 ZETA(5)=B5(1)+B5(2)*RINC+B5(3)*RINC**2+B5(4)*RINC**3+B5(5)*RINC
1+*4
0031 IF(RS(I)-RS3)512,514,516
0032 ZETAR(I)=ZETA(I)+(RS(I)-RS1)/(RS3-RS1)*(ZETA(3)-ZETA(1))
0033 GO TO 518
0034 ZETAR(I)=ZETA(3)
0035 GO TO 518
0036 ZETAR(I)=ZETA(3)+(RS(I)-RS3)/(RS5-RS3)*(ZETA(5)-ZETA(3))
0037 ZETAPR(I)=ZETAR(I)/2.0
0038 CONTINUE

```



```

0039
0040
0041
0042
0043
0044
0045
0046
0047
0048
0049
0050
0051

DSDX(1)=(S(2)-S(1))/(X2(2)-X2(1))
DSDX(2)=0.5*(DSDX(1)+S(3)/(X2(3)-X2(2)))
DSDX(3)=(S(4)-S(3))/(X2(4)-X2(3))+S(2)/(X2(3)-X2(2))
DSDX(4)=(S(4)-S(3))/(X2(5)-X2(4))
DSDX(5)=0.5*(DSDX(1)+S(4)/(X2(5)-X2(4)))/(X2(4)-X2(3))
DHEDX(1)=(HE(2)-HE(1))/(X2(2)-X2(1))
DHEDX(2)=0.5*(DHEDX(1)+(HE(3)-HE(2))/(X2(3)-X2(2)))
DHEDX(3)=0.5*(DHEDX(1)+(HE(3)-HE(2))/(X2(3)-X2(2))+HE(4)-HE(3))/
1 (X2(4)-X2(3))
DHEDX(5)=(HE(5)-HE(4))/(X2(5)-X2(4))
DHEDX(4)=0.5*(DHEDX(5)+(HE(4)-HE(3))/(X2(4)-X2(3)))
522 CONTINUE
RETURN
END

```

```

0001 SUBROUTINE ROTR2 (BETA2, HE, DHEDX, DSDX1, DSDX2, VA2, WU2, W2, WU2, V2,
0002 X2, Y2, YETAR, RI1, RI2, RI3, RI4, RI, SPI, SR2, AA, SA, ITE, PTE, I2, P2, PRAT2,
0003 BETA2, BETAM, ARI, ARI, CBI, A92, BR2, CR2, RRF, DELR, CL, CK, DR, R,
0004 DIMENSION BETA2(10), HE(10), DHEDX(10), DSDX1(10), DSDX2(10), VA2(10),
0005 WU2(10), W2(10), YETAR(10), Y2(10), YU(10), YR(10), YETAR(10),
0006 RI1(10), RI2(10), RI3(10), RI4(10), RI(10), SPI(10), SR2(10), YU(10),
0007 YR(10), YETAR(10), Y2(10), P2(10), PRAT2(10), I2(10), P2(10), I2(10),
0008 YU(10), YR(10), BETAM(10), AMK(10), DBETDX(10), SETA(10), DELR(10), RI5(10),
0009 Y2(10), P2(10)
0010 COMMON /IND
0011 IND$1=0
0012 C=2.*32.174*778.16
0013 GAM=1.4
0014 C1=C/VA2(3)**2
0015 DO 274 I=1,5
0016 IF(R(I)-RR3)270,271,273
0017 BETA2(I)=BETA2(3)+(R(I)-RR3)/(RR1-RR3)*DBET(1)
0018 GO TO 274
0019 BETA2(I)=BETA2(3)
0020 GO TO 274
0021 BETA2(I)=BETA2(3)+(R(I)-RR3)/(RR5-RR3)*DBET(5)
0022 CONTINUE
0023 DBETDX(1)=(BETA2(2)-BETA2(1))/(X2(2)-X2(1))
0024 DBETDX(5)=(BETA2(5)-BETA2(4))/(X2(5)-X2(4))
0025 DO 280 I=2,4
0026 M(I)=1
0027 N(I)=1
0028 DBETDX(I)=5*(BETA2(N)-BETA2(1))/(X2(N)-X2(1))+(BETA2(I)-BETA2
0029 1(M))/X2(I)-X2(M))
0030 DO 10 I=1,5
0031 TAN(BETA2(I))
0032 PROD=TAN*BDBETDX(I)
0033 SIN1=-2.*SIN(BETA2(I))*2/X2(I)
0034 RI1(I)=PROD+SINI+DSDX1(I)
0035 SR1(I)=-4.*U(3)*COS(BETA2(I))*SIN(BETA2(I))/(VA2(3)*YR(I))
0036 SR2(I)=2.*U(3)*U(1)*COS(BETA2(I))*2/(VA2(3))*2*YR(I)**2
0037 YOLD(I)=YR(I)
0038 AAI1=(VA2(3)*YR(I)/COS(BETA2(I)))*2/(C*HE(I))
0039 AAI3(I)=C*COS(BETA2(I))*2/(VA2(3)*YR(I))*2*D+EDX(I)
0040 IF (IND$1-1)10,250,250
0041 CONTINUE
0042 IFCIND-1,201,282,282
0043 WRITE(6,121)(RI1(I),I=1,5)
0044 FORMAT(234) CONSTANT INTEGRAND 1-5, 5F8.5)
0045 WRITE(6,122)
0046 FORMAT(60H) SLINE INDS1 GRAD S INT2 INT3 INT4 INT
0047 1,22

```

```

0040 1Y VAL)
0041 DO 20 J=1,13
0042 I=1,5
0043 AA(I)=AA(I)*YR(I)/YOLD(I)**2
0044 ANUM=1.-AA(I)
0045 ADEN=1.-AA(I)/(1.-ZETAR(I))
0046 AB=ANUM/ADEN
0047 IF (CAB) 130,130,30
0048
0049
0050
0051
0052
130 IND5=1
GO TO 150
30 SR(I)=ALOG(ANUM/ADEN)
DSDX2(1)=(SR(2)-SR(1))/(X2(2)-X2(1))
DSDX2(2)=0.5*(DSDX2(1)+(SR(3)-SR(2))/(X2(3)-X2(2)))
DSDX2(3)=0.5*(DSDX2(2)+(SR(4)-SR(3))/(X2(4)-X2(3)))
DSDX2(4)=0.5*(DSDX2(3)+(SR(5)-SR(4))/(X2(5)-X2(4)))
DSDX2(5)=0.5*(DSDX2(4)+(SR(6)-SR(5))/(X2(6)-X2(5)))
DO 40 I=1,5
SR(I)=SR(I)*YOLD(I)/YR(I)
SR2(I)=SR2(I)*YOLD(I)/YR(I)**2
R1(I)=R1(I)*YOLD(I)/YR(I)**2
R2(I)=R2(I)*YOLD(I)/YR(I)**2
R3(I)=R3(I)*YOLD(I)/YR(I)**2
R4(I)=R4(I)*YOLD(I)/YR(I)**2
R5(I)=R5(I)*YOLD(I)/YR(I)**2
31 RI+II=DSDX2(I)-(DSDX1(I)+DSDX2(I))*CI*HE(I)
GO TO 40
32 R15(I)=-((DSDX1(I)+DSDX2(I))*CI*HE(I))*COS(BETA2(I))/YR(I)**2
R15(I)=-((DSDX1(I)+DSDX2(I))*CI*HE(I))*SIN(BETA2(I))*2+COS(BETA2(I))*2
1*(CL**2+(DR(I)/2.0)**2)/CL**2
2DELR(I))/CL**2
40 RI(I)=R1(I)+R2(I)+R3(I)+R4(I)+R5(I)
SUM1=(RI(1)+RI(2))*X2(2)-X2(1)/4.
SUM2=(RI(3)+RI(4))*X2(3)-X2(2)/4.
SUM3=(RI(5)+RI(6))*X2(4)-X2(3)/4.
SUM4=(RI(7)+RI(8))*X2(5)-X2(4)/4.
EN2=-(SUM2+SUM1)
EN3=-SUM2
EN4=-SUM3
EN5=-SUM4
DO 50 I=1,5
YR(I)=YR(I)+EN1**2/2.+EN2**3/6.+EN3**4/24.+EN4**5/120.
YR(I)=YR(I)+EN1**2/2.+EN2**3/6.+EN3**4/24.+EN4**5/120.
YR(I)=YR(I)+EN1**2/2.+EN2**3/6.+EN3**4/24.+EN4**5/120.
YR(I)=YR(I)+EN1**2/2.+EN2**3/6.+EN3**4/24.+EN4**5/120.
YR(I)=YR(I)+EN1**2/2.+EN2**3/6.+EN3**4/24.+EN4**5/120.
NCOUNT=0
0062
0063
0064
0065
0066
0067
0068
0069
0070
0071
0072
0073
0074
0075
0076
0077
0078
0079
0080
0081
0082

```

```

0083 DO 110, I=1,5
0084 TEST=ABS(YCLD(I))-YR(I)
0085 IF(TEST<.005)GO,119,119
0086 NCOUNT=NCOUNT+1
0087 IF(NCOUNT-5)119,140,119
0088 IF(IND-1)20,120,120
0089 IF(J-3)80,100,80
0090 IF(J-9)140,100,80
0091 IF(J-12)20,100,20
0092 DO 60, I=1,5
0093 FORMAT(I4,I7,F10.5,F8.4)
0094 WRITE(6,123) I,INDSL,DSDX2(I),RI2(I),RI3(I),RI4(I),RI(I),YR(I)
0095 CONTINUE
0096 DO 70, I=1,5
0097 VA2(I)=YR(I)*VA2(3)
0098 Y2(I)=VA2(I)/COS(BETA2(I))
0099 YZ(I)=YE(I)-W2(I)*Z(O.24*C)
0100 IF(INDSL-1)251,149,149
0101 INDSL=INDSL+1
0102 DO 250, I=1,5
0103 AMR(I)=W2(I)/(49.01*SQRT(T2(I)))
0104 IF(AMR(I)-.75)1,4,5
0105 IF(AMR(I)-.5)2,2,3
0106 BETA(3)=BETAM(I)
0107 GO TO 6
0108 BETA(3)=AB1+RB1*AMR(I)+CB1*AMR(I)**2
0109 GO TO 6
0110 BETA(3)=BETAM(3)
0111 GO TO 6
0112 BETA(3)=AB2+RB2*AMR(I)+CB2*AMR(I)**2
0113 IF(R(I)-R63)221,222,223
0114 BETA2(1)=BETA(3)+(R(I)-RR3)/(RR1-RR3)*DBET(1)
0115 GO TO 250
0116 BETA2(1)=BETA(3)
0117 GO TO 250
0118 BETA2(1)=BETA(3)+(R(I)-RR3)/(RR5-RR3)*DBET(5)
0119 CONTINUE
0120 DBETDX(1)=(BETA2(2)-BETA2(1))/(X2(2)-X2(1))
0121 DBETDX(5)=(BETA2(5)-BETA2(4))/(X2(5)-X2(4))
0122 DO 224, I=2,4
0123 M=I-1
0124 N=I+1
0125 DBETDX(I)=5*((BETA2(N)-BETA2(I))/(X2(N)-X2(I))+(BETA2(I)-BETA2
0126 1(M))/(X2(I)-X2(M)))
0127 DO 225, I=1,5
0128 TANI=-2.*TAN(BETA2(I))
0129 PROD=TANI*CBETDX(I)

```

```

0130
0131
0132
0133
0134
0135
0136
0137
0138
0139
0140
0141
0142
0143
0144
0145
0146
-----
SIN1=-2.*SIN(BETA2(I))**2/X2(I)
R1(I)=PROD+SIN1+DSDX1(I)
SR1(I)=-4.*U(3)*COS(BETA2(I))*SIN(BETA2(I))/(VA2(3)**2*YR(I))
SR2(I)=2.*U(3)*U(I)*COS(BETA2(I))**2/(VA2(3)**2*YR(I)**2)
YOLD(I)=YR(I)
AA(I)=(VA2(3)*YR(I)/COS(BETA2(I))**2/(C*HE(I)))
R13(I)=C*COS(BETA2(I))**2/(VA2(3)*YR(I))**2*D*EDX(I)
CONTINUE
GO TO 281
225
149 DO 190 I=1,5
WU2(I)=VA2(I)*TAN(BETA2(I))
WU3(I)=WU2(I)+U(I)
Y2(I)=WU3(I)-TIE(I)-T2(I)/(1.-ZETA(I))
P2(I)=P1(I)*(Y2(I)/TIE(I))**(GAM/(GAM-1.))
PRAT2(I)=P2(I)/PTE(I)
190 RETURN
150 END

```

STATOR SOLUTION TABLE V

SET NO.	PTD	TTC	RPM	PR	
1	17.20	568.00	12000.	1.30	
SLINE	RI	ZETAS	ZETAPS	Y	A
1	3.309	0.09040	0.04520	1.01316	0.3801
2	3.720	0.08411	0.04205	1.00784	0.5082
3	4.220	0.07924	0.03662	1.00097	0.7191
4	4.609	0.07520	0.03380	0.98457	0.7123
5	4.949	0.07340	0.03370	0.96925	0.8017
SLINE	PI	ALFAI	BETAI	UI	W-FRAC
1	11.65	76.77	60.35	345.58	0.0
2	542.40	74.61	42.91	397.84	0.2507
3	546.54	73.78	16.50	441.94	0.4998
4	549.16	72.40	-11.09	481.73	0.7503
5	551.26	71.60	-33.20	518.31	1.0000
SLINE	VAI	VI	WUI	MI	PTO/PI
1	148.1	623.5	260.1	0.550	1.2539
2	147.3	534.8	136.9	201.1	1.1932
3	146.2	507.8	144.4	152.7	1.1579
4	143.9	457.5	-28.2	146.6	1.1365
5	141.7	448.6	-92.7	169.3	1.1198

ROTOR SOLUTION TABLE VI

SEI NO.	PTO	ITO	RPM	PR	VA2		
1	17.20	568.00	12000.	1.30			
SLINE	R29	TIE	PIE	ZETA	ZETAPR	Y	VA2
1	0.729	541.37	14.23	0.18994	0.08447	0.9085	129.7
2	0.876	544.35	14.60	0.18121	0.08080	0.9731	138.9
3	0.889	547.33	14.95	0.10912	0.08456	1.0000	142.8
4	0.552	550.35	15.27	0.16709	0.08354	1.0454	149.2
5	0.929	553.46	15.58	0.21749	0.10875	1.1002	157.1
SLINE	T2	PTO/P2	ALFA2	BETA2	U2	M-FRAC	A
1	532.03	1.300	2.209	-67.104	312.01	0.0	0.3515
2	531.17	1.299	0.911	-69.578	375.17	0.25023	0.3662
3	530.42	1.319	0.817	-71.654	428.18	0.50011	0.3731
4	533.28	1.299	-0.304	-71.432	476.66	1.75143	0.3639
5	533.90	1.298	20.116	-71.104	516.22	1.00000	0.3639
SLINE	M2	V2	WU2	BD	STALI	INCID	
1	0.352	129.8	-307.0	33.3	13.48	-2.09	
2	0.402	138.8	-373.0	398.0	62.42	0.80	
3	0.419	142.8	-420.3	428.5	42.12	-3.94	
4	0.428	152.7	-428.7	468.5	20.84	-6.48	
5	0.428	167.3	-458.7	488.8	21.61	-8.28	
SLINE	DELH	PI1	IT2	T2S	T2S		
1	8.30	16.84	533.33	526.96	530.15		
2	8.46	16.94	532.98	527.06	529.35		
3	8.11	17.00	534.22	526.54	528.32		
4	7.63	17.03	534.22	527.12	528.62		
5		17.06	536.23	527.19	528.46		
SLINE	ETAL	ETAS	ETAR	PSIR	RSTAR	AKIS	DELR
1	0.8425	0.9096	0.8310	0.9116	0.3323	4.129	0.07775
2	0.8614	0.9159	0.8788	0.9374	0.3129	3.109	0.05974
3	0.8664	0.9208	0.8909	0.9439	0.3191	2.551	0.03721
4	0.8283	0.9238	0.8329	0.9126	0.3016	2.117	0.01286
5	0.7786	0.9266	0.7825	0.8846	0.3520	1.825	0.01000
MOMENT	F-LB	REF	REF	REF	REF	REF	REF
1	17.16	3.342	14.663	14.663	14.663	11464.1	2.990
2							
3							
4							
5							
MOMENT	PTO/P2	M-STATION	AKIS	RSTAR			
1	0.8412	1.3003	2.689	0.40041			
2							
3							
4							
5							

INITIAL DISTRIBUTION LIST

	No. Copies
1. Defense Documentation Center Cameron Station Alexandria, Virginia 22314	20
2. Library Naval Postgraduate School Monterey, California 93940	2
3. Commander, Naval Air Systems Command Navy Department Washington, D.C. 20360	1
4. Commander, Naval Ship Systems Command Navy Department Washington, D.C. 20360	1
5. Capt. A. Bodnaruk, USN Naval Ship Systems Command (Code 6140) Navy Department Washington, D.C. 20360	1
6. Office of Naval Research (Power Branch) Attn. Mr. J. K. Patton, Jr. Navy Department Washington, D.C. 20360	1
7. Mr. R. Beichel Liquid Rocket Plant Aerojet-General Corporation Sacramento, California 95809	1
8. Chairman, Department of Aeronautics Naval Postgraduate School Monterey, California 93940	2
9. Professor M. H. Vavra Department of Aeronautics Naval Postgraduate School Monterey, California 93940	3
10. Lt R. G. Harrison, USN Naval Air Turbine Test Station 1440 Parkway Ave. P.O. Box 1716 Trenton, New Jersey 08628	3

DOCUMENT CONTROL DATA - R&D

(Security classification of title, body of abstract and indexing annotation must be entered when the overall report is classified)

1. ORIGINATING ACTIVITY (Corporate author) Naval Postgraduate School Monterey, California 93940		2. REPORT SECURITY CLASSIFICATION UNCLASSIFIED	
3. REPORT TITLE AN ANALYSIS OF SINGLE STAGE AXIAL-FLOW TURBINE PERFORMANCE USING THREE-DIMENSIONAL CALCULATING METHODS			
4. DESCRIPTIVE NOTES (Type of report and inclusive dates) Engineer Thesis, September 1967			
5. AUTHOR(S) (Last name, first name, initial) HARRISON, Robert G.			
6. REPORT DATE September 1967		7a. TOTAL NO. OF PAGES 144	7b. NO. OF REFS 9
8a. CONTRACT OR GRANT NO. a. PROJECT NO. c. d. <i>Distribution unlimited</i>		8b. ORIGINATOR'S REPORT NUMBER(S) 8b. OTHER REPORT NO(S) (Any other numbers that may be assigned this report)	
10. AVAILABILITY/LIMITATION NOTICES <u>Qualified requesters may obtain copies of this report from DDC.</u>			
11. SUPPLEMENTARY NOTES		12. SPONSORING MILITARY ACTIVITY Naval Air Systems Command Navy Department Washington, D.C. 20360	
13. ABSTRACT <p>The method of turbine performance prediction developed by Vavra and Eckert has been refined in this analysis to realize more of the potential of the three-dimensional calculating methods. Mach number and rotor tip clearance effects on blade outlet angles and loss coefficients have been localized rather than averaged over the blade height. An approximation for streamline curvature has been used.</p> <p>Performance curves were determined for two single stage axial-flow turbines located at the Propulsion Laboratory of the Naval Postgraduate School. Test results were available for one of the turbines. Agreement between predicted and experimental performance values was generally within 3 per cent.</p>			

14 KEY WORDS	LINK A		LINK B		LINK C	
	ROLE	WT	ROLE	WT	ROLE	WT
ANALYSIS SINGLE-STAGE AXIAL-FLOW TURBINE PERFORMANCE THREE-DIMENSIONAL CALCULATING METHODS						

—

thesH29343

DUDLEY KNOX LIBRARY



3 2768 00414777 7

DUDLEY KNOX LIBRARY